Theses and Dissertations

12-9-2011

Static and Free Vibration Analyses of Composite Shells Based on Different Shell Theories

Ebrahim Asadi

Follow this and additional works at: https://scholarsjunction.msstate.edu/td

STATIC AND FREE VIBRATION ANALYSES OF

COMPOSITE SHELLS BASED ON

DIFFERENT SHELL

THEORIES

By

Ebrahim Asadi

A Dissertation
Submitted to the Faculty of
Mississippi State University
in Partial Fulfillment of the Requirements
for the Degree of Doctor of Philosophy
in Mechanical Engineering
in the Department of Mechanical Engineering

Mississippi State, Mississippi

December 2011

STATIC AND FREE VIBRATION ANALYSES OF

COMPOSITE SHELLS BASED ON

DIFFERENT SHELL

THEORIES

By

Ebrahim Asadi

Approved:

<table>
<tr><td>Mohamad S. Qatu
Professor of Mechanical Engineering
Department of Mechanical Engineering
(Director of Dissertation)</td><td>Haitham El Kadiri
Assistant Professor of Mechanical
Engineering
Department of Mechanical Engineering
(Major Professor)</td></tr>
<tr><td>Rani W. Sullivan
Associate Professor of Aerospace
Engineering
Department of Aerospace Engineering
(Committee Members)</td><td>Oliver Myers
Assistant Professor of Mechanical
Engineering
Department of Mechanical Engineering
(Committee Member)</td></tr>
<tr><td>Youssef Hammi
Research Assistant Professor
Center for Advanced Vehicular Systems
(CAVS)
(Committee Member)</td><td>Steven R. Daniewicz
Professor of Mechanical Engineering
Graduate Coordinator of Department of
Mechanical Engineering</td></tr>
<tr><td>Sarah A. Rajala
Dean of the Bagley College of
Engineering</td><td></td></tr>
</table>

Name: Ebrahim Asadi

Date of Degree: December 9, 2011

Institution: Mississippi State University

Major Field: Mechanical Engineering

Major Professor: Haitham El Kadiri

Title of Study: STATIC AND FREE VIBRATION ANALYSES OF COMPOSITE SHELLS BASED ON DIFFERENT SHELL THEORIES

Pages in Study: 169

Candidate for Degree of Doctor of Philosophy

Equations of motion with required boundary conditions for doubly curved deep and thick composite shells are shown using two formulations. The first is based upon the formulation that was presented initially by Rath and Das (1973, J. Sound and Vib.) and followed by Reddy (1984, J. Engng. Mech. ASCE). In this formulation, plate stiffness parameters are used for thick shells, which reduced the equations to those applicable for shallow shells. This formulation is widely used but its accuracy has not been completely tested. The second formulation is based upon that of Qatu (1995, Compos. Press. Vessl. Indust.; 1999, Int. J. Solids Struct.). In this formulation, the stiffness parameters are calculated by using exact integration of the stress resultant equations. In addition, Qatu considered the radius of twist in his formulation. In both formulations, first order polynomials for in-plane displacements in the z-direction are utilized allowing for the inclusion of shear deformation and rotary inertia effects (first order shear deformation theory or FSDT). Also, FSDTQ has been modified in this dissertation using the radii of each laminate instead of using the radii of mid-plane in the moment of inertias and stress

resultants equations. Exact static and free vibration solutions for isotropic and symmetric and anti-symmetric cross-ply cylindrical shells for different length-to-thickness and length-to-radius ratios are obtained using the above theories. Finally, the equations of motion are put together with the equations of stress resultants to arrive at a system of seventeen first-order differential equations. These equations are solved numerically with the aid of General Differential Quadrature (GDQ) method for isotropic, cross-ply, angle-ply and general lay-up cylindrical shells with different boundary conditions using the above mentioned theories. Results obtained using all three theories (FSDT, FSDTQ and modified FSDTQ) are compared with the results available in literature and those obtained using a three-dimensional (3D) analysis. The latter (3D) is used here mainly to test the accuracy of the shell theories presented here.

DEDICATION

I wish to dedicate this work to my beloved wife, Hoda. Without the encouragement and support of my wife through difficult times, none of this would have been possible. I'm forever grateful to her.

ACKNOWLEDGEMENTS

TABLE OF CONTENTS

LIST OF TABLES

CHAPTER 1

INTRODUCTION

Light weight and high stiffness characteristics of structures made of laminated composite materials have provided excellent new opportunities in the design of many engineering structures. These include applications in automotive, aerospace and submarine structures. The relative simplicity of shell and plate theories and complexity of composite structures (which often makes these structures hard to analyze by three dimensional (3D) elasticity methods) have led to the development of different shell and plate theories. In the development of plate theories, the thickness ratios of the shell and plate are the main issue in categorizing different types of these plate theories. These classifications are mainly called Classical Theories, First-order Shear Deformation Theories (FSDTs) and Higher-order Shear Deformation Theories (HSDTs). Besides the effect of the thickness of shells, the effect of depth ratio of shells should be included in the development of shell theories. Some researchers included the effects of depth ratio in the development of shell theories, e.g. Qatu[1,2]. However, in spite of the effects of thickness ratio which are fairly addressed in literature, the effects of depth ratio need to be examined in the development of different shell theories. **This is one of the main contributions of this work.**

In the basic equations derived for shells, difficulties arise as a term $(1+z/R)$ appears in both the strain displacement and stress resultant equations. This term

introduced difficulty early in the development of shell theories. Some researchers included the term even for thin isotropic shells like Flügge [3] and Vlasov [4] while others ignored it like Love [5]. Significant analyses of isotropic thin shells showed that indeed the term is negligible for such thin isotropic shells.

The term was neglected by first analysts of composite thin shells (e.g. Ambartsumian [6]). While this is understandable for thin shells, the importance of the inclusion of the term needs to be tested for thicker shells. In addition to the inclusion of this term, both shear deformation and rotary inertia should be included for composite thick shells. Early treatment of composite thick shells [7, 8] included both shear deformation and rotary inertia but failed to include the z/R terms. We will refer to these as simply the first order shear deformation theory (FSDT). Qatu [1,2] presented equations where the term is carefully considered in the shell equations for composite deep thick shells. However, Qatu only presented the exact solution for free vibration problem of cross-ply cylindrical shells and the accuracy of his equations regarding other FSDTs needs to be examined. We will refer to his equations as the first order shear deformation shell theory by Qatu (FSDTQ). These equations will be described and modified in detail here.

1.1. Motivation and Objectives

There are a considerable number of shell theories in the literature and each one of them uses certain assumptions. However, most of them fail to provide accurate analysis when the radius of the shells is relatively large. This dissertation deals with different type of shell theories, their accuracy when comparing them with three dimensional solutions,

possible modification of them to achieve a higher level of accuracy, and the limitation of each of the shell theories regarding the thickness and depth ratios of the shell.

1.2.   Overview

This dissertation is divided into seven chapters. In the second chapter a general and complete literature review on the analyses of composite shells is done. As a prelude, the third chapter deals with the vibration of doubly curved shells with different boundaries. In this chapter, a classical shell theory is employed to treat cylindrical, spherical and paraboidal shells and plate with all possible type of boundary conditions with Ritz method. Exact solution for both static and free vibration of composite shells based on FSDTQ and FSDT are obtained in chapter four. Also, FSDTQ has been modified to take in to account the radii of each laminate instead of the mid-surface in the formulation. This modification improves the accuracy of the results. These results are obtained for the case of fully simply supported boundary conditions and the results are compared with those of 3D analysis by finite element software. Static analysis of composite shells based on FSDTQ and FSDT with different boundary conditions has been done by General Differential Quadrature (GDQ) method in chapter five. Six types of boundary conditions are selected for this study and the results are compared with the available results in literature and those obtained from 3D finite element analysis. Chapter six deals with the same problem as chapter five but it is for the free vibration problem of composite shells. Finally, concluding remarks and suggestions for future works from this dissertation are presented in chapter seven.

In summary, the major contributions of this dissertation are:

- Test the accuracy of various shell theories in static and vibration analyses

- Develop exact and approximate solutions for various set of shell problems (different boundaries, static, and vibration) and test their accuracy

- Improve on existing shell theories to achieve higher level of accuracy

1.3. References

1. Qatu MS. Accurate stress resultants equations for laminated composite deep thick shells. Compos Press Vessl Indust 1995; 302: 39-44.

2. Qatu MS. Accurate equations for laminated composite deep thick shells. Int J Solids Struct 1999; 36: 2917-2941.

3. Flügge W. Stresses in Shells. Berlin: Springer-Verlag; 1962.

4. Vlasov VZ. General Theory of Shells and Its Application to Engineering. GITTL: Moskva-Leningrad; 1949, English Translation, NASA Technical Translation TTF-99; 1964.

5. Love AEH. A Treatise on the Mathematical Theory of Elasticity, 1st Edition. Cambridge Univ. Press; 1892, 4th Edition, New York: Dover Publishing Inc.; 1944.

6. Ambartsumian SA. Contribution to the theory of anisotropic laminated shells. Appl Mech Rev 1962; 15: 245-249.

7. Rath BK, and Das YC. Vibration of layered shells. J Sound Vib 1973; 28: 737-757.

8. Reddy JN. Exact solution of moderately thick laminated shells. J Eng Mech ASCE 1984; 110: 794-809.

CHAPTER 2

LITERATURE REVIEW

The use of laminated composite shells in many engineering applications has been expanding rapidly in the past four decades due to their higher strength and stiffness to weight ratios when compared to most metallic materials. Composite shells now constitute a large percentage of recent aerospace or submarine structures. They are used increasingly in areas such as automotive engineering, biomedical engineering and other applications.

Literature on composite shell research can be found in many national and international conferences and journals. A recent article [3] focused on the recent research done on the dynamic behavior of composite shells wherein problems of free vibration, shock, wave propagation, dynamic stability, damping and viscoplastic behavior related to laminated shells are discussed. Several review articles on the subject, such as Qatu [2, 4], Kapania [5], Noor and Burton [6, 7], Noor et al. [8], and Soldatos [9] covered much of the research done in past decades. Computational aspects of the research were covered by Noor and Burton [6, 7], Noor et al. [8, 10] and Noor and Venneri [11]. Carrera [12] presented a historical review of zigzag theories for multilayered plates and shells. He also reviewed the theories and finite elements for multilayered, anisotropic, composite plates and shells [13]. Among the recent books on the subject are those by Reddy [14], Ye [15], Lee [16], and Shen [17].

This article reviews only recent research (2000 through 2010) done on the static and buckling analyses of composite shells. It includes stress, deformation, buckling and post buckling analyses under mechanical, thermal, hygrothermal or electrical loading.

This article classifies research based upon the shell theories typically used. These include thin (or classical) and thick shell theories (including shear deformation and three dimensional theories), shallow and deep theories, linear and nonlinear theories, and others. Most theories are classified based on the thickness ratio of the shell being treated (defined as the ratio of the thickness of the shell to the shortest of the span lengths and/or radii of curvature), its shallowness ratio (defined as the ratio of the shortest span length to one of the radii of curvature) and the magnitude of deformation (compared mainly to its thickness). Fundamental equations are listed for the types of shells used by most researchers in other publications [1-4]. Finite element analysis is gaining notable increase in its usage for solving composite shell problems.

The literature is reviewed while focusing on various aspects of research. Focus will first be placed on the various shell geometries that are receiving attention in recent years. Among classical shell geometries are the cylindrical, spherical, conical shells and other shells of revolution; other shells like shallow shells are also included in this review. Stress and deformation analyses, in which various boundary conditions and/or shell geometries are considered, buckling and post-buckling problems, and finally research dealing with thermal and/or hygrothermal environments will be reviewed. The third aspect of research will focus on material-related complexities, which include piezoelectric or other complex materials. Structural-related complexities will be the final

category that will be addressed. This will include stiffened shells, shells with cut-outs, shells with imperfections or other complexities.

2.1. Shell theories

Shells are three dimensional bodies bounded by two, relatively close, curved surfaces. The three dimensional equations of elasticity are complicated when written in curvilinear, or shell, coordinates. Researchers simplify such shell equations by making certain assumptions for particular applications. Almost all shell theories (thin and thick, deep and shallow …) reduce the three-dimensional (3D) elasticity problem into a two dimensional (2D) problem. The accuracy of thin and thick shell theories is established when their results are compared to those of 3D theory of elasticity.

2.1.1. Three dimensional elasticity theory

A shell is a three dimensional body confined by two parallel (unless the thickness is varying) surfaces. In general, the distance between those surfaces is small compared with other shell parameters. In this section, the equations from the theory of 3D elasticity in curvilinear coordinates are presented. The literature regarding vibrations of laminated shells using 3D elasticity theory will then be reviewed.

Consider a shell element of thickness h, radii of curvature $R\alpha$ and $R\beta$ (a radius of twist $R\alpha\beta$ is not shown here) (Fig. 2.1). Assume that the deformation of the shell is small compared to the shell dimensions. This assumption allows us to neglect nonlinear

8

terms in the subsequent derivation. It will also allow us to refer the analysis to the original configuration of the shell. The strain displacement relations can be written as [1]

$$\varepsilon_\alpha = \frac{1}{(1+z/R_\alpha)}\left(\frac{1}{A}\frac{\partial u}{\partial \alpha} + \frac{v}{AB}\frac{\partial A}{\partial \beta} + \frac{w}{R_\alpha}\right)$$

$$\varepsilon_\beta = \frac{1}{(1+z/R_\beta)}\left(\frac{1}{B}\frac{\partial v}{\partial \beta} + \frac{u}{AB}\frac{\partial B}{\partial \alpha} + \frac{w}{R_\beta}\right)$$

$$\varepsilon_z = \frac{\partial w}{\partial z}$$

$$\gamma_{\alpha\beta} = \frac{1}{(1+z/R_\alpha)}\left(\frac{1}{A}\frac{\partial v}{\partial \alpha} - \frac{u}{AB}\frac{\partial A}{\partial \beta} + \frac{w}{R_{\alpha\beta}}\right) + \frac{1}{(1+z/R_\beta)}\left(\frac{1}{B}\frac{\partial u}{\partial \beta} - \frac{v}{AB}\frac{\partial B}{\partial \alpha} + \frac{w}{R_{\alpha\beta}}\right)$$

(1)

$$\gamma_{\alpha z} = \frac{1}{A(1+z/R_\alpha)}\frac{\partial w}{\partial \alpha} + A(1+z/R_\alpha)\frac{\partial}{\partial z}\left(\frac{u}{A(1+z/R_\alpha)}\right) - \frac{v}{R_{\alpha\beta}(1+z/R_\alpha)}$$

$$\gamma_{\beta z} = \frac{1}{B(1+z/R_\beta)}\frac{\partial w}{\partial \beta} + B(1+z/R_\beta)\frac{\partial}{\partial z}\left(\frac{v}{B(1+z/R_\beta)}\right) - \frac{u}{R_{\alpha\beta}(1+z/R_\beta)}$$

The laminated composite shells are assumed to be composed of plies of unidirectional long fibers embedded in a matrix material. On a macroscopic level, each layer may be regarded as being homogeneous and orthotropic. However, the fibers of a typical layer may not be parallel to the coordinates in which the shell equations are expressed. The stress-strain relationship for a typical nth lamina in a laminated composite shell made of N laminas is shown in Fig. 2.2 and given by Eq. (2) [1].

$$
\begin{bmatrix} \sigma_\alpha \\ \sigma_\beta \\ \sigma_z \\ \sigma_{\beta z} \\ \sigma_{\alpha z} \\ \sigma_{\alpha\beta} \end{bmatrix} = \begin{bmatrix} \overline{Q}_{11} & \overline{Q}_{12} & \overline{Q}_{13} & 0 & 0 & \overline{Q}_{16} \\ \overline{Q}_{12} & \overline{Q}_{22} & \overline{Q}_{23} & 0 & 0 & \overline{Q}_{26} \\ \overline{Q}_{13} & \overline{Q}_{23} & \overline{Q}_{33} & 0 & 0 & \overline{Q}_{36} \\ 0 & 0 & 0 & \overline{Q}_{44} & \overline{Q}_{45} & 0 \\ 0 & 0 & 0 & \overline{Q}_{45} & \overline{Q}_{55} & 0 \\ \overline{Q}_{16} & \overline{Q}_{26} & \overline{Q}_{36} & 0 & 0 & \overline{Q}_{66} \end{bmatrix} \begin{bmatrix} \varepsilon_\alpha \\ \varepsilon_\beta \\ \varepsilon_z \\ \gamma_{\beta z} \\ \gamma_{\alpha z} \\ \gamma_{\alpha\beta} \end{bmatrix}
$$

(2)

The positive notations of the stresses are shown in Fig. 2.1.

In order to develop a consistent set of equations, the boundary conditions and the equations of motion will be derived using Hamilton's principle [1], which yields the following equations of motion

$$
\frac{\partial(B\sigma_\alpha)}{\partial\alpha} + \frac{\partial(A\sigma_{\alpha\beta})}{\partial\beta} + \frac{\partial(AB\sigma_{\alpha z})}{\partial z} + \sigma_{\alpha\beta}\frac{\partial A}{\partial\beta} + \sigma_{\alpha z}B\frac{\partial A}{\partial z} - \sigma_\beta\frac{\partial B}{\partial\alpha} + ABq_\alpha = \rho\frac{\partial^2 u}{\partial t^2}
$$

$$
\frac{\partial(B\sigma_{\alpha\beta})}{\partial\alpha} + \frac{\partial(A\sigma_\beta)}{\partial\beta} + \frac{\partial(AB\sigma_{\beta z})}{\partial z} + \sigma_{\beta z}A\frac{\partial B}{\partial z} + \sigma_{\alpha\beta}\frac{\partial B}{\partial\alpha} - \sigma_\alpha\frac{\partial A}{\partial\beta} + ABq_\beta = \rho\frac{\partial^2 v}{\partial t^2}
$$

$$
\frac{\partial(B\sigma_{\alpha z})}{\partial\alpha} + \frac{\partial(A\sigma_{\beta z})}{\partial\beta} + \frac{\partial(AB\sigma_z)}{\partial z} - \sigma_\beta A\frac{\partial B}{\partial z} - \sigma_\alpha B\frac{\partial A}{\partial z} + ABq_z = \rho\frac{\partial^2 w}{\partial t^2}
$$

(3)
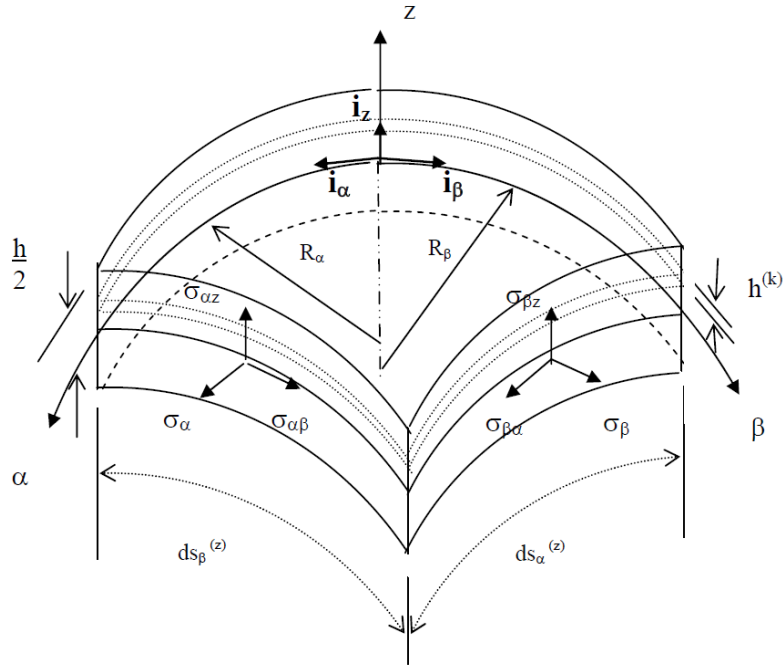
Figure 2.1:   Stresses in shell coordinates (free outer surfaces)

Hamilton's principle will also yield boundary terms that are consistent with the other equations. The boundary terms for z = constant are:

$$\sigma_{0z} - \sigma_z = 0 \qquad or \qquad w^0 = 0$$
$$\sigma_{0\alpha z} - \sigma_{\alpha z} = 0 \qquad or \qquad u^0 = 0$$
$$\sigma_{0\beta z} - \sigma_{\alpha z} = 0 \qquad or \qquad v^0 = 0$$

(4)

where σ_{0z}, $\sigma_{0\alpha z}$ and $\sigma_{0\beta z}$ are surface tractions and u0, v0 and w0 are displacement functions at z = constant.   Similar results are obtained for the boundaries α = constant and β = constant. A three dimensional shell element has six surfaces. With three

equations at each surface, a total of 18 equations can be obtained for a single-layered shell.

The above equations are valid for single-layered shells. To use 3D elasticity theory for multi-layered shells, each layer must be treated as an individual shell. Both displacements and stresses must be continuous between each layer (layer k to layer k+1) in a n-ply laminate to insure that there are no free internal surfaces (i.e., delamination) between the layers.

$$u(\alpha,\beta,z = h_k / 2) \big|_{k=i} = u(\alpha,\beta,z = -h_k / 2) \big|_{k=i+1}$$
$$v(\alpha,\beta,z = h_k / 2) \big|_{k=i} = v(\alpha,\beta,z = -h_k / 2) \big|_{k=i+1}$$
$$w(\alpha,\beta,z = h_k / 2) \big|_{k=i} = w(\alpha,\beta,z = -h_k / 2) \big|_{k=i+1}$$
$$\sigma_z(\alpha,\beta,z = h_k / 2) \big|_{k=i} = \sigma_z(\alpha,\beta,z = -h_k / 2) \big|_{k=i+1}$$
$$\sigma_{\alpha z}(\alpha,\beta,z = h_k / 2) \big|_{k=i} = \sigma_{\alpha z}(\alpha,\beta,z = -h_k / 2) \big|_{k=i+1}$$
$$\sigma_{\beta z}(\alpha,\beta,z = h_k / 2) \big|_{k=i} = \sigma_{\beta z}(\alpha,\beta,z = -h_k / 2) \big|_{k=i+1} \quad \text{For k= 1, ..., N-1} \quad (5)$$

Among the recent work that used 3D theory of elasticity is the work of Sheng and Ye [18] who presented a 3D state space finite element solution for composite cylindrical shells. Wu and Lo [19] discussed 3D elasticity solutions of laminated annular spherical shells. Wang and Zhong [20] used 3D theory to solve problems with smart laminated anisotropic circular cylindrical shells with imperfect bonding. Li and Shen [21] studied postbuckling of 3D textile composite cylindrical shells under axial compression in thermal environments. Santos et al [22, 23] showed a finite element model for the analysis of 3D axisymmetric laminated shells with piezoelectric sensors and actuators. Sprenger et al [24] investigated delamination growth in laminated structures with 3D-shell elements and a viscoplastic softening model. Li and Shen [25, 26] analyzed

12

postbuckling of 3D braided composite cylindrical shells under various loading in thermal environments. Alibeigloo and Nouri [27] found a three-dimensional solution for static analysis of functionally graded (FG) cylindrical shells with bonded piezoelectric layers by utilizing differential quadrature method (DQM) to the edge boundary conditions and in-plane differentials and using state-space approach for discrete points. Fagiano et al. [28] used 3-D finite element method to accurately predict interlaminar stresses for multilayer composite shells.

2.1.2. Thick shell theory

Thick shells are defined as shells with a thickness smaller by at least one order of magnitude when compared with other shell parameters such as wavelength and/or radii of curvature (thickness is at least 1/10th of the smallest of the wavelength and/or radii of curvature). The main differentiation between thick shell and thin shell theories is the inclusion of shear deformation and rotary inertia effects. Theories that include shear deformation are referred to as thick shell theories or shear deformation theories.

Thick shell theories are typically based on either a displacement or stress approach. In the former, the midplane shell displacements are expanded in terms of shell thickness, which can be a first order expansion, referred to as first order shear deformation theories.

The 3D elasticity theory is reduced to a 2D theory using the assumption that the normal strains acting upon the plane parallel to the middle surface are negligible compared with other strain components. This assumption is generally valid except within the vicinity of a highly concentrated force (St. Venant's principle). In other words, no

stretching is assumed in the z-direction (i.e., $\varepsilon z=0$). Assuming that normals to the

midsurface strains remain straight during deformation but not normal, the displacements

can be written as [1]

$$u(\alpha,\beta,z) = u_0(\alpha,\beta) + z\psi_\alpha(\alpha,B)$$
$$v(\alpha,\beta,z) = v_0(\alpha,\beta) + z\psi_\beta(\alpha,B)$$
$$w(\alpha,\beta,z) = w_0(\alpha,\beta)$$

(6)
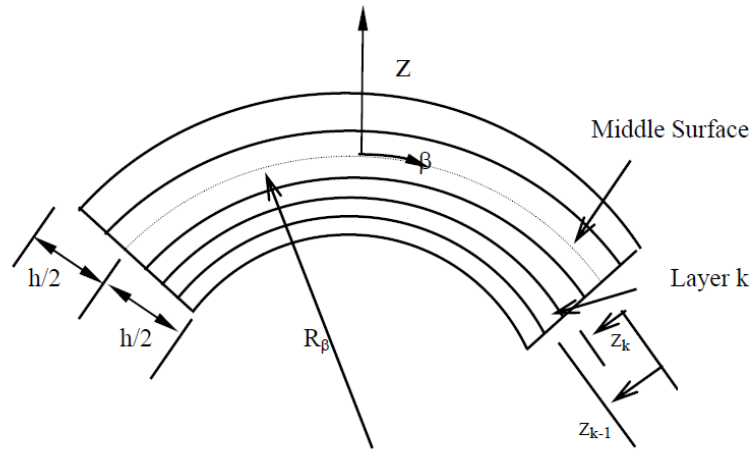
Figure. 2.2:   Lamination parameters in shells

where u0, v0 and w0 are midsurface displacements of the shell and $\psi\alpha$ and $\psi\beta$ are

midsurface rotations. An alternative derivation can be made with the assumption $\sigma z = 0$.

The subscript (0) will refer to the middle surface in subsequent equations. The above

equations describe a typical first-order shear deformation shell theory, and will constitute

14

the only assumption made in this analysis when compared with the 3D theory of elasticity. As a result, strains are written as [1]

$$\varepsilon_\alpha = \frac{1}{(1+z/R_\alpha)}(\varepsilon_{0\alpha} + z\kappa_\alpha), \qquad \varepsilon_\beta = \frac{1}{(1+z/R_\beta)}(\varepsilon_{0\beta} + z\kappa_\beta)$$

$$\varepsilon_{\alpha\beta} = \frac{1}{(1+z/R_\alpha)}(\varepsilon_{0\alpha\beta} + z\kappa_{\alpha\beta}), \qquad \varepsilon_{\beta\alpha} = \frac{1}{(1+z/R_\beta)}(\varepsilon_{0\beta\alpha} + z\kappa_{\beta\alpha})$$

(7)

$$\gamma_{\alpha z} = \frac{1}{(1+z/R_\alpha)}\left(\gamma_{0\alpha z} - z(\psi_\beta/R_{\alpha\beta})\right)$$

$$\gamma_{\beta z} = \frac{1}{(1+z/R_\beta)}\left(\gamma_{0\beta z} - z(\psi_\alpha/R_{\alpha\beta})\right)$$

where the midsurface strains are:

$$\varepsilon_{0\alpha} = \frac{1}{A}\frac{\partial u_0}{\partial\alpha} + \frac{v_0}{AB}\frac{\partial A}{\partial\beta} + \frac{w_0}{R_\alpha}, \qquad \varepsilon_{0\beta} = \frac{1}{B}\frac{\partial v_0}{\partial\beta} + \frac{u_0}{AB}\frac{\partial B}{\partial\alpha} + \frac{w_0}{R_\beta}$$

$$\varepsilon_{0\alpha\beta} = \frac{1}{A}\frac{\partial v_0}{\partial\alpha} - \frac{u_0}{AB}\frac{\partial A}{\partial\beta} + \frac{w_0}{R_{\alpha\beta}}, \qquad \varepsilon_{0\beta\alpha} = \frac{1}{B}\frac{\partial u_0}{\partial\beta} - \frac{v_0}{AB}\frac{\partial B}{\partial\alpha} + \frac{w_0}{R_{\alpha\beta}}$$

(8a)

$$\gamma_{0\alpha z} = \frac{1}{A}\frac{\partial w_0}{\partial\alpha} - \frac{u_0}{R_\alpha} - \frac{v_0}{R_{\alpha\beta}} + \psi_\alpha, \qquad \gamma_{0\beta z} = \frac{1}{B}\frac{\partial w_0}{\partial\beta} - \frac{v_0}{R_\beta} - \frac{u_0}{R_{\alpha\beta}} + \psi_\beta$$

and the curvature and twist changes are:

$$\kappa_\alpha = \frac{1}{A}\frac{\partial\psi_\alpha}{\partial\alpha} + \frac{\psi_\beta}{AB}\frac{\partial A}{\partial\beta}, \quad \kappa_\beta = \frac{1}{B}\frac{\partial\psi_\beta}{\partial\beta} + \frac{\psi_\alpha}{AB}\frac{\partial B}{\partial\alpha}$$

$$\kappa_{\alpha\beta} = \frac{1}{A}\frac{\partial\psi_\beta}{\partial\alpha} - \frac{\psi_\alpha}{AB}\frac{\partial A}{\partial\beta}, \quad \kappa_{\beta\alpha} = \frac{1}{B}\frac{\partial\psi_\alpha}{\partial\beta} - \frac{\psi_\beta}{AB}\frac{\partial B}{\partial\alpha}$$

(8b)
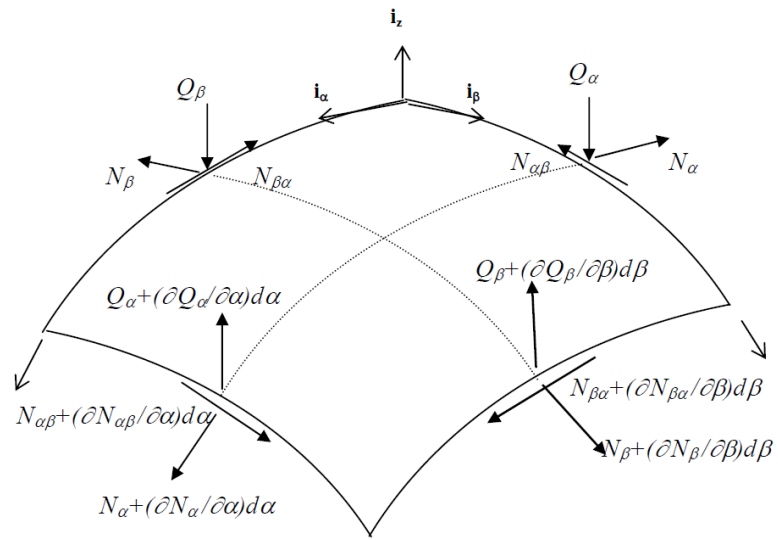
Figure 2.3:   Force resultants in shell coordinates
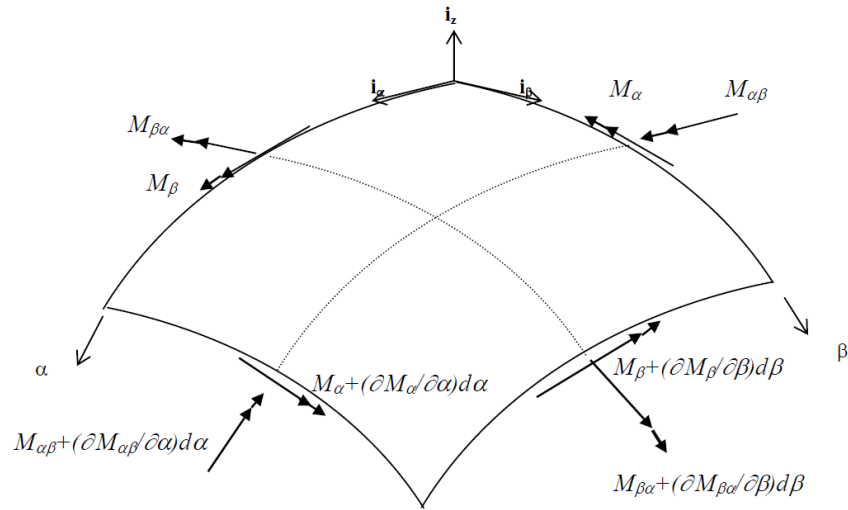
Figure 2.4:   Moment resultants in shell coordinates

The force and moment resultants (Figs 2.3 and 2.4) are obtained by integrating the stresses over the shell thickness considering the (1+z/R) term that appears in the denominator of the stress resultant equations [5]. The stress resultant equations are:

$$
\begin{bmatrix} N_\alpha \\ N_\beta \\ N_{\alpha\beta} \\ N_{\beta\alpha} \\ M_\alpha \\ M_\beta \\ M_{\alpha\beta} \\ M_{\beta\alpha} \end{bmatrix} = \begin{bmatrix} \bar{A}_{11} & A_{12} & \bar{A}_{16} & A_{16} & \bar{B}_{11} & B_{12} & \bar{B}_{16} & B_{16} \\ A_{12} & \hat{A}_{22} & A_{26} & \hat{A}_{26} & B_{12} & \hat{B}_{22} & B_{26} & \hat{B}_{26} \\ \bar{A}_{16} & A_{26} & \bar{A}_{66} & A_{66} & \bar{B}_{16} & B_{26} & \bar{B}_{66} & B_{66} \\ A_{16} & \hat{A}_{26} & A_{66} & \hat{A}_{66} & B_{16} & \hat{B}_{26} & B_{66} & \hat{B}_{66} \\ \bar{B}_{11} & B_{12} & \bar{B}_{16} & B_{16} & \bar{D}_{11} & D_{12} & \bar{D}_{16} & D_{16} \\ B_{12} & \hat{B}_{22} & B_{26} & \hat{B}_{26} & D_{12} & \hat{D}_{22} & D_{26} & \hat{D}_{26} \\ \bar{B}_{16} & B_{26} & \bar{B}_{66} & B_{66} & \bar{D}_{16} & D_{26} & \bar{D}_{66} & D_{66} \\ B_{16} & \hat{B}_{26} & B_{66} & \hat{B}_{66} & D_{16} & \hat{D}_{26} & D_{66} & \hat{D}_{66} \end{bmatrix} \begin{bmatrix} \varepsilon_{0\alpha} \\ \varepsilon_{0\beta} \\ \varepsilon_{0\alpha\beta} \\ \varepsilon_{0\beta\alpha} \\ \kappa_\alpha \\ \kappa_\beta \\ \kappa_{\alpha\beta} \\ \kappa_{\beta\alpha} \end{bmatrix}
$$

(9)

$$
\begin{bmatrix} Q_\alpha \\ Q_\beta \\ P_\alpha \\ P_\beta \end{bmatrix} = \begin{bmatrix} \bar{A}_{55} & A_{45} & \bar{B}_{55} & B_{45} \\ A_{45} & \hat{A}_{44} & B_{45} & \hat{B}_{44} \\ \bar{B}_{55} & B_{45} & \bar{D}_{55} & D_{45} \\ B_{45} & \hat{B}_{44} & D_{45} & \hat{D}_{44} \end{bmatrix} \begin{bmatrix} \gamma_{0\alpha z} \\ \gamma_{0\beta z} \\ -\psi_\beta / R_{\alpha\beta} \\ -\psi_\alpha / R_{\alpha\beta} \end{bmatrix}
$$

(10)

where A_{ij}, B_{ij}, D_{ij}, $\bar{A}_{ij}$, $\bar{B}_{ij}$, $\bar{D}_{ij}$, $\hat{A}_{ij}$, $\hat{B}_{ij}$, and $\hat{D}_{ij}$, are defined in [1].

It has been shown [1,5] that the above Eqs. (9) and (10) yield more accurate results when compared with those of plates and those traditionally used for shells [18]. Hamilton's principle can be used to derive the consistent equations of motion and boundary conditions. The equations of motion are [1-4]:

$$\frac{\partial}{\partial\alpha}\left(BN_\alpha\right)+\frac{\partial}{\partial\beta}\left(AN_{\beta\alpha}\right)+\frac{\partial A}{\partial\beta}N_{\alpha\beta}-\frac{\partial B}{\partial\alpha}N_\beta+\frac{AB}{R_\alpha}Q_\alpha+\frac{AB}{R_{\alpha\beta}}Q_\beta+ABq_\alpha=AB\left(\bar{I}_1\ddot{u}_0+\bar{I}_2\ddot{\psi}_\alpha\right)$$

$$\frac{\partial}{\partial\beta}\left(AN_\beta\right)+\frac{\partial}{\partial\alpha}\left(AN_{\alpha\beta}\right)+\frac{\partial B}{\partial\alpha}N_{\beta\alpha}-\frac{\partial A}{\partial\beta}N_\alpha+\frac{AB}{R_\beta}Q_\beta+\frac{AB}{R_{\alpha\beta}}Q_\alpha+ABq_\beta=AB\left(\bar{I}_1\ddot{v}_0+\bar{I}_2\ddot{\psi}_\beta\right)$$

$$-AB\left(\frac{N_\alpha}{R_\alpha}+\frac{N_\beta}{R_\beta}+\frac{N_{\alpha\beta}+N_{\beta\alpha}}{R_{\alpha\beta}}\right)+\frac{\partial}{\partial\alpha}\left(BQ_\alpha\right)+\frac{\partial}{\partial\beta}\left(AQ_\beta\right)+ABq_n=AB\left(\bar{I}_1\ddot{w}_0\right)$$

$$\frac{\partial}{\partial\alpha}\left(BM_\alpha\right)+\frac{\partial}{\partial\beta}\left(AM_{\beta\alpha}\right)+\frac{\partial A}{\partial\beta}M_{\alpha\beta}-\frac{\partial B}{\partial\alpha}M_\beta-ABQ_\alpha+\frac{AB}{R_{\alpha\beta}}P_\beta+ABm_\alpha=AB\left(\bar{I}_2\ddot{u}_0+\bar{I}_3\ddot{\psi}_\alpha\right)$$

$$\frac{\partial}{\partial\beta}\left(AM_\beta\right)+\frac{\partial}{\partial\alpha}\left(BM_{\alpha\beta}\right)+\frac{\partial B}{\partial\alpha}M_{\beta\alpha}-\frac{\partial A}{\partial\beta}M_\alpha-ABQ_\beta+\frac{AB}{R_{\alpha\beta}}P_\alpha+ABm_\beta=AB\left(\bar{I}_2\ddot{v}_0+\bar{I}_3\ddot{\psi}_\beta\right)$$

$$(11)$$

where the two dots over the terms represent the second derivative of these terms with respect to time, and where:

$$\bar{I}_i=\left(I_i+I_{i+1}\left(\frac{1}{R_\alpha}+\frac{1}{R_\beta}\right)+\frac{I_{i+2}}{R_\alpha R_\beta}\right),\quad i=1,2,3$$

$$(12a)$$

and

$$[I_1,I_2,I_3,I_4,I_5]=\sum_{k=1}^{N}\int_{h_{k-1}}^{h_k}\rho^{(k)}\left[1,z,z^2,z^3,z^4\right]dz$$

$$(12b)$$

The boundary terms for the boundaries with α =constant are

$$N_{0\alpha}-N_\alpha=0\qquad or\qquad u_0=0$$
$$N_{0\alpha\beta}-N_{\alpha\beta}=0\qquad or\qquad v_0=0$$
$$Q_{0\alpha}-Q_\alpha=0\qquad or\qquad w_0=0$$
$$M_{0\alpha}-M_\alpha=0\qquad or\qquad \psi_\alpha=0$$
$$M_{0\alpha\beta}-M_{\alpha\beta}=0\qquad or\qquad \psi_\beta=0$$

$$(13)$$

Similar equations can be obtained for β = constant. Eqs. (9) and (10) are significantly different from those that cover most of first order shear deformation theories (FSDTs) for shells which neglect the effect of z / R in the stress resultant equations.

Shear deformation theories were used by many authors (e.g. Qatu [4]). Chaudhuri [29] presented a nonlinear zigzag theory for finite element analysis of shear-deformable laminated shells. Krejaa and Schmidt [30] studied large rotations in shear deformation finite element analysis of laminated shells. Non-linear buckling and postbuckling of a moderately thick anisotropic laminated cylindrical shell of finite length subjected to lateral pressure, hydrostatic pressure and external liquid pressure based on a higher order shear deformation shell theory with von Kármán–Donnell-type of kinematic non-linearity and including the extension/twist, extension/flexural and flexural/twist couplings were presented by Li and Lin [31] wherein the material property of each layer could be linearly elastic, anisotropic and fiber-reinforced. A mixed meshless computational method based on the Local Petrov–Galerkin approach for analysis of plate and shell structures was presented by Sorić and Jarak [32]. They overcame the undesired locking phenomena and demonstrated that this meshless method is numerically more efficient than the available meshless fully displacement approaches. Shen [33, 34] investigated postbuckling of shear deformable cross-ply laminated cylindrical shells under combined loading. Piskonov et al [35] were interested in a rotational higher order shear deformation theory of anisotropic laminated plates and shells. Iozzi and Gaudenzi [36] showed shear deformable shell elements for adaptive laminated structures. Han et al [37] performed a geometrically nonlinear analysis of laminated composite thin shells using a modified first-order shear deformable element. Other studies that used a shear deformation shell theory include

those of Li [38], Zenkour [39], Shen [40], Shen and Li [41], Balah and Al-Ghamedy [42], and Ferriera [43].

Zhen and Wanji [44] presented a higher order theory for multilayered shells and performed analysis on laminated cylindrical shell panels. Khare et al [45] discussed closed-form thermo-mechanical solutions of higher-order theories of cross-ply laminated shallow shells. Khare and Rode [46] showed similar solutions for thick laminated sandwich shells. Ferreira et al [47] modeled cross-ply laminated elastic shells by a higher-order theory. Alijani and Aghdam [48] presented a semi-analytical solution for stress analysis of moderately thick laminated cylindrical panels with various boundary conditions. Pinto Correia et al [49] analyzed laminated conical shell structures for buckling using higher order models. Matsunaga [50] studied thermal buckling of cross-ply laminated composite shallow shells according to a higher order deformation theory. Oh and Cho [51] investigated a higher order zigzag theory for smart composite shells under mechanical-thermo-electric loading. Yaghoubshahi et al. [52] employed general higher-order shear deformation theory and formulated it to analyze deep composite shells with mixed boundary conditions. Benson et al. [53] presented a Reissner–Mindlin shell formulation based on a degenerated solid is implemented for NURBS-based isogeometric analysis. They constructed a user-defined element in LS-Dyna for industrial purposes to analyze elasto-plastic behavior of shells.

In general, layer-wise laminate theories are used to properly represent local effects, such as interlaminar stress distribution, delaminations, etc. These theories are typically employed for cases involving anisotropic materials in which transverse shear effects

cannot be ignored. Recent studies include Yuan et al [54] in which a stress projection, layer-wise-equivalent formulation was used for accurate predictions of transverse stresses in laminated plates and shells. Kim and Chaudhuri [55-56] and Chaudhuri and Kim [57] described a layer-wise linear displacement distribution theory and based their analysis on it to investigate the buckling and shear behavior of a long cross-ply cylindrical shell (ring). Leigh and Tafreshi [58] used layerwise shell finite element based on first order shear deformation theory to investigate delamination buckling of composite cylindrical shells. A static analysis of thick composite circular arches using a layerwise differential quadrature technique was performed by Malekzadeh [59]. Roh et al [60, 61] investigated the thermo-mechanical behavior of shape memory alloys using a finite element method based on layerwise theory. The theory of layerwise displacement field was used to perform a finite element analyses of aero-thermally buckled composite shells by Shin et al [62]. The displacement field of a layerwise theory was also used to develop laminated beam theories by Tahani [63].

2.1.3. Thin shell theory

If the shell thickness is less than 1/20th of the other shell dimensions (e.g. length) and/or radii of curvature, a thin shell theory, where shear deformation and rotary inertia are negligible, is generally acceptable. Depending on various assumptions made during the derivation of the strain-displacement relations, stress-strain relations, and the equilibrium equations, various thin shell theories can be derived [5]. All these theories were initially derived for isotropic shells and expanded later for laminated composite

shells by applying the appropriate integration through laminas, and stress-strain relations. For very thin shells, the shell is thin such that the ratio of the thickness compared to any of the shell's radii or any other shell parameter, i.e., width or length, is negligible when compared to unity. Also, for thin shells, the normals to the middle surface remain straight and normal when the shell undergoes deformation. These assumption assures that certain parameters in the shell equations (including the z/R) term mentioned earlier in the thick shell theory can be neglected. The shear deformation can be neglected in the kinematic equations allowing the in-plane displacement to vary linearly through the shell's thickness as given by

$$
\begin{aligned}
\varepsilon_\alpha &= \varepsilon_{0\alpha} + z\kappa_\alpha \\
\varepsilon_\beta &= \varepsilon_{0\beta} + z\kappa_\beta \\
\gamma_{\alpha\beta} &= \gamma_{0\alpha\beta} + z\tau_{\alpha\beta}
\end{aligned}
\tag{14}
$$

where the midsurface strains, curvature and twist changes are

$$
\varepsilon_{0\alpha} = \frac{1}{A}\frac{\partial u_0}{\partial \alpha} + \frac{v_0}{AB}\frac{\partial A}{\partial \beta} + \frac{w_0}{R_\alpha}
$$

$$
\varepsilon_{0\beta} = \frac{1}{B}\frac{\partial v_0}{\partial \beta} + \frac{u_0}{AB}\frac{\partial B}{\partial \alpha} + \frac{w_0}{R_\beta}
$$

$$
\gamma_{0\alpha\beta} = \frac{1}{A}\frac{\partial v_0}{\partial \alpha} - \frac{u_0}{AB}\frac{\partial A}{\partial \beta} + \frac{1}{B}\frac{\partial u_0}{\partial \beta} - \frac{v_0}{AB}\frac{\partial B}{\partial \alpha} + 2\frac{w_0}{R_{\alpha\beta}}
\tag{15a}
$$

$$
\kappa_\alpha = \frac{1}{A}\frac{\partial \psi_\alpha}{\partial \alpha} + \frac{\psi_\beta}{AB}\frac{\partial A}{\partial \beta}, \quad \kappa_\beta = \frac{1}{B}\frac{\partial \psi_\beta}{\partial \beta} + \frac{\psi_\alpha}{AB}\frac{\partial B}{\partial \alpha}
$$

$$
\tau = \frac{1}{A}\frac{\partial \psi_\beta}{\partial \alpha} - \frac{\psi_\alpha}{AB}\frac{\partial A}{\partial \beta} + \frac{1}{B}\frac{\partial \psi_\alpha}{\partial \beta} - \frac{\psi_\beta}{AB}\frac{\partial B}{\partial \alpha}
\tag{15b}
$$

and where

22

$$\psi_\alpha = \frac{u}{R_\alpha} + \frac{v_0}{R_{\alpha\beta}} - \frac{1}{A}\frac{\partial w}{\partial \alpha}, \qquad \psi_\beta = \frac{v}{R_\beta} + \frac{u_0}{R_{\alpha\beta}} - \frac{1}{A}\frac{\partial w}{\partial \beta}. \tag{15c}$$

Applying Kirchhoff hypothesis of neglecting shear deformation and the assumption that εz is negligible, the stress-strain equations for an element of material in the kth lamina may be written as [1]

$$\begin{bmatrix} \sigma_\alpha \\ \sigma_\beta \\ \sigma_{\alpha\beta} \end{bmatrix}_k = \begin{bmatrix} Q_{11} & Q_{12} & Q_{16} \\ Q_{12} & Q_{22} & Q_{26} \\ Q_{16} & Q_{26} & Q_{66} \end{bmatrix}_k \begin{bmatrix} \varepsilon_\alpha \\ \varepsilon_\beta \\ \gamma_{\alpha\beta} \end{bmatrix}_k \tag{16}$$

where σα and σβ are normal stress components, ταβ is the in-plane shear stress component [1], εα and εβ are the normal strains, and γαβ is the in-plane engineering shear strain. The terms Qij are the elastic stiffness coefficients for the material. If the shell coordinates (α,β) are parallel or perpendicular to the fibers, then the terms Q16 and Q26 are both zero. Stresses over the shell thickness (h) are integrated to get the force and moment resultants as given by

$$\begin{bmatrix} N_\alpha \\ N_\beta \\ N_{\alpha\beta} \\ M_\alpha \\ M_\beta \\ M_{\alpha\beta} \end{bmatrix} = \begin{bmatrix} A_{11} & A_{12} & A_{16} & B_{11} & B_{12} & B_{16} \\ A_{12} & A_{22} & A_{26} & B_{12} & B_{22} & B_{26} \\ A_{16} & A_{26} & A_{66} & B_{16} & B_{26} & B_{66} \\ B_{11} & B_{12} & B_{16} & D_{11} & D_{12} & D_{16} \\ B_{12} & B_{22} & B_{26} & D_{12} & D_{22} & D_{26} \\ B_{16} & B_{26} & B_{66} & D_{16} & D_{26} & D_{66} \end{bmatrix} \begin{bmatrix} \varepsilon_{0\alpha} \\ \varepsilon_{0\beta} \\ \gamma_{0\alpha\beta} \\ k_\alpha \\ k_\beta \\ \tau \end{bmatrix} \tag{17}$$

where Aij , Bij , and Dij are the stiffness coefficients arising from the piecewise integration over the shell thickness (Eq. 10b).   For shells which are laminated symmetrically with respect to their midsurfaces, all the Bij terms become zero. Note that

23

the above equations are the same as those for laminated plates, which are also valid for thin laminated shells. Using Hamilton's principle yields the following equations of motion.

$$\frac{\partial}{\partial\alpha}\left(BN_\alpha\right)+\frac{\partial}{\partial\beta}\left(AN_{\beta\alpha}\right)+\frac{\partial A}{\partial\beta}N_{\alpha\beta}-\frac{\partial B}{\partial\alpha}N_\beta+\frac{AB}{R_\alpha}Q_\alpha+\frac{AB}{R_{\alpha\beta}}Q_\beta+ABq_\alpha=AB\left(\bar{I}_1\ddot{u}_0\right)$$

$$\frac{\partial}{\partial\beta}\left(AN_\beta\right)+\frac{\partial}{\partial\alpha}\left(AN_{\alpha\beta}\right)+\frac{\partial B}{\partial\alpha}N_{\beta\alpha}-\frac{\partial A}{\partial\beta}N_\alpha+\frac{AB}{R_\beta}Q_\beta+\frac{AB}{R_{\alpha\beta}}Q_\alpha+ABq_\beta=AB\left(\bar{I}_1\ddot{v}_0\right)$$

$$-AB\left(\frac{N_\alpha}{R_\alpha}+\frac{N_\beta}{R_\beta}+\frac{N_{\alpha\beta}+N_{\beta\alpha}}{R_{\alpha\beta}}\right)+\frac{\partial}{\partial\alpha}\left(BQ_\alpha\right)+\frac{\partial}{\partial\beta}\left(AQ_\beta\right)+ABq_n=AB\left(\bar{I}_1\ddot{w}_0\right)$$

where

$$ABQ_\alpha=\frac{\partial}{\partial\alpha}\left(BM_\alpha\right)+\frac{\partial}{\partial\beta}\left(AM_{\beta\alpha}\right)+\frac{\partial A}{\partial\beta}M_{\alpha\beta}-\frac{\partial B}{\partial\alpha}M_\beta$$

$$ABQ_\beta=\frac{\partial}{\partial\beta}\left(AM_\beta\right)+\frac{\partial}{\partial\alpha}\left(BM_{\alpha\beta}\right)+\frac{\partial B}{\partial\alpha}M_{\beta\alpha}-\frac{\partial A}{\partial\beta}M_\alpha$$

$$(18)$$

The following boundary conditions can be obtained for thin shells for α = constant (similar equations can be obtained for β = constant).

$$N_{0\alpha}-N_\alpha=0 \qquad or \qquad u_0=0$$

$$\left(N_{0\alpha\beta}-\frac{N_{0\alpha\beta}}{R_\beta}\right)-\left(N_{\alpha\beta}-\frac{N_{\alpha\beta}}{R_\beta}\right)=0 \qquad or \qquad v_0=0$$

$$\left(Q_{0\alpha}-\frac{1}{B}\frac{\partial M_{0\alpha\beta}}{\partial\beta}\right)-\left(Q_\alpha-\frac{1}{B}\frac{\partial M_{\alpha\beta}}{\partial\beta}\right)=0 \qquad or \qquad w_0=0$$

$$M_{0\alpha}-M_\alpha=0 \qquad or \qquad \psi_\alpha=0$$

$$M_{0\alpha\beta}w\ ]_{\beta_1}^{\beta_2}=0$$

$$(19)$$

Shen [64] studied buckling and postbuckling of laminated thin cylindrical shells under hygrothermal environments. Soldatos and Shu [65] discussed modeling of perfectly and weakly bonded laminated plates and shallow shells. Chaudhuri et al [66] presented admissible boundary conditions and solutions to internally pressurized thin cylindrical

shells. Khosravi et al [67] illustrated a shell element for co-rotational nonlinear analysis of thin and moderately thick laminated structures. Sofiyev et al [68] discussed buckling of laminated cylindrical thin shells under torsion. Weicker et al. [69,70] in two companion papers derived governing equilibrium conditions for a thin-walled pipe subjected to general loading based on thin shell theory and found exact and finite element solutions and compared them with each others. Kiendla et al. [71] proposed an isogeometric formulation for rotation-free thin shell analysis of structures comprised of multiple patches and applied that to real wind turbine problems. Prabu et al. [72] performed a parametric study on buckling behavior of dented short carbon steel cylindrical thin shell subjected to uniform axial compression by non-linear static buckling analysis. The elastic modulus reduction method (EMRM) proposed by Yu and Yang [73] to calculate lower-bound limit loads of thin plate and shell structures. Challagulla et al [74] performed micromechanical analysis of grid-reinforced thin composite shells. Stress, deformation and stability conditions for thin doubly curved shallow bimetallic shells with taking to account large displacements under homogenous thermal field were done by Jakomina et al. [75]. Ghassemi et al. [76] employed a finite element model in order to analyze large displacements. Since, the finite-element implementation for this kind of problems suffers from membrane and shear locking, especially for very thin shells, the mid-surface of the shell is regarded as a Cosserat surface with one inextensible director to overcome these numerical problems. Other studies include those of Morozov [77], Guz' and Shnerenko [78], and Maksimyuk and Chernyshenko [79].

2.1.4. Nonlinear theories

The magnitude of transverse displacement compared to shell thickness is the third criterion used in classifying shell equations. In many cases, nonlinear terms in the fundamental shell equations are expanded using perturbation methods, and smaller orders of the rotations are retained. Most frequently, the first order only is retained and occasionally third orders have been included in nonlinear shell theories. In some shell problems, the material used can also be nonlinear (e.g., rubber, plastics and others). Theories that include nonlinear material constants are also referred to as nonlinear shell theories as well. The vast majority of shell theories, however, deal with geometric nonlinearity only.

Galishin and Shevchenko [80] determined the axisymmetric nonlinear thermoelastoplastic state of laminated orthotropic shells. Wang et al [81] studied the nonlinear dynamic response and buckling of laminated cylindrical shells with axial shallow grooves. Nonlinear finite element analyses were performed by Kundu et al [82], Naidu and Sinha [83] and Guo et al [84]. Patel et al [85, 86] investigated nonlinear thermo-elastic buckling characteristics of cross-ply laminated joined conical and cylindrical shells. Xu et al. [87] studied Nonlinear stability of double-deck reticulated circular shallow spherical shell based on the variational equation of the nonlinear bending theory. Panda and Singh [88] studied thermal buckling and post-buckling analysis of a laminated composite spherical shell panel embedded with shape memory alloy fibers using non-linear finite element methods. Sze and Zheng [89] studied a hybrid-stress solid element for geometrically nonlinear laminated shell analyses. Andrade et al [90] and Kima et al [91] performed geometrically nonlinear analysis of laminated composite plates

and shells using various shell elements. Huang [92] performed nonlinear buckling of composite shells of revolution. Ferreira et al [93] conducted a nonlinear finite element analysis of rubber composite shells. Material nonlinearity was discussed by Khoroshun et al [94,95].

Other nonlinear analyses include Chaudhuri [29], Khosravi et al [67], Han et al [37], Hsia [96], Wang et al [97], Moitaa et al [98], Jakomina et al. [75], Li and Lin [31], and Razzaq and El-Zafrany [99].

2.1.5. Shell geometries

Shells may have different geometries based mainly on their curvature characteristics. In most shell geometries, the fundamental equations have to be treated at a very basic level. The equations are affected by the choice of the coordinate system, the characteristics of the Lame parameters and curvature [1-4]. Equations for cylindrical, spherical, conical and barrel shells can be derived from the equations of the more general case of shells of revolution. Equations for cylindrical, barrel, twisted and shallow shells can also be derived from the general equations of doubly curved shells. Cylindrical shells, doubly curved shallow shells, spherical and conical shells are the most treated geometries in research.

Bespalova and Urusova [100] studied contact interaction between prestressed laminated shells of revolution and a flat foundation. Pinto Correia et al [101] investigated modeling and optimization of laminated adaptive shells of revolution. Vasilenko et al [102] described contact interaction between a laminated shell of revolution and a rigid or

elastic foundation. Khoroshun and Babich [103] discussed stability of laminated convex shells of revolution with micro-damages in laminate components. Vasilenko et al [104] analyzed stresses in laminated shells of revolution with an imperfect interlayer contact. Gureeva et al. [105] analyzed an arbitrary loaded shell of revolution based on the finite element method in a mixed formulation. Merzlyakov and Galishin [106] investigated thermoelastoplastic non-axisymmetric stress-strain analysis of laminated shells of revolution. Ye and Zhou [107] analyzed the bending of composite shallow shells of revolution. Stability of composite shells of revolution was picked up by Trach [108] and Khoroshun and Babich [109].

Shin et al [110] investigated thermal post-buckled behaviors of cylindrical composite shells with viscoelastic damping treatments. Bhaskar and Balasubramanyam [111] showed accurate analysis of end-loaded laminated orthotropic cylindrical shells. Merglyakov and Gatishin [112] performed analysis of the thermoelastoplastic non-axisymmetric laminated circular cylindrical shells. Weaver et al [113] investigated anisotropic effects in the compression buckling of laminated cylindrical shells. Huang and Lu [114], Shen and Xiang [115] studied buckling and postbuckling of cylindrical shells under combined compression and torsion. Diaconu et al [116] studied buckling characteristics and layup optimization of long laminated composite cylindrical shells subjected to combined loads. Fu and Yang [117] and Yang and Fu [118] described delamination growth for composite laminated cylindrical shells under external pressure. Shen [119] conducted a study on the hygrothermal effects on the postbuckling of laminated cylindrical shells. Wang and Dong [120] were interested in local buckling for triangular delaminations near the surface of laminated cylindrical shells under

hygrothermal effects. Goldfeld and Ejgenberg [121] were interested in linear bifurcation analysis of laminated cylindrical shells. Shen [122,123] and Shen and Li [124] analyzed postbuckling of axially-loaded laminated cylindrical shells with piezoelectric actuators. Panda and Ramachandra [125] studied postbuckling analysis of cross-ply laminated cylindrical shell panels under parabolic mechanical edge loading. Rahman and Jansen [126] presented a finite element formulation of Koiter's initial post-buckling theory using a multi-mode approach for coupled mode initial post-buckling analysis of a composite cylindrical shell.

Studies on buckling of cylindrical shells include Wangi and Xiao [127], Shen [128-130], Wang et al [131], Geier et al [132], Weaver et al [133], Wang and Dai [134], Zhu et al [135], Patel et al [136], Yang and Fu [137], Hilburger and Starnes [138], Semenyuk et al [139], Tafreshi [140], Solaimurugan and Velmurugan [141], Semenyuk and, Zhukova [142], Tafreshi [143], Weaver and Dickenson [144], Kere and Lyly [145], Vaziri [146], Semenyuk et al [147], Tafreshi [148,149], Babich and Semenyuk [150], Biagi and Medico [151], Sheinman and Jabareen [152], Prabu et al. [72], Li and Lin [31], and De Faria [153].

Wang et al [154] presented a method for interlaminar stress analysis in a laminated cylindrical shell. Lin and Jen [155] performed analysis of laminated anisotropic cylindrical shell by chebyshev collocation method. Lemanski and Weaver [156] were interested in optimization of a 4-layer laminated cylindrical shell. Gong and Ling-Feng [157] did experimental study and numerical calculation of stability and load-carrying capacity of cylindrical shell with initial dent. Khoroshun and Babich [158] investigated

29

stability of cylindrical shells with damageable components. Alibeigloo [159] performed a static analysis of an anisotropic laminated cylindrical shell with piezoelectric layers. Goldfeld [160] studied the influence of the stiffness coefficients on the imperfection sensitivity of laminated cylindrical shells. Zenkour and Fares [161] picked up the problem of thermal bending analysis of composite laminated cylindrical shells. Jinhua et al [162] performed variational analysis of delamination growth for composite laminated cylindrical shells under concentrated load. Meink et al [163] studied filament wound composite cylindrical shells. Solaimurugan and Velmurugan [164] researched progressive crushing of stitched glass-polyester composite cylindrical shells.

Other analyses include those of Sheng and Ye [18], Li and Shen [21, 25, 26], Shen [33, 34], Li [38], Zenkour [39], Shen and Li [41], Zen and Wanji [44], Chaudhuri et al [66], Sofiyev et al [68], Patel et al [85], Khoroshun et al [94,95], Wang et al [97], Zhu et al [135], Seif et al [165], Burgueño and Bhide [166], Belozerov and Kireev [167], Alibeigloo and Nouri. [27], Semenyuk and Trach [168], Paris and Costello [169] and Movsumov and Shamiev [170]. As can be seen from the above review, cylindrical shells received the most attention (as compared with other shell geometries.

Khare et al [45] presented closed-form thermo-mechanical solutions of cross-ply laminated shallow shells. Soldatos and Shu [65] discussed modeling of perfectly and weakly bonded laminated plates and shallow shells. Zang et al [171] were interested in nonlinear dynamic buckling of laminated shallow spherical shells. Kioua and Mirza [172] investigated piezoelectric induced bending and twisting of laminated shallow shells. Niemi [173] developed a four-node bilinear shell element of arbitrary quadrilateral shape

and applied that to find the solution of static and vibration problems of shallow shells. Zarivnyak [174] researched the probability of the critical state of glue joints of a shallow laminated shell. Other studies on shallow shells include those of Grigorenko et al [175] Matsunaga [50], Wang et al [81], Ye and Zhou [107], Jakomina et al. [75], Xu et al. [87], Gupta [176], and Zhu et al [135].

Conical shells are other special cases of shells of revolution. For these shells, a straight line revolves about an axis to generate the surface. Wu et al [177] discussed a refined asymptotic theory of laminated circular conical shells. Das and Chakravorty [178] suggested selection guidelines of point-supported composite conoidal shell roofs based on a finite element analysis. Mahdi et al [179] investigated the effect of material and geometry on crushing behavior of laminated conical shells. Goldfeld [180] studied the imperfection sensitivity of laminated conical shells. Goldfeld et al [181] performed a multi-fidelity optimization of laminated conical shells for buckling. Mahdi et al [182] were interested in the effect of residual stresses in a filament wound laminated conical shell. Singh and Babu [183] studied thermal buckling of laminated piezoelectric conical shells. Wu and Chiu [184] picked up the problem of thermoelastic buckling of laminated conical shells. Rezadoust et al [185] investigated the crush behavior of conical composite shells. Goldfeld et al [186] presented design and optimization of laminated conical shells for buckling. Kosonen [187] described specification for mechanical analysis of conical composite shells. Other studies on conical include Patel et al [85, 188-189], and Pinto Correia [49].

Spherical shells are other special cases of shells of revolution. For these shells, a circular arc, rather than a straight line, revolves about an axis to generate the surface. If the circular arc is half a circle and the axis of rotation is the circle's own diameter, a closed sphere will result. Smithmaitrie and Tzou [190] discussed actions of actuator patches laminated on hemispherical shells. Marchuk and Khomyak [191] presented refined mixed finite element solutions of laminated spherical shells. He and Hwang [192] investigated identifying damage in spherical laminated shells. Kadoli and Ganesan [193] Analyzed thermoelastic buckling of composite hemispherical shells with a cut-out at the apex. Saleh et al [194] described crushing behavior of composite hemispherical shells subjected to axial compressive load. Other studied on spherical shells include those of Zang et al [171], Wu and Lo [19], Xu et al. [87], Panda and Singh [88], and others.

Tzou et al [195] studied sensitivity of actuator patches laminated on toroidal shells. Mitkevich and Kul'kov [196] investigated design optimization and forming methods for toroidal composite shells.

Sai et al [197,198] investigated shells with and without cut-outs. Other studies include Latifa and Sinha [199].

2.2.   Types of analyses

Analyses can be dynamic in nature. These include free and transient vibrations, wave propagation, dynamic stability, shock and impact loadings and others. These were covered in another review article [3]. The types of analyses that this work focuses on are static, buckling, post buckling, thermal and hygrothermal, and failure and damage.

2.2.1. Static analysis

Pinto Correiaa et al [200] described a finite element semi-analytical model for laminated axisymmetric shells under static and other loads. Prusty [201] performed linear static analysis of composite hat-stiffened laminated shells using finite elements. Park et al [202] analyzed laminated composite plates and shells using a shell element. Alijani et al [203] studied application of the extended Kantorovich method to the bending of clamped cylindrical panels. Santos et al [23] presented a finite element bending analysis of 3D axisymmetric laminated piezoelectric shells. Babeshko and Shevchenko [204-206], Babeshko [207] and Shevchenko and Babeshko [208,209] discussed elastoplastic laminated shells made of isotropic, transversely isotropic and laminated materials. Maslov et al [210] presented a method of stressed state analysis of thick-walled composite shells.

Other static analyses include Yuan et al [54], Maksimyuk and Chernyshenko [79], Razzaq and El-Zafrany [99], Vasilenko et al [104], Ye and Zhou [107], Tafreshi [140], Wang et al [154], Alibeigloo [159], Zenkour and Fares [161], Seif et al [165], Semenyuk and Trach [168], Paris and Costello [169], Kioua and Mirza [172], Grigorenko et al [175], Mahdi et al [182], Marchuk and Khomyak [191], Saleh et al [194], Alibeigloo and Nouri [27], and Sai et al [197,198].

2.2.2. Buckling analysis

Lee and Lee [211] discussed a numerical analysis of the buckling and postbuckling behavior of laminated composite shells. Sai-Ram et al [212] studied buckling of laminated composite shells under transverse load. Fan et al [213] investigated creep buckling of viscoelastic laminated plates and circular cylindrical shells. Li et al [214] performed buckling analysis of rotationally periodic laminated composite shells by finite elements. Sofiyev [215] conducted torsional buckling analysis of cross-ply laminated orthotropic composite cylindrical shells. Patel et al [216] were interested in thermo-elastic buckling of angle-ply laminated elliptical cylindrical shells. Hilburger and Starnes [217] studied the effects of imperfections of the buckling response of composite shells. Rickards et al [218] analyzed buckling of composite stiffened shells.

Studies on buckling of cylindrical shells include Wangi and Xiao [127], Shen [128-130], Wang et al [131], Geier et al [132], Weaver et al [133], Wang and Dai [134], Zhu et al [135], Patel et al [136], Yang and Fu [137], Hilburger and Starnes [138], Semenyuk [139], Tafreshi [140], Solaimurugan and Velmurugan [141], Semenyuk and, Zhukova [142], Tafreshi [143], Weaver and Dickenson [144], Kere and Lyly [145], Vaziri [146], Semenyuk et al [147], Tafreshi [148,149], Babich and Semenyuk [150], Biagi and Medico [151], Sheinman and Jabareen [152], Prabu et al. [72], Li and Lin [31], and De Faria [153].

Other buckling analyses include Matsunaga [50], Shen [64], Sofiyev et al. [68], Wang et al [81], Huang [92], Wang et al [97], Weaver et al. [113], Huang and Lu [114], Shen and Xiang [115], Diaconu et al [116], Wang and Dong [120], Hilburger and

Starnes [138], Semenyuk et al [139], Tafreshi [140], Zang et al [171], Goldfeld et al [181, 186], Singh and Babu [183], Wu and Chiu [184], Kadoli and Ganesan [193], and Pinto Correiaa [200].

2.2.3. Postbuckling analysis

Shin et al [110] discussed thermal postbuckled behavior of cylindrical composite shells. Shen [219,220] discussed the same problem with piezoelectric actuators and thermal-dependant properties. Kim et al [221] presented an 8-node shell element for postbuckling analysis of laminated composite plates and shells. Kundu and Sinha [222] analyzed postbuckling of laminated shells. Kundu et al [223] performed postbuckling analysis of smart laminated doubly curved shells. Xie and Biggers [224] conducted postbuckling analysis with progressive damage modeling in tailored laminated plates and shells with a cutout. Merazzi et al. [225] employed implicit finite element methods to analyze postbuckling behavior of shell-wised tools.

Other studied on postbuckling analysis include Shen [33, 34, 40, 64, 119, 122, 123 128-130], Li and Shen [21, 25, 26], Li [38], Shen and Xiang [115], Shen and Li [41, 124], Tafreshi [140, 143, 144], Semenyuk and Zhukova [142], Kere and Lyly [145], Sheinman and Jabareen [152], Patel et al [188, 189], Lee and Lee [211], Rahman and Jansen [126], Li and Lin [31], Panda and Singh [85], Panda and Ramachandra [125], and Sai-Ram et al [212].

2.2.4. Thermal and hygrothermal loading

Galishin [226] and Babeshko and Shevchenko [227, 205] performed analysis of the axisymmetric thermoelastoplastic state of laminated transversally isotropic shells. Swamy and Sinha [228] investigated nonlinear analysis of laminated composite shells in hygrothermal environments. Babeshko [204] and Babeshko and Shevchenko [229] were interested in thermoelastoplastic state of flexible laminated shells under axisymmetric loading. Cheng and Batra [230] showed thermal effects on laminated composite shells containing interfacial imperfections. Kewei [231] conducted weak Formulation Study for thermoelastic analysis of thick open laminated shell. Ghosh [232] studied hygrothermal effects on the initiation and propagation of damage in composite shells. Saha and Kalamkarov [233] presented a micromechanical thermoelastic model for sandwich composite shells. El-Damatty et al [234] performed thermal analysis of composite chimneys using finite shell elements. Roy et al. [235] developed an improved shell element for smart fiber reinforced composite structures under coupled piezothermoelastic loading. Also, Kulikov and Plotinkova [236] constructed a seven parameter geometrically exact shell element to study coupled problem of thermopiezoelectricity in laminated plates and shells.

Studies that treated thermal and/or hygrothermal effects include those of Li and shen [21, 25, 26], Li [38], Shen [36, 37, 58, 103], Khare et al [45], Matsunaga [50], Oh and Cho [51], Galishin and Shevchenko [80], Kundu et al [82], Naidu and Sinha [83], Wang et al [91, 131], Merzlyakov and Galishin [106], Shin [110], Wang and Dong [120], Patel et al [136, 188, 189, 216], Shevchenko and Babeshko [209], Babeshko [208], Zenkour and Fares [161], Wang and Dai [134], Zhu et al [135], Singh and Babu [183],

36

Wu and Chiu [184], Kadoli and Ganesan [193],Panda and Singh [88], and in addition to articles that can be found on the dynamic problems in the review by Qatu [3].

2.2.5. Failure, delamination and damage analyses

Zhang et al [237] studied progressive failure analysis for advanced grid stiffened composite plates/shells. Ikonomopoulos and Perreux [238] investigated reliability of laminates through a damage tolerance approach. Khoroshun and Babich [239] discussed stability of plates and shells made of homogeneous and composite materials subject to short-term microdamage. Zozulya [240] studied laminated shells with debonding between laminas in temperature field. Larsson [241] discussed discontinuous shell-interface element for delamination analysis of laminated composite structures. Mahdi et al [242] performed an experimental investigation into crushing behavior of filament-wound laminated cone-cone intersection composite shell. Huang and Lee [243] investigated the static contact crushing of composite laminated shells. Wagner and Balzani [244] performed simulation of delamination in stringer stiffened fiber-reinforced composite shells.

Other studies on failure of composite shells include those of Galishin [226], Xie and Biggers [224], He and Hwang [192], Khoroshun et al [94, 95], Khoroshun and Babich [103, 109, 158, 239], Mahdi et al [179], Rezadoust [185], Saleh et al [194], Solaimurugan and Velmurugan [164], and Ghosh [232].

37

2.2.6. Other Analyses

Morozov [245] conducted a theoretical and experimental analysis of filament wound composite shells under compressive loading. Hossain et al [246], Kim et al [247] and Szea et al [248] presented a finite element formulation for the analysis of laminated composite shells. Wu and Burguen [249] studied an integrated approach to shape and laminate stacking sequence optimization of composite shells. Balah and Al-Ghamedy [250] discussed finite element formulation of a third order laminated finite rotation shell element. Trach et al [251] investigated stability of laminated shells made of materials with one plane of elastic symmetry. Kabir et al [252] presented a triangular element for arbitrarily laminated general shells. Kalamkarov et al [253] delivered an asymptotic model of flexible composite shells of a regular structure. Haussya and Ganghoffer [254] investigated modeling of curved interfaces in composite shells. Roque and Ferreira [255] described new developments in the radial basis functions analysis of shells.

2.3. Material complexity

Material complexity in composites occurs in various ways. Composite shells can have active or piezoelectric layers. They can also be braided or made of wood or natural fibers or a combination of materials.

2.3.1. Piezoelectric shells

Ren and Parvizi-Majidi [256] presented a model for shape control of cross-ply laminated shells using a piezoelectric actuator. Bhattacharya et al [257] and Zallo and

Gaudenzi [258] presented finite element models for laminated shells with actuation capability. Pinto Correia et al [259] conducted an analysis of adaptive shell structures using a refined laminated model. Bhattacharya et al [260] investigated smart laminated shells and deflection control strategy. Xue [261] studied effective dielectric constant of composite shells.

Other studies on piezoelectric shells include Santos et al [22], Kioua and Mirza [172], Shen [115, 119, 122], Alibeigloo [159], Alibeigloo and Nouri [27], Kulikov and Plotnikova [236], Singh and Babu [183], as well as others that dealt with dynamic response [3].

2.3.2. Other materials

Picha et al [262] studied composite polymeric shells. Yan et al [263] investigated post-tensioned composite shells for concrete confinement. Lopez-Anido et al [264] studied repair of wood piles using prefabricated polymer composite shells. Burgueño and Bhide [166] discussed shear response of concrete-filled composite cylindrical shells. Other studies on concrete shells include Ferreira [43].

2.4. Structural complexity

Structural complexity occurs when the geometry or boundary conditions of the shells deviate from the classical shells described earlier. These include stiffened shells, shells with internal boundaries from cracks, imperfect shells as well as other types of complexities.

2.4.1. Stiffened shells

Janunky and Ambur [265] demonstrated a design optimization process while investigating the local buckling behavior of stiffened structures with variable curvature. Optimum design of stiffened cylindrical shells with added T-rings subjected to external pressure was also performed by Bushnell [266]. The reliability of a postbuckled composite isogrid stiffened shell structure subjected to a compression load was studied by Kim [267]. Zeng and Wu [268] performed a post-buckling analysis of stiffened braided cylindrical shells subjected to combined external pressure and axial compression loads. For the same combined loading, Poorveis and Kabir [269] analyzed the static buckling of orthotropic stringer stiffened composite cyclindrical shells. The postbuckling behavior of stringer stiffened panels by using strip elements was determined by Mocker and Reimerdes [270]. Bisagni and Cordisco [271,272] tested stiffened carbon composite stringer-stiffened shells in the postbuckling range until failure. Rao [273] and Rickards et al [218] used finite elements for buckling and vibration analysis of laminated composite stiffened shells. Prusty [201] used the finite element method to perform a linear static analysis of composite hat-stiffened laminated shells. Bai et al [274] performed a numerical analysis using a finite element method to investigate the buckling behavior of an advanced grid stiffened structure. Kidane et al [275] developed an analytical model to study the global buckling load of grid stiffened composite cylinders. De Vries [276] used a hierarchical method to analyze localized buckling of thin-walled stiffened or unstiffened metallic and composite shells. Accardo et al [277] discuss the design of a combined loads test machine and test fixture to perform experimental investigations on

curved reinforced metallic and composite stiffened panels. Linde et al [278] discussed the development of a virtual test platform used for parametric modeling and simulation of stiffened test shells to study the static behavior in the buckling and postbuckling range. Park et al [202] and Patel et al [279] used shell elements to perform both linear and dynamic analysis of laminated stiffened composite shells. An optimization design procedure based on surrogate modeling of stiffened composite shells was presented by Rikards et al [280]. Using the finite element method, Wong and Teng [281] investigated the buckling behavior of axisymmetric stiffened composite shell structures and Apicella et al [282] studied the behavior of a stiffened bulkhead subjected to ultimate pressure load. Chen and Guedes Soares [283] modeled ship hulls as stiffened composite panels to perform a strength analysis under sagging moments. Rais-Rohani and Lokits [284] conducted an optimization study to study reinforcement layout and sizing parameters of composite submarine sail structures. Wu et al [285] conducted an experimental investigation to study the behavior of grid stiffened steel-concrete composite panels under a buckling load. Chen et al [286] used a nonlinear finite element method to study the thermal mechanical behavior of advanced composite grid stiffened shells with multi-delaminations. The finite element method was used by Chen and Xu [287] and by Prusty [288] to study the buckling and postbuckling response of doubly curved stiffened composite panels under general loading. Sahoo and Chakravorty [289] used finite elements to solve a bending problem of a composite stiffened hypar shell subjected to a concentrated load. Zhang et al [290] and Lu et al [291] performed a stability analysis of advanced composite grid stiffened shells. A buckling load analysis of composite grid stiffened structures was investigated by the finite element method by He et al [292].

41

Progressive failure analysis of composite laminated stiffened plates using a finite strip method for non-linear static analysis was performed by Zahari and El-Zafrany [293].

Studies on stiffened composite shells include Prusty [201], Goldfeld [160], Zhang et al [237], Wagner and Balzani [244], and others on dynamic analysis [3].

2.4.2. Shells with cutouts

Several recent studies have focused on various composite shell structures with cutouts. Hillburger and Starnes [138] and Hillburger [294] performed numerical and experimental studies to determine the effects of unreinforced and reinforced cutouts in composite cylindrical shells subjected to compression loading. Li et al [295] performed a three-dimensional finite element analysis to study the buckling response of sandwich composite shells with cutouts under axial compression. The principle of minimum potential energy was used by Madenci and Barut [296] to investigate the effects of an elliptical cutout in a composite cylindrical shell subjected to compression. Nanda and Bandyopadhyay [297] looked at the nonlinear transient responses from static and dynamic analyses of composite cylindrical and spherical shell laminates with cutouts. The finite element method was used to study the bending behavior of laminated composite shells without a cutout [197] and with a central circular cutout [198]. Buckling and post-buckling due to internal pressure and compression loading of composite shells with various size cutouts was investigated through the finite element method by Tafreshi [143]. Xie and Biggers [224] performed analysis on tailored laminated plates and shells with a central cutout subjected to compressive buckling loads. Other studies include Kadoli and Ganesan [193] and Hilburger and Starnes [138].

42

2.4.3. Imperfect shells

Starnes and Hilburger [298] conducted an experimental and analytical study to investigate the effects of initial imperfections on the buckling response of graphite-epoxy cylindrical shells. Arbocz and Hillburger [299] used a probability-based analysis to investigate section properties such as geometric imperfections to determine more accurate buckling-load "knockdown factors". Biagi and Perugini [300] investigated the buckling behavior of the front composite skirt using linear and nonlinear finite element analysis to study the relationship between various shapes of geometrical imperfections and amplitudes and failure modes. Bisagni [301] studied the buckling and post-buckling characteristics of carbon composite cylindrical shells with geometric imperfections under axial compression using eigenvalue analysis. Carvelli et al [302,303] performed a non-linear buckling analysis to study the geometric imperfections of composite shells in an underwater sea environment. Hilburger and Starnes [304,305] investigated the effects of imperfections such as shell-wall thickness variations, imperfections due to composite fabrication, shell-end geometric imperfections, and nonuniformly applied end-loads, on the buckling and post-buckling response of un-stiffened thin-walled graphite-epoxy cylindrical shells. Jayachandran et al [306] also investigated the postbuckling behavior of imperfect thin shells by using secant matrices with the finite element method to study postbuckling behavior of thin composite shells with initial imperfections. Kere and Lyly [145] considered geometric shape imperfections and demonstrated that the best numerical-experimental correlation was achieved with diamond shape imperfections. Rahman and Jansen [126] investigated imperfection sensitivity of composite cylindrical

shells under axial compression using a finite element method. Tafreshi and Bailey [308] investigated the effects of combined loading on imperfect composite shell structures. Wardle and Lagace [308] compared experimental and numerical computations of the buckling response from transversely loaded composite shell structures. Other studies on imperfect shells include Goldfeld [160, 180], Vasilenko [102], Cheng and Batra [230], Shen and Li [41], Wang and Zhong [20], and Hilburger and Starnes [217].

Vasilenko [87] studied contact interaction between a laminated shell of revolution and a rigid or elastic foundation. Other studies include Abouhamze et al [309].

2.5.   Conclusions

It is interesting to see that despite advances made in computational power, researchers avoided in general usage of 3D theory of elasticity. Experience shows that extensive usage of 3D elements in practical problems is not feasible even with advanced computers. Researchers looked for, developed and used thick shell theories to solve engineering problems. Finite element is the most used method in the analysis. Its ability to treat general boundary conditions, loading and geometry have certainly attributed to its popularity.

Cylindrical shells are still the subject of research of most recent articles. Doubly curved shallow shells have also received considerable interest. These shells can be spherical, barrel, cylindrical, or other shape.

Complicating effects of various kinds have received considerable interest. The use of piezoelectric shells necessitated by various applications and certain advanced materials resulted in considerable literature in the field. Other complicating effect of stiffened shells received some attention.

Looking at recent innovations in the area of composite plates, authors think that it is a matter of time before these composites start making strong presence in research on shells. Areas of innovation include the use of natural fiber, single-walled and multi-walled carbon nano tubes, varying fiber orientation (both short and long fibers) as we as others. Such innovation are becoming more necessary as composite materials are required to deliver simultaneously structural functions (strength, stiffness, damping, toughness, …) and non-structural ones (thermal and electrical conductivity). Both modeling and testing of such composites can be a corner-stone of future research on composite shells.

2.6. References

1. Qatu, MS. Recent research advances in the dynamic behavior of shells. part 1: laminated composite shells. Appl Mech Rev 2002; 55: 325-350.

2. Qatu, MS, Sullivan RW, Wang W. Recent research advances in the dynamic behavior of composite shells: 2000-2009. Compos Struct 2010; 93:14-31.

3. Qatu, MS. Accurate theory for laminated composite deep thick shells. Int J Solids and Struct 1999; 36: 2917-2941.

4. Kapania, PK. Review on the analysis of laminated shells. J Press Vessel Tech 1989;111: 88-96.

5. Noor AK, and Burton WS. Assessment of computational models for multilayered composite shells. Appl Mech Rev 1990; 43: 67-97.

6. Noor AK, and Burton WS, Computational models for high-temperature multilayered composite plates and shells. Appl Mech Rev 1992; 45:419-446.

7. Noor AK, Burton WS and Peters JM. Assessment of computational models for multilayered composite cylinders. Int J Solids Struct 1991;27: 1269-1286.

8. Soldatos KP. Mechanics of cylindrical shells with non-circular cross-section. Appl Mech Rev, 1999; 52: 237-274

9. Noor AK, Burton WS and Bert CW. Computational models for sandwich panels and shells. Appl Mech Rev 1996; 49: 155-200.

10. Noor AK, and Venneri SL. High-performance computing for flight vehicles. Comput Syst Eng 1992;3: 1-4.

11. Carrera, E. Historical review of Zig-Zag theories for multilayered plates and shells. Appl. Mech. Rev., 2003; 56:287-309.

12. Carrera, E. Theories and finite elements for multilayered, anisotropic, composite plates and shells. J Arch Comput Meth Eng 2002; 9:87-140.

13. Reddy, JN. Mechanics of laminated composite plates and shells: theory and analysis. Second Edition, CRC press, 2003.

14. Ye. J. Laminated composite plates and shells: 3D modeling. Springer, 2003.

15. Lee, CY. Geometrically correct laminated composite shell modeling, VDM Verlag, 2008.

16. Shen, HS. Functionally graded materials: nonlinear analysis of plates and shells.

CRC Press, 2009.

17. Sheng HY, Ye JQ. A three-dimensional state space finite element solution for laminated composite cylindrical shells. Comput Meth Appl. Mech. Engrg. 2003;192:2441-2459.

18. Wu CP, Lo JY. Three-dimensional elasticity solutions of laminated annular spherical shells. J Engineering Mechanics 2000;882-885.

19. Wang X, Zhong Z. Three-dimensional solution of smart laminated anisotropic circular cylindrical shells with imperfect bonding. Int J Solids and Struct 2003;40:5901–5921.

20. Li ZM, Shen HS. Postbuckling analysis of three-dimensional textile composite cylindrical shells under axial compression in thermal environments. Compos Science Tech 2008; 68:872–879.

21. Santos H, Mota Soares CM, Mota Soares CA, Reddy JN. A finite element model for the analysis of 3D axisymmetric laminated shells with piezoelectric sensors and actuators. Compos Struct 2006;75:170-178.

22. Santos H, Mota Soares CM, Mota Soares CA, Reddy JN. A finite element model for the analysis of 3D axisymmetric laminated shells with piezoelectric sensors and actuators: bending and free vibrations. Comput Struct 2008;86:940-947.

23. Sprenger W, Gruttmann F, Wagner W. Delamination growth analysis in laminated structures with continuum-based 3D-shell elements and a viscoplastic softening model. Comput Meth Appl Mech Engrg. 2000:185;123-139.

24. Li ZM, Shen HS. Postbuckling analysis of 3D braided composite cylindrical shells under torsion in thermal environments. Compos Struct 2009;87:242–256.

25. Li ZM, Shen HS. Postbuckling of 3D braided composite cylindrical shells under combined external pressure and axial compression in thermal environments. Int J Mech Sci 2008;50:719–731.

26. Alibeigloo A, Nouri V. Static analysis of functionally graded cylindrical shell with piezoelectric layers using differential quadrature method. Comp Struc 2010; 92 (8): 1775-1785.

27. Fagiano C, Abdalla MM, Gürdal Z. Interlaminar stress recovery of multilayer composite shell structures for three-dimensional finite elements. Finite Elem Anal Design 2010; 46 (12): 1122-1130.

28. Chaudhuri RA. A nonlinear zigzag theory for finite element analysis of highly shear-deformable laminated anisotropic shells. Compos Struct 2008;85:350-359.

29. Krejaa I, Schmidt R. Large rotations in first-order shear deformation FE analysis of laminated shells. Int J Non-Linear Mechanics 2006:41;101–123.

30. Li Z-M, Lin Z-Q. Non-linear buckling and postbuckling of shear deformable anisotropic laminated cylindrical shell subjected to varying external pressure loads. Comps Struct 2010; 92 (2): 553-567.

31. Sorić J, Jarak T. Mixed meshless formulation for analysis of shell-like structures. . Computer Meth Appl Mech Eng 2010; 199: 1153-1164.

32. Shen HS. Postbuckling of shear deformable cross-ply laminated cylindrical shells under combined external pressure and axial compression. Int J Mech Sci 2001:43;2493-2523.

33. Shen HS. Postbuckling of shear deformable laminated cylindrical shells. J Engineering Mechanics 2002:128;296-307.

34. Piskonov VG, Verijenko VE, Adali S, Tabakov PY, Prisyazknyouk VK, Buryhin SJ. Rational transverse shear deformation higher order theory of anisotropic laminated plates and shells. Int J Solids and Struct 2001:38;6491-6523.

35. Iozzi R, Gaudenzi P. Effective shear deformable shell elements for adaptive laminated structures. J Intelligent Material Systems and Struct 2001:12;415-421.

36. Han SC, Tabiei A, Park WT. Geometrically nonlinear analysis of laminated composite thin shells using a modified first-order shear deformable element-based Lagrangian shell element. Compos Struct 2008:82;465–474.

37. Li ZM. Postbuckling of a shear-deformable anisotropic laminated cylindrical shell under external pressure in thermal environments. Mech Comp Mat 2007:43;535-560.

38. Zenkour AM. Stress analysis of axisymmetric shear deformable cross-ply laminated circular cylindrical shells. J Eng Math 2001;40: 315–332.

39. Shen HS. The effects of hygrothermal conditions on the postbuckling of shear deformable laminated cylindrical shells. Int J Solids Struct 2001;38:6357-6380.

40. Shen HS, Li QS. Thermomechanical postbuckling of shear deformable laminated cylindrical shells with local geometric imperfections. Int J Solids Struct 2002;39:4525–4542.

41. Balah M, Al-Ghamedy HN. Third order shear deformation model for laminated shells with finite rotations- Formulation and consistent linearization. Acta Mech Sinica 2004;20:484-498.

42. Ferreira AJM. On the shear-deformation theories for the analysis of concrete shells

reinforced with external composite laminates. Strength Mat 2003;35:128-135.

43. Zhen W, Wanji C. A global-local higher order theory for multilayered shells and the analysis of laminated cylindrical shell panels. Compos Struct 2008;84:350–361.

44. Khare RK, Kant T, Garg AK. Closed-form thermo-mechanical solutions of higher-order theories of cross-ply laminated shallow shells. Compos Struct 2003:59;313-340.

45. Khare RK, Rode V. Higher-order closed-form solutions for thick laminated sandwich shells. J Sandwich Struct Mat 2005:7;335-358.

46. Ferreira AMA, Roque CMC, Jorge RMN. Modeling cross-ply laminated elastic shells by a higher-order theory and multiquadrics. Comput Struct 2006:84;1288-1299.

47. Alijani F, Aghdam MM. A semi-analytical solution for stress analysis of moderately thick laminated cylindrical panels with various boundary conditions, Compos Struct 2009;89: 543–550.

48. Pinto Correia IF, Mota Soares CM, Mota Soares CA, J. Herskovits J. Analysis of laminated conical shell structures using higher order models. Compos Struct 2003:62;383–390.

49. Matsunaga H. Thermal buckling of cross-ply laminated composite shallow shells according to a global higher-order deformation theory. Compos Struct 2007;81:210–221.

50. Oh J, Cho M. Higher order zig-zag theory for smart composite shells under mechanical-thermo-electric loading. Int J Solids Struct 2007;44:100–127.

51. Yaghoubshahi M, Asadi E, Fariborz SJ. A higher-order shell model applied to shells with mixed boundary conditions. J Mech Eng Sci 2011;225 (2): 292-303.

52. Benson DJ, Bazilevsa Y, Hsua MC, Hughes TJR. Isogeometric shell analysis: The Reissner–Mindlin shell. Computer Meth Appl Mech Eng 2010; 199: 276-289.

53. Yuan YZ, Saleeb AF, Gendy AS. Stress projection, layerwise-equivalent, formulation for accurate predictions of transverse stresses in laminated plates and shells. Int J Comput Eng Sci 2000;1:91-138.

54. Kim D, Chaudhuri RA. Effect of lamination sequence on the localization and shear crippling instability in thick imperfect cross-ply rings under external pressure. Compos Struct 2007;80:504.

55. Kim D, Chaudhuri RA. Effect of thickness on buckling of perfect cross-ply rings under external pressure. Compos Struct 2007; 81:525.

56. Chaudhuri RA, Kim D. Sensitivity of the post-localization response of a thick cross-ply imperfect ring to transverse Young's modulus nonlinearity. Compos Struct 2008;84:44.

57. Leigh T, Tafreshi A. Delamination buckling of composite cylindrical panels under axial compressive load. ASME 7th Biennial Conference on Eng Sys Des Anal Paper no. ESDA2004-58578 pp. 387-396 (2004)

58. Malekzadeh P. A two-dimensional layerwise-differential quadrature static analysis of thick laminated composite circular arches. Appl Math Model 2009;33:1850.

59. Roh J-H, Han J-H, Lee I. Effects of shape memory alloys on structural modification. Jeju Island, Korea. Trans Tech Publ 2004;270-273:2120.

60. Roh J-H, Oh I-K, Yang S-M, Han J-H, Lee I. Thermal post-buckling analysis of shape memory alloy hybrid composite shell panels. Smart Mat Struct 2004;13:1337.

61. Shin W-H, Oh I-K, Lee I. Nonlinear flutter of aerothermally buckled composite shells with damping treatments. J Sound Vib 2009;324:556.

62. Tahani M. Analysis of laminated composite beams using layerwise displacement theories. Compos Struct 2007;79:535.

63. Shen HS. Buckling and postbuckling of laminated thin cylindrical shells under hygrothermal environments. Appl Math Mech 2001;22:270-281.

64. Soldatos KP, Shu X. Modeling of perfectly and weakly bonded laminated plates and shallow shells. Compos Sci Tech 2001:61;247-260.

65. Chaudhuri RA, Balaraman K, Kunukkasseril VX. Admissible boundary conditions and solutions to internally pressurized thin arbitrarily laminated cylindrical shell boundary-value problems. Compos Struct 2008:86;385–400.

66. Khosravi P, Ganesan R, Sedaghati R. An efficient facet shell element for corotational nonlinear analysis of thin and moderately thick laminated Compos Structures. Comput Struct 2008:86;850–858.

67. Sofiyev AH, Zerin Z, Turkmen M. The buckling of laminated cylindrical thin shells under torsion varying as a linear function of time. Turkish J Eng and Env Sci 2003;27:237-245.

68. Weicker K, Salahifar R, Mohareb M. Shell analysis of thin-walled pipes. Part I – Field equations and solution. Int J Press Vessels Pip 2010; 87 (7): 402-413.

69. Weicker K, Salahifar R, Mohareb M. Shell analysis of thin-walled pipes. Part I – Finite element formulation. Int J Press Vessels Pip 2010; 87 (7): 414-423.

70. Kiendla J, Bazilevsb Y, Hsub M-C, Wüchnera R, Bletzingera K-U. The bending strip method for isogeometric analysis of Kirchhoff–Love shell structures comprised of multiple patches. Computer Meth Appl Mech Eng 2010; 199: 2403-2416

71. Prabu B, Raviprakash AV, Venkatraman A. Parametric study on buckling behaviour of dented short carbon steel cylindrical shell subjected to uniform axial compression. Thin-walled Struct 2010; 48 (8): 639-649.

72. Yu B, Yang L. Elastic modulus reduction method for limit analysis of thin plate and shell structures. Thin-walled Struc 2010; 48: 291-298

73. Challagulla KS, Georgiades AV, Saha GC, Kalamkarov AL. Micromechanical analysis of grid-reinforced thin composite generally orthotropic shells. Composites: Part B 2008;39:627–644.

74. Jakomina M, Koselb F, Kosel T. Thin double curved shallow bimetallic shell of translation in a homogenous temperature field by non-linear theory. Thin-Walled Struct 2010; 48 (3): 243-259.

75. Ghassemi A, Shahidi A, Farzin M. A new element for analyzing large deformation of thin Naghdi shell model. Part 1: Elastic. Appl Math Mod 2010; 34 (12): 4267-4277.

76. Morozov EV. The effect of filament- winding mosaic patterns on the strength of thin-walled composite shells. Compos Struct 2006;76:123–129.

77. Guz' AN, Shnerenko KI. Solution of two-dimensional boundary-value problems of the theory of thin composite shells. Mech Compos Mat 2000;36:273-276.

78. Maksimyuk VA, Chernyshenko IS. Numerical analysis of the efficiency of using theories of thin and thick composite shells in stress concentration problems. J Math Sci 2001;103: 320-324.

79. Galishin AZ, Shevchenko YN. Determining the axisymmetric, geometrically nonlinear, thermoelastoplastic state of laminated orthotropic shells. Int Appl Mech 2003;39;56-63.

80. Wang TL, Tang WN, Zhang SK. Nonlinear dynamic response and buckling of laminated cylindrical shells with axial shallow groove based on a semi-analytical method. J Shanghai Univ (English Edition) 2007:11; 223-228.

81. Kundu CK, Maiti DK, Sinha PK. Nonlinear finite element analysis of laminated composite doubly curved shells in hygrothermal environment. J Reinf Plastics Compos 2007:26;1461-1478.

82. Naidu NVS, Sinha PK. Nonlinear finite element analysis of laminated composite

shells in hygrothermal environments. Compos Struct 2005:69;387-395.

83. Guo X, Lee YY, Mei C. Non-linear random response of laminated composite shallow shells using finite element modal method. Int J Numer. Meth. Eng 2006:67;1467-1489.

84. Patel BP, Nath Y, Shukla KK. Nonlinear thermo-elastic buckling characteristics of cross-ply laminated joined conical–cylindrical shells. Int J Solids Struct 2006:43;4810-4829.

85. Patel BP, Shuklab KK, Nath Y. Nonlinear thermoelastic stability characteristics of cross-ply laminated oval cylindrical/conical shells. Finite Elem Anal Des 2006:42;1061-1070.

86. Xu J-C, Li Y, Wang F, Liu R-H. Nonlinear stability of double-deck reticulated circular shallow spherical shell. Appl Math Mech 2010; 31 (3): 279-290.

87. Panda SK, Singh BN. Thermal post-buckling analysis of a laminated composite spherical shell panel embedded with shape memory alloy fibers using non-linear finite element methods. J Mech Eng Sci 2010; 224 (4): 757-769.

88. Sze KY, Zheng SJ. A stabilized hybrid-stress solid element for geometrically nonlinear homogeneous and laminated shell analyses. Comput. Methods Appl. Mech. Eng 2002:191;1945–1966.

89. Andrade LG, Awruch AM, Morsch IB. Geometrically nonlinear analysis of laminate composite plates and shells using the eight-node hexahedral element with one-point integration. Compos Struct 2007:79 ;571–580.

90. Kima KD, Hanb SC, Suthasupradit S. Geometrically non-linear analysis of laminated Compos Structures using a 4-node co-rotational shell element with enhanced strains. Int J Non-Linear Mech 2007:42;864 – 881.

91. Huang J. Nonlinear buckling of composite shells of revolution. J Aero Eng 2002;15:64-71.

92. Ferreira AJM, Sá JMAC, Marques AT. Nonlinear finite element analysis of rubber composite shells. Strength Mat 2003;35:225-235.

93. Khoroshun LP, Babich DV, Shikula EN. Stability of cylindrical shells made of a particulate composite with nonlinear elastic inclusions and damageable matrix. Int Appl Mech 2007;43:1123-1131.

94. Khoroshun LP, Babich DV, Shikula EN. Stability of cylindrical shells made of a particulate composite with nonlinear elastic matrix and damaged inclusions. Int Appl Mech 2007;43:893-902.

95. Hsia, LR. Nonlinear response of thick laminated shells with inter-laminar deformation, PhD Thesis, Univ Utah, 2006, pp. 88.

96. Wang X, Lub G, Xiao DG. Non-linear thermal buckling for local delamination near the surface of laminated cylindrical shell. Int J Mech Sci 2002:44;947–965.

97. Moitaa JS, Infante Barbosab J, Mota Soaresb CM, Mota Soares CA. Sensitivity analysis and optimal design of geometrically non-linear laminated plates and shells. Comput Struct 2000:76;407-420.

98. Razzaq RJ, El-Zafrany A. Non-linear stress analysis of composite layered plates and shells using a mesh reduction method. Eng Anal Bound Elem 2005;29:1115–1123.

99. Bespalova EI, Urusova GP. Contact interaction between prestressed laminated shells of revolution and a flat foundation. Int Appl Mech 2006:42;1137-1144.

100. Pinto Correia IF, Martins PG, Mota Soares CM, Mota Soares CA, Herskovits J. Modelling and optimization of laminated adaptive shells of revolution. Compos Struct 2006:75;49-59.

101. Vasilenko AT, Bespalova EI, Urusova GP. Contact interaction between a laminated shell of revolution and a rigid or elastic foundation. Int Appl Mech 2005:41;520-525.

102. Khoroshun LP, Babich DV. Stability of laminated convex shells of revolution with microdamages in laminate components. Int Appl Mech 2006:42;810-817.

103. Vasilenko AT, Emel'yanov IG, Kuznetsov VY. Stress analysis of laminated shells of revolution with an imperfect interlayer contact. Int Appl Mech 2001;37:662-669.

104. Gureeva NA, Klochkov YV, Nikolaev AP. Analysis of an arbitrary loaded shell of revolution based on the finite element method in a mixed formulation. Russian Aeronautics (IZ VUZ) 2010, 53 (3): 7-10.

105. Merzlyakov VA, Galishin AZ. Thermoelastoplastic nonaxisymmetric stress-strain analysis of laminated shells of revolution. Int Appl Mech, Vol. 2001;37:1166-1174.

106. Ye Z, Zhou Z. The bending of composite shallow revolutional shells. Proc Inst Mech Engrs 2000;214:369-376.

107. Trach VM. Stability of composite shells of revolution. Int Appl Mech 2008;44:331-344.

108. Khoroshun LP, Babich DV. Stability of shells of revolution made of granular composite with damageable components. Int Appl Mech 2004;40:1028-1036.

109. Shin WH, Lee SJ, Oh IK, Lee I. Thermal post-buckled behaviors of cylindrical composite shells with viscoelastic damping treatments. J Sound Vib 2009;323:93–111.

110. Bhaskar K, Balasubramanyam G. Accurate analysis of end-loaded laminated orthotropic cylindrical shells. Compos Struct 2002;58:209-216.

111. Merglyakov VA, Gatishin AZ. Analysis of the thermoelastoplastic nonaxisymmetric stress-strain state of laminated circular cylindrical shells. Int Appl Mech 2000;36:241-246.

112. Weaver PM, Driesen JR, Roberts P. Anisotropic effects in the compression buckling of laminated composite cylindrical shells. Compos Sci Tech 2002;62:91–105.

113. Huang X, Lu G. Buckling analysis of laminated circular cylindrical shells using a two-surface theory. Int J Mech Eng Educ 2000;30:171-183.

114. Shen HS, Xiang Y. Buckling and postbuckling of anisotropic laminated cylindrical shells under combined axial compression and torsion. Compos Struct 2008;84:375–386.

115. Diaconu CG, Sato M, Sekine H. Buckling characteristics and layup optimization of long laminated composite cylindrical shells subjected to combined loads using lamination parameters. Compos Struct 2002;58:423–433.

116. Fu YM, Yang JH. Delamination growth for composite laminated cylindrical shells under external pressure. Appl Math Mech 2007:28;1133-1144

117. Yang JH, Fu YM. Delamination growth of laminated composite cylindrical shells. Theor Appl Fract Mech 2006:45;192-203.

118. Shen HS. Hygrothermal effects on the postbuckling of composite laminated cylindrical shells. Compos Sci Tech 2000:60;1227-1240.

119. Wang X, Dong K. Local buckling for triangular and lemniscate delaminations near the surface of laminated cylindrical shells under hygrothermal effects. Compos Struct 2007:79;67-75.

120. Goldfeld Y, Ejgenberg EA. On the different formulations in linear bifurcation analysis of laminated cylindrical shells. Int J Solids Struct 2007:44;8613-8626.

121. Shen HS. Postbuckling analysis of axially-loaded laminated cylindrical shells with piezoelectric actuators. Eur. J. Mech. A/Solids 2001:20;1007-1022.

122. Shen HS. Postbuckling of laminated cylindrical shells with piezoelectric actuators under combined external pressure and heating. Int J Solids Struct 2002:39;4271-

4289.

123. Shen HS , Li QS. Postbuckling of cross-ply laminated cylindrical shells with piezoelectric actuators under complex loading conditions. Int J   Mech Sci 2002:44;1731-1754.

124. Panda SK, Ramachandra LS. Postbuckling analysis of cross-ply laminated cylindrical shell panels under parabolic mechanical edge loading. Thin-walled Struct 2010; 48 (6): 660-667.

125. Rahman T, Jansen EL. Finite element based coupled mode initial post-buckling analysis of a composite cylindrical shell. Thin-Walled Struct 2010; 48 (1): 25-32.

126. Wangi XI, Xiao DG. A study of buckling of near surface local delamination in a cylindrical laminated shell. J Rein Plastics Compos 2001:20;1633-1643.

127. Shen HS. Boundary layer theory for the buckling and postbuckling of an anisotropic laminated cylindrical shell. Part I: Prediction under axial compression. Compos Struct 2008:82;346–361.

128. Shen HS. Boundary layer theory for the buckling and postbuckling of an anisotropic laminated cylindrical shell, Part II: Prediction under external pressure. Compos Struct 2008:82;362–370.

129. Shen HS. Boundary layer theory for the buckling and postbuckling of an anisotropic laminated cylindrical shell, Part III: Prediction under torsion. Compos Struct 2008:82;371–381.

130. Wang X, Zhang YC, Dai HL. Critical strain for a locally elliptical delamination near the surface of a cylindrical laminated shell under hydrothermal effects. Compos Struct 2005:67;491–499.

131. Geier B, Meyer-Piening HR, Zimmermann R. On the influence of laminate stacking on buckling of composite cylindrical shells subjected to axial compression. Compos Struct 2002:55;467–474.

132. Weaver PM, Driesen JR, Robers P. The effect of flexural-twist anisotropy on compression buckling of quasi-isotropic laminated cylindrical shells. Compos Struct 2002;44:195-204.

133. Wang X, Dai HL. Thermal buckling for local delamination near the surface of laminated cylindrical shells and delaminated growth. J   Thermal Stresses 2003;26:423–442.

134. Zhu Y, Wang F, Liu RH. Thermal buckling of axisymmetrically laminated cylindrically orthotropic shallow spherical shells including transverse shear. Appl Math Mech 2008;29:291–300.

135. Patel BP, Shukla KK, Nath Y. Thermal buckling of laminated cross-ply oval cylindrical shells. Compos Struct 2004;65:217–229.

136. Yang J, Fu Y. Analysis of energy release rate for composite delaminated cylindrical shells subjected to axial compression. Acta Mech Sin 2006; 22:537–546.

137. Hilburger MW, Starnes Jr. JH. Buckling behavior of compression-loaded composite cylindrical shells with reinforced cutouts. Int J Non-Linear Mech 2005;40:1005 – 1021.

138. Semenyuk NP, Babich IY, Zhukova NB. Buckling instability of sectional noncircular cylindrical composite shells under axial compression. Mech Comp Mat 2003;39:541-552.

139. Tafreshi A. Delamination buckling and postbuckling in composite cylindrical shells under combined axial compression and external pressure. Compos Struct 2006;72:401–418.

140. Solaimurugan, S, Velmurugan R. Influence of fiber orientation and stacking sequence on petalling of glass-polyester composite cylindrical shells under axial compression. Int J Solids Struct 2007;44:6999–7020.

141. Semenyuk NP, Zhukova NB. Initial postbuckling behavior of cylindrical composite shells under axisymmetric deformation. Int Appl Mech 2006;42:461-470.

142. Tafreshi A. Instability of delaminated composite cylindrical shells under combined axial compression and bending. Compos Struct 2008;82:422–433.

143. Weaver PM, Dickenson R. Interactive local/Euler buckling of composite cylindrical shells. Comput Struct 2003;81:2767–2773.

144. Kere P, Lyly M. On post-buckling analysis and experimental correlation of cylindrical composite shells with Reissner–Mindlin–Von Kármán type facet model. Comput Struct 2008;86:1006–1013.

145. Vaziri A. On the buckling of cracked composite cylindrical shells under axial compression. Compos Struct 2007;80:152–158.

146. Semenyuk NP, Zhukova NB, Ostapchuk VV. Stability of corrugated composite noncircular cylindrical shells under external pressure. Int Appl Mech 2007;43:1380-1389.

147. Tafreshi A. Buckling and post-buckling analysis of composite cylindrical shells with cutouts subjected to internal pressure and axial compression loads. Int J Press Vess Piping 2002;79: 351-359.

148. Tafreshi A. Delamination buckling and postbuckling in composite cylindrical shells

under external pressure. Thin-Walled Struct 2004;10:1379-1404.

149. Babich IY, Semenyuk NP. The stability of cylindrical and conic shells made of composite materials with an elastoplastic matrix. Int Appl Mech 2000;36:697-728.

150. Biagi M, Medico FD. Reliability-based knockdown factors for composite cylindrical shells under axial compression. Thin-Walled Struct 2008;46:1351-1358.

151. Sheinman I, Jabareen M. Postbuckling of laminated cylindrical shells in different formulation. AIAA J 2005;43:1117-1123.

152. De Faria, AR. Buckling optimization of composite plates and cylindrical shells: uncertain load combinations. PhD Thesis, Univ Toronto, 2000, pp 167

153. Wang X, Cai W, Yu ZY. An analytic method for interlaminar stress in a laminated cylindrical shell. Mech Adv Mat Struct 2002:9;119–131.

154. Lin CH, Jen MHR. Analysis of laminated anisotropic cylindrical shell by Chebyshev collocation method. J Appl Mech 2003:70;391-403.

155. Lemanski S, Weaver P. Optimisation of a 4-layer laminated cylindrical shell to meet given cross-sectional stiffness properties. Compos Struct 2006:72;163–176.

156. Gong Y-G, Ling-Feng HE. Experimental study and numerical calculation of stability and load-carrying capacity of cylindrical shell with initial dent. J Exp Mech 2010; 1: 1-11.

157. Khoroshun LP, Babich DV. Stability of cylindrical shells made of a laminate material with damageable components. Int Appl Mech 2006:42;677-683.

158. Alibeigloo A. Static analysis of an anisotropic laminated cylindrical shell with piezoelectric layers using differential quadrature method. Mechanical Engineering Science 2008:222;865-880.

159. Goldfeld Y. The influence of the stiffness coefficients on the imperfection sensitivity of laminated cylindrical shells. Compos Struct 2004;64:243–247.

160. Zenkour AM, Fares ME. Thermal bending analysis of composite laminated cylindrical shells using a refined first-order theory. J Therm Stress 2000;23:505 - 526.

161. Jinhua Y, Yiming F, Xianqiao W. Variational analysis of delamination growth for composite laminated cylindrical shells under circumferential concentrated load. Compos Sci Tech 2007;67:541–550.

162. Meink TE, Huybrechts S, Shen MHH. Processing induced warpage of filament wound composite cylindrical shells. J Compos Mat 2002;36:1025-1047.

163. Solaimurugan S, Velmurugan R. Progressive crushing of stitched glass-polyester composite cylindrical shells. Compos Sci Tech 2007;67:422–437.

164. Seif H, Sofiyev AH, Yusufoglu E, Karaca Z. Semi-analytical solution of stability of composite orthotropic cylindrical shells under time dependant a-periodic axial compressive load. Iranian J Scie Tech 2006;30:343-347.

165. Burgueño R, Bhide KM. Shear response of concrete-filled FRP composite cylindrical shells. J Struc Eng 2006;132:949-960.

166. Belozerov LG, Kireev VA. An economical method of determining the elasticity characteristics of the composite material of cylindrical shells. Measurement Tech 2001;44:1224-1233.

167. Semenyuk NP, Trach VM. Bending of cord composite cylindrical shells with noncoincident directions of layer reinforcements and coordinate lines. Mech Comp Mat 2005;41:437-444.

168. Paris AJ, Costello GA. Bending of cord composite cylindrical shells. J Appl Mech 2000;67:117-127.

169. Movsumov EA, Shamiev FH. Yield condition for circular cylindrical shells made of a fiber-reinforced composite. Mech Comp Mat 2006;42:459-466.

170. Zang YQ, Zhang D, Zhou HY, Mab HZ, Wang TK. Non-linear dynamic buckling of laminated composite shallow spherical shells. Compos Sci Tech 2000:60;2361-2363.

171. Kioua H, Mirza S. Piezoelectric induced bending and twisting of laminated composite shallow shells. Smart Mater. Struct. 2000:9;476-484.

172. Niemi AH. A bilinear shell element based on a refined shallow shell model. Int J Num Meth Eng 2010; 81 (4): 485-512.

173. Zarivnyak IS. Probability of the critical state of glue joints of a shallow laminated shell with random irregularities. Strength Mat 2006:38;99-107.

174. Grigorenko YM, Kryukov NN, Ivanova YI. Stress analysis of biconvex laminated orthotropic shells that are shallow to a variable degree. Int Appl Mech 2003:39;688-695.

175. Gupta KM. An Orthotropic adaptive shallow cylindrical shell on elastic foundation. Int J Research Reviews Appl Sci 2010; 2 (1): 67-87.

176. Wu CP, Hung YC, Lo JY. A refined asymptotic theory of laminated circular conical shells. Europ J Mech A/Solids 2002;21:281-300.

177. Das HS, Chakravorty D. A finite element application in the analysis and design of point-supported composite conoidal shell roofs: suggesting selection guidelines. J Strain Anal Eng Design 2010; 45 (3): 165-177.

178. Mahdi E, Hamouda AMS, Sahari BB, Khalid YA. Effect of material and geometry on crushing behaviour of laminated conical composite shells. Appl Compos Mat 2002:9;265-290.

179. Goldfeld Y. Imperfection sensitivity of laminated conical shells. Int J Solids Struct 2007:44;1221-1241.

180. Goldfeld Y, Vervenne K, Arbocz J, Keulen FV. Multi-fidelity optimization of laminated conical shells for buckling. Struct Multidisc Optim 2005:30;128–141.

181. Mahdi E, Hamoudaa AMS, Saharib BB, Khalid YA. Effect of residual stresses in a filament wound laminated conical shell. J Mat Proc Tech 2003:138;291–296.

182. Singh BN, Babu JB. Thermal buckling of laminated conical shells embedded with and without piezoelectric layer. J Rein Plastics Comp 2009;28: 791-812.

183. Wu CP, Chiu SJ. Thermoelastic buckling of laminated composite conical shells. J Thermal Stresses 2001;24:881-901.

184. Rezadoust AM, Esfandeh M, Sabet SA. Crush behavior of conical composite shells- effect of cone angle and diameter-wall thickness ratio. Polymer-Plastics Tech and Eng 2008;47: 147–151.

185. Goldfeld Y, Arbocz J, Rothwell A. Design and optimization of laminated conical shells for buckling. Thin-Walled Struct 2005;43:107-133.

186. Kosonen, J. Specification for mechanical analysis of conical composite shells, MS Thesis, Helsinki Univ Tech, 2003.

187. Patel BP, Shukla KK, Nath Y. Thermal postbuckling analysis of laminated cross-ply truncated circular conical shells. Compos Struct 2005;71:101–114.

188. Patel BP, Nath Y, Shukla KK, Thermal postbuckling characteristics of laminated conical shells with temperature-dependent material properties. AIAA J 2005;43:1380-1388.

189. Smithmaitrie P, Tzou HS. Micro-control actions of actuator patches laminated on hemispherical shells. J Sound Vib 2004:277;691-710.

190. Marchuk MV, Khomyak NN. Refined mixed finite element solution of the problem on the stress state of laminated spherical shells. Int Appl Mech 2001:37;1594-1601.

191. He RS, Hwang SF. Identifying damage in spherical laminate shells by using a

hybrid real-parameter genetic algorithm. Compos Struct 2007:80;32–41.

192. Kadoli R, Ganesan N. A theoretical analysis of linear thermoelastic buckling of composite hemispherical shells with a cut-out at the apex. Compos Struct 2005;68:87–101.

193. Saleh MA, Mahdi E, Hamouda AMS, Khalid YA. Crushing behaviour of composite hemispherical shells subjected to quasi-static axial compressive load. Compos Struct 2004;66:487–493.

194. Tzou HS, Chai WK, Wang DW. Micro-control actions and location sensitivity of actuator patches laminated on toroidal shells. J Vib Acous 2006:126;284-297.

195. Mitkevich AB, Kul'kov AA. Design optimization and forming methods for toroidal composite shells. Mech Compos Mat, 2006;42:95-108.

196. Sai Ram KS, Sreedhar Babu T. Study of bending of laminated composite shells. Part 1. Shells without a cutout. Compos Struct 2001;51:103-116.

197. Sai Ram KS, Sreedhar Babu T. Study of bending of laminated composite shells. Part II: Shells with a cutout. Compos Struct 2001;51:117.

198. Latifa SK , Sinha PK. Improved finite element analysis of multilayered, doubly curved composite shells. J Rein Plastics Compos 2005; 24:385-404.

199. Pinto Correiaa IF, Barbosa JI, Mota Soares CA, Mota Soares CA. A finite element semi-analytical model for laminated axisymmetric shells: statics, dynamics and buckling. Comput Struct 2000;76:299-317.

200. Prusty BG. Linear static analysis of composite hat-stiffened laminated shells using finite elements. Finite Elem Anal Des 2003:39;1125-1138.

201. Park T, Kim K, Han S. Linear static and dynamic analysis of laminated composite plates and shells using a 4-node quasi-conforming shell element. Composites: Part B 2006:37;237-248.

202. Alijani F, Aghdam MM, Abouhamze M. Application of the extended Kantorovich method to the bending of clamped cylindrical panels. Eur J Mech–A/Solids 2008;378- 388.

203. Babeshko ME, Shevchenko YN. Elastoplastic axisymmetric stress–strain state of laminated shells made of isotropic and transversely isotropic materials with different moduli. Int Appl Mech 2005:41;910-916.

204. Babeshko ME, Savchenko VG. Study of the elastoplastic axisymmetric stress-strain state of irradiated laminated shells with a loading history. Int Appl Mech 2001;37:1441-1446.

205. Babeshko ME, Shevchenko YN. Thermoelastoplastic axisymmetric stress–strain state of laminated orthotropic shells. Int Appl Mech 2001;40:1378-1384.

206. Babeshko ME. Thermoelastoplastic state of flexible laminated shells under axisymmetric loading along various planes paths. Int Appl Mech 2003;39:177-184.

207. Shevchenko VG, Babeshko ME. The elastoplastic axisymmetric stress–strain state of flexible laminated shells exposed to radiation. Int Appl Mech 2000;36:1218-1224

208. Shevchenko YN, Babeshko ME. Numerical analysis of the thermoelastoplastic stress-strain state of laminated orthotropic shells under axisymmetric loading. J Therm Stress 2006:29;1143-1162.

209. Maslov BP, Zhukov VB, Pogrebnyak AD. Method of stressed state analysis of thick-walled GTE shells from composite materials. Strength Mat 2003;35:376-382.

210. Lee HJ, Lee JJ. A numerical analysis of the buckling and postbuckling behavior of laminated composite shells with embedded shape memory alloy wire actuators. Smart Mater Struct 2000;9:780-787.

211. Sai-Ram KS, Sreedhar BT. Buckling of laminated composite shells under transverse load. Compos Struct 2002;55:157-168.

212. Fan P, YiMing FU, YiFan L. On the durable critic load in creep buckling of viscoelastic laminated plates and circular cylindrical shells. Sci China Ser G-Phys Mech Astron 2008:51;873-882.

213. Li J, Xiang ZH, Xue MD. Buckling analysis of rotationally periodic laminated composite shells by a new multilayered shell element. Compos Struct 2005:70;24–32.

214. Sofiyev AH. Torsional buckling of cross-ply laminated orthotropic composite cylindrical shells subject to dynamic loading. Europ J Mech A/Solids 2003;22:943–951.

215. Patel BP, Nath Y, Shukla KK. Thermo-elastic buckling characteristics of angle-ply laminated elliptical cylindrical shells. Compos Struct 2007;77:120–124.

216. Hilburger MW, Starnes Jr. JH. Effects of imperfections of the buckling response of composite shells. Thin-Walled Struct 2004;42:369-397.

217. Rickards R, Chate A, Ozolinch O. Analysis for buckling and vibrations of composite stiffened shells and plates. Compos Struct 2001;51:361-370.

218. Shen HS. Thermal postbuckling analysis of laminated cylindrical shells with piezoelectric actuators. Compos Struct 2002;55:13-22.

219. Shen HS. Thermal postbuckling behavior of anisotropic laminated cylindrical shells with temperature-dependent properties. AIAA J 2008;46:185.

220. Kim KD, Lomboy GR, Han SC. A co-rotational 8-node assumed strain shell element for postbuckling analysis of laminated composite plates and shells. Comput Mech 2003;30:330-342.

221. Kundu CK, Sinha PK. Postbuckling analysis of laminated composite shells. Compos Struct 2007:78;316-324.

222. Kundu CK, Maiti DK, Sinha PK. Postbuckling analysis of smart laminated doubly curved shells. Compos Struct 2007:81;314-322.

223. Xie D, Biggers Jr SB. Postbuckling analysis with progressive damage modeling in tailored laminated plates and shells with a cutout. Compos Struct 2003:59;199-216.

224. Merazzi E, Degenhardt R, Rohwer K. Postbuckling analysis of composite shell structures toward fast and accurate tools with implicit FEM methods. International Journal of Structural Stability and Dynamics 2010; 10 (4): 941-947.

225. Galishin AZ. Analysis of the axisymmetric thermoelastoplastic state of branched laminated transversally isotropic shells. S. P. Timoshenko Institute of Mechanics 2000;36:I25-131.

226. Babeshko MA, Shevchenko YN. Axisymmetric thermoelastoplastic stress-strain state of transversely isotropic laminated shells. Int Appl Mech 2006;42:669-676.

227. Swamy NV, Sinha PK. Nonlinear transient analysis of laminated composite shells in hygrothermal environments. Compos Struct 2006:72;280-288.

228. Babeshko ME, Shevchenko YN. Thermoelastoplastic stress–strain state of laminated shells under axisymmetric loading along arbitrary plane paths. Int Appl Mech 2002;38:1464-1472.

229. Cheng ZQ, Batra RC. Thermal effects on laminated composite shells containing interfacial imperfections. Compos Struct 2001:52;3-11.

230. Kewei D. Weak formulation study for thermoelastic analysis of thick open laminated shell. Mech Adv Mat Struct 2008;15:33–39.

231. Ghosh A. Hygrothermal effects on the initiation and propagation of damage in composite shells. Aircraft Eng Aero Tech: An Int J 2008;80:386–399.

232. Saha GC, Kalamkarov AL. Micromechanical thermoelastic model for sandwich composite shells made of generally orthotropic materials. J Sandwich Struct Mat 2009;11:27-56.

233. El Damatty AA, Awadb AS, Vickery BJ. Thermal analysis of FRP chimneys using consistent laminated shell element. Thin-Walled Struct 2000;37:57-76.

234. Roy T, Manikandan P, Chakraborty D. Improved shell finite element for piezothermoelastic analysis of smart fiber reinforced composite structures. Finite Elem Anal Des 2010; 46 (9):710-720.

235. Kulikov GM, Plotnikova V. Solution of a coupled problem of thermopiezoelectricity based on a geometrically exact shell element. Mech Comp Mat 2010; 46 (4): 513-534.

236. Zhang Z, Chen H, Ye L. Progressive failure analysis for advanced grid stiffened composite plates/shells. Compos Struct 2008;86:45–54.

237. Ikonomopoulos G, Perreux D. Reliability of composite laminates through a damage tolerance approach- applications into carbon-epoxy and glass-epoxy composite shells.

238. Khoroshun LP, Babich DV. Stability of plates and shells made of homogeneous and composite materials subject to short-term microdamage. Int Appl Mech 2008;44:239-267.

239. Zozulya VV. Laminated shells with debonding between laminas in temperature field. Int Appl Mech 2006:42;842-848.

240. Larsson R. A discontinuous shell-interface element for delamination analysis of laminated Compos Structures. Comput. Methods Appl Mech Eng 2004:193;3173-3194.

241. Mahdi E, Sahari BB, Hamouda AMS, Khalid YA. An experimental investigation into crushing behaviour of filament-wound laminated cone-cone intersection composite shell. Compos Struct 2001:51;211-219.

242. Huang CH, Lee YJ. Static contact crushing of composite laminated shells. Compos Struct 2004;63:211–217.

243. Wagner W, Balzani C. Simulation of delamination in stringer stiffened fiber-reinforced composite shells. Comput Struct 2008;86:930–939.

244. Morozov EV. Theoretical and experimental analysis of the deformability of filament wound composite shells under axial compressive loading. Compos Struct 2001;54:255-260.

245. Hossain SJ, Sinha PK, Sheikh AH. A finite element formulation for the analysis of laminated composite shells. Comput Struct 2004;82:1623-1638.

246. Kim KD, Lee CS, Han SC. A 4-node co-rotational ANS shell element for laminated

Compos Structures. Compos Struct 2007:80;234-252.

247. Szea KY, Yaoa LQ, Pian THH. An eighteen-node hybrid-stress solid-shell element for homogenous and laminated structures. Finite Elem Anal Des 2002:38;353–374.

248. Wu J, Burguen R. An integrated approach to shape and laminate stacking sequence optimization of free-form FRP shells. Comput Meth Appl Mech Eng 2006:195;4106–4123.

249. Balah M, Al-Ghamedy HN. Finite element formulation of a third order laminated finite rotation shell element. Comput Struct 2002:80;1975–1990.

250. Trach VM, Podvornyi AV. Stability of laminated shells made of materials with one plane of elastic symmetry. Int Appl Mech 2004:40;573-579.

251. Kabir HRH, Al-Shaleh K. Three-node triangular element for arbitrarily laminated general shells. Compos Struct 2007;77:18–29.

252. Kalamkarov AL, Duvaut G, Lene F. A new asymptotic model of flexible composite shells of a regular structure. Int J Eng Sci 2002;40:333-343.

253. Haussya B, Ganghoffer JF. Modelling of curved interfaces in composite shells. Int J Mech Sci 2006;48:1234–1245.

254. Roque CMC, Ferreira AJM. New developments in the radial basis functions analysis of composite shells. Compos Struct 2009;87:141–150.

255. Ren L, Parvizi-Majidi A. A model for shape control of cross-ply laminated shells using a piezoelectric actuator. J Compos Mat 2006;40:1271-1285.

256. Bhattacharya P, Suhail H, Sinha PK. Finite element analysis and distributed control of laminated composite shells using LQR/IMSC approach. Aero Sci Tech 2002:6;273-281.

257. Zallo A, Gaudenzi P. Finite element models for laminated shells with actuation capability. Comput Struct 2003:81;1059-1069.

258. Pinto Correia IF, Mota Soares CM, Mota Soares CA, Herskovits J. Analysis of adaptive shell structures using a refined laminated model. Compos Struct 2004:66;261–268.

259. Bhattacharya P, Suhail H, Sinha PK. Smart laminated shells and deflection control strategy with optimal voltage. J Rein Plastics Comp 2000:19;1293-1316.

260. Xue Q. Effective dielectric constant of composite with interfacial shells. Physica B 2004; 344:129–132.

261. Picha A, Haina J, Protsb Y, Adler HJ. Composite polymeric particles with ZnS shells. Polymer 2005;46:7931–7944.

262. Yan Z, Pantelides CP, Reaveley LD. Post-tensioned FRP Composite Shells for Concrete Confinement. J Composites For Construction 2007;11:81-90.

263. Lopez-Anido R, Michael AP, Sandford TC, Goodell B. Repair of wood piles using prefabricated fiber-reinforced polymer composite shells. J Performance of Constructed Facilities 2005;19:78-87.

264. Jaunky N, Ambur DR. Optimal design of grid-stiffened panels and shells with variable curvature. AIAA 2000;1:654.

265. Bushnell D. Global optimum design of externally pressurized iso-grid stiffened cylindrical shells with added T-rings. Int J Non-Linear Mechanics 2002;37:801.

266. Kim TD. Postbuckled behavior of composite isogrid stiffened shell structure. Advanced Composite Materials: The Official J the Japan Society of Composite Materials 2000;9:253.

267. Zeng T, Wu L. Post-buckling analysis of stiffened braided cylindrical shells under combined external pressure and axial compression. Compos Struct 2003;60:455.

268. Poorveis D, Kabir MZ. Buckling of discretely stringer-stiffened composite cylindrical shells under combined axial compression and external pressure. Scientia Iranica 2006;13:113.

269. Mocker T, Reimerdes HG. Load carrying capability of stringer stiffened curved composite panels in the postbuckling region. Europ Space Agency 2005:1077.

270. Bisagni C, Cordisco P. Testing of stiffened composite cylindrical shells in the postbuckling range until failure. AIAA J 2004;42:1806.

271. Bisagni C, Cordisco P. Post-buckling and collapse experiments of stiffened composite cylindrical shells subjected to axial loading and torque. Compos Struct 2006;73:138.

272. Rao KP. Study of the behaviour of laminated composite beam, plate and shell structures using some specifically developed finite elements. J Spacecraft Tech 2000;10:1.

273. Bai R, Wang M, Chen H. Buckling behavior of composite AGS with delamination. Fuhe Cailiao Xuebao/Acta Materiae Compos Sinica 2005;22:136.

274. Kidane S, Li G, Helms J, Pang S-S, Woldesenbet E. Buckling load analysis of grid stiffened composite cylinders. Compos Part B: Eng 2003;34:1.

275. De Vries J. Analysis of localized buckling of cylindrical shell using a hierarchical approach. AIAA 2006;11:8061.

276. Accardo AF, Ricci F, Lucariello D, Polese P, Leone B, Cozzolino D, Sollo, Palmiero F. Design of a combined loads machine for tests on fuselage barrels and curved panels. AIAA 2004;2:1249.

277. Linde P, Schulz A, Rust W. Influence of modelling and solution methods on the FE-simulation of the post-buckling behaviour of stiffened aircraft fuselage panels. Compos Struct 2006;73:229.

278. Patel SN, Datta PK, Sheikh AH. Dynamic instability analysis of laminated composite stiffened shell panels subjected to in-plane harmonic edge loading. Struct Eng Mech 2006;22:483.

279. Rikards R, Abramovich H, Kalnins K, Auzins J. Surrogate modeling in design optimization of stiffened composite shells. Compos Struct 2006;73:244.

280. Wong HT, Teng JG. Buckling behaviour of model steel base shells of the Comshell roof system. J Const Steel Res 2006;62:4-19.

281. Apicella A, Armentani E, Esposito R, Pirozzi M. Finite element analysis of a composite bulkhead structure. Laubisrutistr.24, Stafa-Zuerich, CH-8712 2007;348-349:553.

282. Chen N-Z, Guedes Soares C. Longitudinal strength analysis of ship hulls of composite materials under sagging moments. Compos Struct 2007;77:36.

283. Rais-Rohani M, Lokits J. Reinforcement layout and sizing optimization of composite submarine sail structures. Struct Multi Opt 2007;34:75.

284. Wu D, Xu Y, Wan Q. Global buckling load analysis of grid stiffened composite panels. Fuhe Cailiao Xuebao/Acta Mat Compos Sinica 2007;24:168.

285. Chen H-R, Zhou B-H, Bai R-X. Thermal-mechanical buckling behavior of advanced composite grid stiffened shell with multi-delaminations. Gongcheng Lixue/Engin Mech 2008;25:58.

286. Chen W, Xu X. Buckling and postbuckling response analysis of the doubly-curved composite shell by nonlinear FEM. Fuhe Cailiao Xuebao/Acta Mat Compos Sinica 2008;25:178.

287. Prusty BG. Free vibration and buckling response of hat-stiffened composite panels under general loading. Int J Mech Sci 2008;50:1326.

288. Sahoo S, Chakravorty D. Bending of composite stiffened hypar shell roofs under point load. J Engineering Mechanics 2008;134:441.

289. Zhang Z-F, Chen H-R, Bai R-X. Stability analysis of advanced composite grid stiffened cylindrical shell. Dalian Ligong Daxue Xuebao/J Dalian University of Technology 2008;48:631.

290. Lu W, Ma Y, Liang W, Lu Z. Analysis system of stability and strength for airframe composite stiffened plate/shell. Hangkong Xuebao/Acta Aero Astr Sinica 2009;30:895.

291. He J-X, He G-Q, Ren M-F, Hou X. Buckling load analysis of composite grid stiffened structure skirts. Guti Huojian Jishu/J Solid Rocket Tech 2009;32:331.

292. Zahari R, El-Zafrany A. Progressive failure analysis of composite laminated stiffened plates using the finite strip method. Compos Struct 2009;87:63.

293. Hilburger MW. Buckling and failure of compression-loaded composite laminated shells with cutouts. AIAA 2007;6:6366.

294. Li J, Xiang ZH, Xue MD. Three-dimensional finite element buckling analysis of honeycomb sandwich composite shells with cutouts. Comput Mat Cont 2005;2:139.

295. Madenci E, Barut A. The influence of geometric irregularities on the linear buckling of cylindrical shells with an elliptic cutout. AIAA 2003;7:4817.

296. Nanda N, Bandyopadhyay JN. Nonlinear transient response of laminated composite shells. J Eng Mech 2008;134:983.

297. Starnes JJH, Hilburger MW, Nemeth MP. The effects of initial imperfections on the buckling of composite cylindrical shells. ASTM Special Tech Pub 2000:529.

298. Arbocz J, Hilburger MW. Towards a probabilistic preliminary design criterion for buckling critical composite shells. AIAA 2003;6:4076.

299. Biagi M, Perugini P. Nonlinear analysis of the vega launcher first stage composite skirts with geometrical imperfections. Vol. 5. Waikiki, HI: AIAA, 2007. p.5015.

300. Bisagni C. Numerical analysis and experimental correlation of composite shell buckling and post-buckling. Compos Part B: Eng 2000;31:655.

301. Carvelli V, Panzeri N, Poggi C. Buckling strength of GFRP under-water vehicles. Compos Part B: Eng 2001;32:89.

302. Carvelli V, Panzeri N, Poggi C. Effects of material failure on buckling behaviour of medium-thick GFRP cylindrical shells for submarine applications. ASME Appl Mechanic Div 2001:81.

303. Hilburger MN, Starnes J.H, Jr. High-fidelity nonlinear analysis of compression-loaded composite shells. AIAA 2001;3:1564.

304. Hilburger MW, Starnes Jr JH. Effects of imperfections on the buckling response of compression-loaded composite shells. AIAA 2000;1:423.

305. Jayachandran SA, Kalyanaraman V, Narayanan R. Marguerre shell type secant matrices for the postbuckling analysis of thin, shallow composite shells. Struct Eng Mech 2004;18:41.

306. Tafreshi A, Bailey CG. Instability of imperfect composite cylindrical shells under combined loading. Compos Struct 2007;80:49.

307. Wardle BL, Lagace PA. Bifurcation, limit-point buckling, and dynamic collapse of transversely loaded composite shells. AIAA J 2000;38:507.

308. Abouhamze M, Aghdam MM, Alijani F. Bending analysis of symmetrically laminated Cylindrical panels using the extended Kantorovich method. Mech Adv Mater Struct 2007;14(7):523–30.

CHAPTER 3

VIBRATION OF DOUBLY CURVED SHALLOW

SHELLS WITH ARBITRARY

BOUNDARIES

A shell is a three dimensional body confined by two parallel (unless the thickness is varying) surfaces. The distance between those surfaces is small compared with other shell parameters. Shell structures constitute a major component of today's aerospace, submarine, automotive and other machine or structural elements. They can be used for aerodynamic, aesthetic and/or other reasons. From a structural viewpoint, shells are considerably stiffer than flat plates. In addition, their theory is reasonably more complex than that of a plate. This is a direct result of the coupling between extensional and bending stiffness parameters that a shell has and a flat plate does not.

Shallow shells are shells that are open and have large radii of curvatures compared with other shell parameters (e.g. length and width). They can have circular, rectangular, triangular or any other planform. They can be singly-curved (i.e. cylindrical) or doubly-curved (e.g. spherical). They can also have their principal radii of curvature not align with the geometric boundaries, introducing a radius of twist (e.g. turbomachinery blades).

Unlike plates, where there is a widely accepted plate theory, shells can be modeled relatively accurately using many theories. In this work, we will use a Donnel-Mushtari

theory [1-5] which is accurate for shallow shells and will be sufficient for the structures treated here. It is also accurate for higher frequencies of deeper shells. The literature on shallow shell vibration has been the subject of various articles [6-9]. Leissa and Narita [10] and Narita and Leissa [11] studied vibrations of completely free and corner point supported shallow shells of rectangular planform. Also, Liew and Lim [12-14] studied vibration behavior of doubly curved shallow shells with rectangular planform as well as curvilinear planform including those of rounded corners. Other detailed vibration studies include cantilevered shallow cylindrical [15, 16], doubly-curved [17] and twisted [18] shells of rectangular planform. Qatu and Leissa [19] studied shallow shells with two adjacent edges clamped and the others free. Qatu [20] showed mode shape analysis of laminated composite shallow shells. Effects of edge constraints upon the frequencies of shallow shells having three free boundaries were also investigated [21]. Clear differences between frequencies obtained for shallow shells and those for plates are outlines in a recent publication [22]. Lim et al [23] and Liew et al [24, 25] analyzed the vibratory characteristics of cantilevered conical shallow shells of initial twist. They used a special version of the Ritz method [26, 27]. Vibration studies on completely free shallow shells having triangular and trapezoidal planforms and cantilevered shallow shells with right triangular and trapezoidal planforms were the subject of two studies [28-29].

This chapter presents the first comprehensive and accurate study of vibrations of shallow thin shells for all combinations of practical boundary conditions. These can be directly used by acoustic and vibration engineers for various applications (structures, automotive, submarine, aerospace, …). They can also be used for benchmarking of researchers in the field. In this paper, the Ritz method is used to solve for natural

vibrations of shallow shells with arbitrary boundary conditions using the same algorithm. Thin shallow shell theory is used in the analysis and natural frequencies are presented for various shell curvatures including spherical, cylindrical and hyperbolic paraboloidal shells.

3.1. Basic equations of thin shallow shells

The middle surface of a shallow shell of arbitrary curvature is depicted in Fig. 3.1 In terms of the rectangular coordinates shown there, its equation is

$$z = \frac{x^2}{2R_x} + \frac{xy}{R_{xy}} + \frac{y^2}{2R_y},$$
(1)

where R_x and R_y are radii of curvature in the x and y directions, respectively, as shown in Fig. 3.1, and R_{xy} is the corresponding coefficient describing the twist of the surface. This analysis will be limited to the case when R_x, R_{xy}, and R_y are constants. In this case, Eq. (1) represents a quadratic surface. Figure 3.2 shows a shallow shell having boundaries which, when projected upon the xy-plane (i.e., its planform), are rectangular. For analysis it is then usually convenient to choose the xy-coordinates to be parallel to the boundaries. However, if the x and y axes were rotated about the z-axis, it is possible to orient them so that $R_{xy} = \infty$ in (1). Then x and y are principal coordinates, and the new values of R_x and R_y are principal radii of curvature. Consider the shell segment shown in Fig. 3.3. It may be circular cylindrical, with $R_x = R$, and $R_y = R_{xy} = \infty$, spherical, with
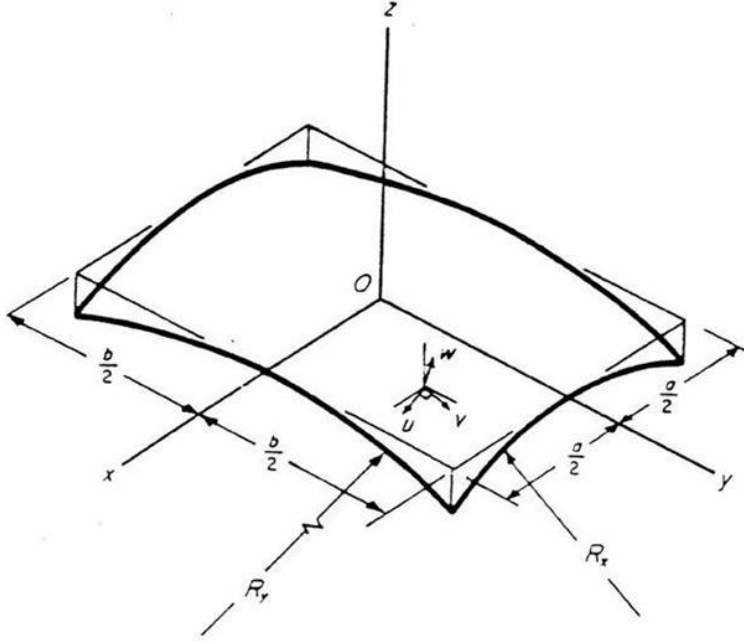
Figure 3.1:   Shallow shell with rectangular planform

$R_x = R_y = R$ and $R_{xy} = \infty$, hyperbolic paraboloidal with $R_x = -R_y = R$ and $R_{xy} = \infty$, or other.

Assuming the Kirchhoff hypothesis for the behavior of the normal to the shell midsurface [1-3], midsurface strains and curvature changes can then be written as:

$$\varepsilon_{0x} = \frac{\partial u_o}{\partial x} + \frac{w_o}{R_x}, \quad \varepsilon_{0y} = \frac{\partial v_o}{\partial y} + \frac{w_o}{R_y}$$

$$\gamma_{0xy} = \frac{\partial v_o}{\partial x} + \frac{\partial u_o}{\partial y} + \frac{2w_o}{R_{xy}}, \quad \kappa_x = -\frac{\partial^2 w_0}{\partial x^2}, \quad \kappa_y = -\frac{\partial^2 w_0}{\partial y^2}, \quad \kappa_{xy} = -\frac{\partial^2 w_0}{\partial x \partial y} \tag{2}$$

where u_0, v_0 and w_0 are midsurface displacements in the x, y and z directions. Strain at any point can be written as

72

$$\varepsilon_x = \varepsilon_{0x} + z\kappa_x$$
$$\varepsilon_y = \varepsilon_{0y} + z\kappa_y$$
$$\gamma_{xy} = \gamma_{0xy} + 2z\kappa_{xy}$$

(3)
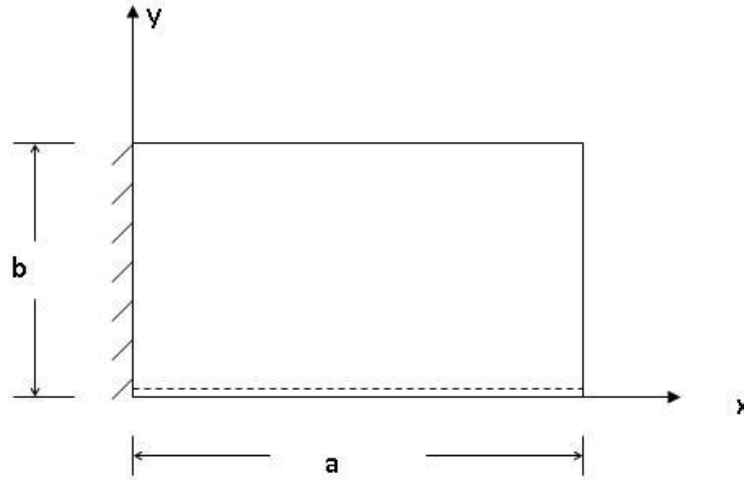
Figure 3.2:   Non-dimensional coordinates for a CSFF shallow shell.

Consider an infinitesimal element of the shell. It will have stress resultants (forces per unit length) N_x, N_y, and N_{xy} tangent to its midsurface called "membrane forces" acting along its edges as well as moment resultants (moments per unit length) M_x, M_y, and M_{xy}. In applying the equilibrium equations including the transverse shearing forces, and performing some mathematical substitutions, the resulting equations of motion are [1]
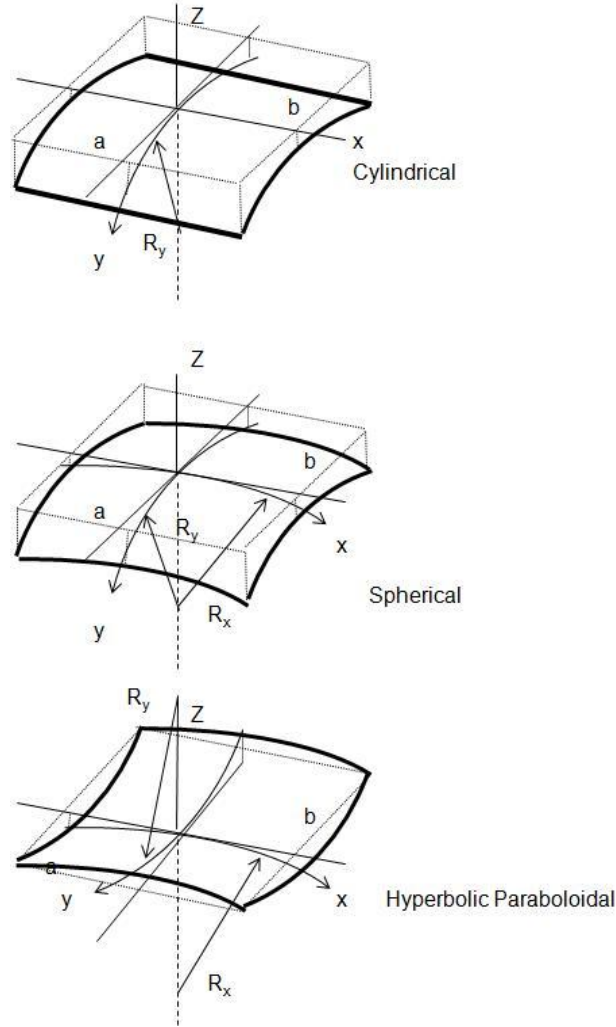
Figure 3.3: Types of curvatures for shallow shells on rectangular planforms : spherical ($R_x / R_y = 1$), circular cylinder ($R_x / R_y = 0$) and hyperbolic paraboloidal ($R_x / R_y = -1$) shallow shells.

$$\frac{\partial N_x}{\partial x} + \frac{\partial N_{xy}}{\partial y} + p_\alpha = -\rho \frac{\partial^2 u_o}{\partial t^2}, \qquad \frac{\partial N_y}{\partial y} + \frac{\partial N_{xy}}{\partial x} + p_y = -\rho \frac{\partial^2 v_o}{\partial t^2},$$

$$-\left(\frac{2N_{xy}}{R_{xy}} + \frac{N_x}{R_x} + \frac{N_y}{R_y} \right) + \frac{\partial^2 M_x}{\partial x^2} + 2\frac{\partial^2 M_{xy}}{\partial y \partial x} + \frac{\partial^2 M_y}{\partial y^2} + (p_n) = -\rho \frac{\partial^2 w_o}{\partial t^2}$$

(4)

For an isotropic shell material the strains are related to the stresses by

74

$$\varepsilon_x = \frac{1}{E}\left(\sigma_x - v\sigma_y\right), \quad \varepsilon_y = \frac{1}{E}\left(\sigma_y - v\sigma_x\right), \quad \gamma_{xy} = \frac{\tau_{xy}}{G}, \tag{5a}$$

or $\quad \sigma_x = \frac{E}{1-v^2}\left(\varepsilon_x + v\varepsilon_y\right), \quad \sigma_y = \frac{E}{1-v^2}\left(\varepsilon_y + v\varepsilon_x\right), \quad \tau_{xy} = \frac{E}{2(1+v)}\gamma_{xy},$ \hfill (5b)

where E is modulus of elasticity (Young's modulus), v is Poisson's ratio, and G is the shear modulus, related to E and v by ($G = E/2(1+v)$). The resultant forces are obtained by carrying the integration of stresses over the cross-section. The bending moments are obtained by integrating the moments of the in-plane stresses over the thickness. That is,

$$N_x = \int_{-h/2}^{h/2} \sigma_x dz \quad N_y = \int_{-h/2}^{h/2} \sigma_y dz \quad N_{xy} = \int_{-h/2}^{h/2} \tau_{xy} dz$$

$$M_x = \int_{-h/2}^{h/2} \sigma_x z dz \quad M_y = \int_{-h/2}^{h/2} \sigma_y z dz \quad M_{xy} = \int_{-h/2}^{h/2} \tau_{xy} z dz \tag{6a}$$

The moment resultant can be written as

$$M_x = D\left(\kappa_x + v\kappa_y\right), \quad M_y = D\left(\kappa_y + v\kappa_x\right), \quad M_{xy} = D(1-v)\kappa_{xy} \tag{6b}$$

where $D = Eh^3/12\left(1-v^2\right)$ \hfill (7)

is the flexural rigidity of the shell. All the needed parts of the classical shallow shell theory are present, and they may be combined to obtain the desired form of the equation of motion.

For the case of coordinates of principal curvature, the resulting equations written in terms of displacements in matrix form, are [3]

$$\frac{Eh}{1-v^2}\begin{bmatrix} L_{11} & L_{12} & L_{13} \\ L_{12} & L_{22} & L_{23} \\ L_{13} & L_{23} & L_{33} \end{bmatrix}\begin{bmatrix} u \\ v \\ w \end{bmatrix} + \rho h\begin{bmatrix} -\dfrac{\partial^2 u}{\partial t^2} \\ -\dfrac{\partial^2 v}{\partial t^2} \\ -\dfrac{\partial^2 w}{\partial t^2} \end{bmatrix} = \begin{bmatrix} -p_x \\ -p_y \\ q \end{bmatrix},$$ (8)

where p_x and p_y, are the tangential components of exciting force (per unit surface area) acting in planes parallel to the xz- and yz-planes, respectively, and the L_{ij} are differential operators given by:

$$L_{11} = -\frac{\partial^2}{\partial x^2} + \frac{1-v}{2}\frac{\partial^2}{\partial y^2}, \qquad L_{22} = \frac{1-v}{2}\frac{\partial^2}{\partial x^2} + \frac{\partial^2}{\partial y^2}, \qquad L_{33} = \frac{1}{R_x^2} + \frac{2v}{R_x R_y} + \frac{1}{R_y^2} + \frac{h}{12}\nabla^4,$$

$$L_{12} = \frac{1+v}{2}\frac{\partial^2}{\partial x \partial y}, \qquad L_{13} = (\frac{1}{R_x} + \frac{v}{R_y})\frac{\partial}{\partial x}, \qquad L_{13} = (\frac{v}{R_x} + \frac{1}{R_y})\frac{\partial}{\partial y},$$ (9)

If one is using an energy approach (e.g. the Ritz method), the total potential energy is due to strain energy. In a deforming shell it is $PE_{max} = PE_s + PE_b$, where PE_s arises from midsurface stretching and PE_b is due to bending [3], where

$$PE_s = \frac{1}{2}\iint \frac{Eh}{1-v^2}[(\varepsilon_{0x} + \varepsilon_{0y})^2 - 2(1-v)(\varepsilon_{0x}\varepsilon_{0y} - \frac{\gamma_{0xy}^2}{4})]dA,$$ (10)

with ε_{0x}, ε_{0y}, and γ_{0xy}, given by (5), and A is the area of the shell midsurface. The potential energy from bending is

$$PE_b = \frac{1}{2}\iint D[(\kappa_x + \kappa_y)^2 - 2(1-v)(\kappa_x\kappa_y - \kappa_{xy}^2)]dA,$$ (11)

The kinetic energy of the vibrating shell is

$$KE_{max} = \frac{1}{2} \iint \rho h [(\frac{\partial u}{\partial t})^2 + (\frac{\partial v}{\partial t})^2 + (\frac{\partial w}{\partial t})^2] dA, \tag{12}$$

It is worth noting that the above energy expressions are written with E, h, ν, D, and ρ in the integrands. This will enable us to treat shells of variable thickness and/or non-homogeneous material straightforwardly.

The boundary terms for the boundaries with x =constant are

$$N_{0x} - N_x = 0 \qquad or \qquad u_0 = 0$$

$$\left(N_{0xy} - \frac{M_{0xy}}{R_y}\right) - \left(N_{xy} - \frac{M_{xy}}{R_y}\right) = 0 \qquad or \qquad v_0 = 0$$

$$\left(Q_{0x} - \frac{\partial M_{0xy}}{\partial y}\right) - \left(Q_x - \frac{\partial M_{xy}}{\partial y}\right) = 0 \qquad or \qquad w_0 = 0 \tag{13}$$

$$M_{0x} - M_x = 0 \qquad or \qquad \frac{\partial w_0}{\partial x} = 0 \qquad\qquad M_{0xy} w_0 \left.\right]_{y_1}^{y_2} = 0$$

Table 3.1: Convergence study and comparison with previous results for frequency parameters $\omega a^2 \sqrt{\rho h / D}$ of plates, a/b = 1, ν = 0.3.

B.C.	Ref. [28], 36-terms and			Exact	Present Analysis (36 term)				Present Analysis (49 term)			
FFFF	13.489	19.789	24.432	35.024	13.469	19.726	24.541	35.288	13.469	19.596	24.271	34.808
SFFF	6.6480	15.023	25.492	26.126	6.6438	14.903	25.378	26.259	6.6438	14.902	25.378	26.001
CFFF	3.4917	8.5246	21.429	27.331	3.4739	8.5128	21.313	27.461	3.4722	8.5121	21.293	27.200
SSFF	3.3687	17.407	19.367	38.291	3.3671	17.316	19.293	38.213	3.3671	17.316	19.293	38.211
CSFF	5.3639	19.171	24.768	43.191	5.3536	19.080	24.680	43.101	5.3529	19.078	24.677	43.096
CCFF	6.9421	24.034	26.681	47.785	6.9247	23.924	26.592	47.670	6.9232	23.918	26.589	47.668
SFSF*	9.6314	16.135	36.726	38.945	9.6316	16.135	37.169	39.127	9.6312	16.134	36.721	38.944
CFSF	15.285	20.673	39.775	49.730	15.203	20.597	40.199	49.500	15.140	20.442	39.709	49.274
SSSF*	11.685	27.756	41.197	59.066	11.684	27.755	41.350	59.131	11.684	27.755	41.195	59.061
CSSF	16.865	31.138	51.631	64.043	16.802	31.124	51.433	64.377	16.808	31.104	51.434	64.031
CCSF	17.615	36.046	52.065	71.194	17.554	36.073	51.855	71.122	17.537	36.025	51.825	71.085
CFCF	22.272	26.529	43.664	61.466	22.200	26.452	44.085	61.252	22.181	26.437	43.611	61.208
SCSF*	12.687	33.065	41.702	63.015	12.687	33.065	41.861	63.119	12.689	33.060	41.701	63.017
CSCF	23.460	35.612	63.126	66.808	23.402	35.593	62.949	67.300	23.315	35.703	62.909	66.761
CCCF	24.020	40.039	63.193	76.761	23.944	40.080	63.247	76.941	23.903	39.972	63.240	76.772
SSSS*	19.739	49.348	49.348	78.957	19.739	49.491	49.492	79.172	19.738	49.343	49.345	78.943
CSSS*	23.646	51.674	58.646	86.135	23.665	51.866	58.665	86.221	23.658	51.513	58.665	86.221
CCSS	27.056	60.544	60.791	92.865	27.026	60.537	60.861	93.313	26.907	60.545	60.554	93.313
CSCS*	28.951	54.743	69.327	94.585	28.962	54.903	69.344	94.699	28.902	54.685	69.344	94.699
CCCS	31.829	63.347	71.084	100.83	31.854	63.175	71.135	99.494	31.686	62.914	71.135	99.494
CCCC	35.992	73.413	73.413	108.27	35.970	73.724	73.756	109.78	35.773	73.182	73.374	108.61

* Exact Solution reported in [28]

Similar equations can be obtained for y = constant. It is clear that four possible combinations at each edge can be made for each of the classical boundary condition known for plates (simply supported, clamped, and free). For the analysis done here, clamped means completely clamped (inplane displacements constrained), free means completely free (inplane displacements are also free) and simply supported boundaries are shear diaphragm boundaries defined as :

$$N_x = 0, \quad v_0 = 0, \quad w_0 = 0, \quad and \quad M_x = 0 \tag{14}$$

3.2. Ritz analysis

The Ritz method with algebraic polynomial displacement functions is used here to solve the vibration problem for shallow shells having different boundary conditions. Convergence studies are made which demonstrate that accurate results (natural frequencies) can be obtained with this analysis. The effects of shell curvature and boundary conditions upon the natural frequencies and mode shapes are studied.

For free vibrations of a shallow shell having the rectangular planform, displacements are assumed as $\omega a^2 \sqrt{\rho h / D}$

$$u_0(x,y,t) = U(x,y)\sin \omega t, \quad v_0(x,y,t) = V(x,y)\sin \omega t, \quad w_0(x,y,t) = W(x,y)\sin \omega t, \tag{15}$$

Algebraic functions may be used as trial functions. The displacement trial functions, in terms of the nondimensional coordinates ξ and η, are taken as:

$$U(\xi,\eta) = \sum_{i=i_0}^{I} \sum_{j=j_0}^{J} \alpha_{ij}\xi^i\eta^j, \quad V(\xi,\eta) = \sum_{k=k_0}^{K} \sum_{\ell=\ell_0}^{L} \beta_{k\ell}\xi^k\eta^\ell, \quad W(\xi,\eta) = \sum_{m=m_0}^{M} \sum_{n=n_0}^{N} \gamma_{mn}\xi^m\eta^n, \tag{16}$$

where $\xi = x/a$ and $\eta = y/b$.

The Ritz method requires satisfaction of geometric (forced) boundary conditions only. One can solve for many boundary conditions with the same analytical procedure by using a suitable selection of the value i_0, j_0, k_0, l_0, m_0 and n_0. Vibration problems for shallow shells having the boundary conditions XXFF, where X can be simply supported (S), clamped (C), or free (F) can be solved. One should keep in mind that for shallow shells there are four types of configurations for each of the simply supported, free and clamped edge conditions.

For other types of boundary conditions, one can use springs at the free ends. These are springs that cover the whole edge and can actually be functions of the boundary coordinates. These springs will be taken as constants along the boundary at which they are acting. Three linear springs and one rotational spring are used at each of the two edges at $x = a$ and at $y = b$. For the free edge at $x = a$, a linear spring in the vertical direction (with a spring constant k_z) can be taken to restrain motion vertically; another linear spring is used to restrain motion in the x direction (with a spring constant k_x); a third linear spring can be used to restrain motion in the tangential direction (with a spring constant k_y); and finally a rotational spring about the edge parallel to the y axis can be used (with a spring constant k_ψ). The strain energy of these springs is:

Table 3.2: Frequency parameters $\omega a^2 \sqrt{\rho h / D}$ of shallow spherical shells, $R_x / R_y = 1$, a/ b = 1, a / h = 20, v = 0.3.

B.C	a/ R = 0.5				a/ R = 0.2			
FFFF	13.42	19.39	32.53	34.98	13.46	19.56	25.99	34.85
SFFF	6.551	16.25	25.47	31.04	6.629	15.34	25.40	27.08
CFFF	4.722	8.390	22.09	28.80	3.754	8.492	21.53	28.26
SSFF	3.332	17.29	24.64	48.04	3.367	17.32	20.79	39.71
CSFF	6.387	19.71	27.98	52.49	5.566	19.35	25.47	44.64
CCFF	11.14	23.83	32.74	57.43	7.894	23.90	27.92	49.27
SFSF	11.12	15.91	42.19	47.47	10.07	16.10	38.89	39.59
CFSF	17.04	26.19	50.89	52.18	15.63	21.68	41.84	49.95
SSSF	13.14	42.40	44.25	64.32	12.22	30.50	41.85	60.14
CSSF	23.52	44.97	55.57	72.75	18.01	33.76	52.05	65.24
CCSF	21.90	50.00	54.17	77.69	18.68	38.58	52.19	72.13
CFCF	36.90	38.37	55.08	62.98	25.30	28.67	45.53	61.34
SCSF	13.67	44.40	47.38	64.32	12.95	35.75	42.26	64.09
CSCF	37.70	49.75	65.08	74.46	26.34	38.07	63.08	68.01
CCCF	37.96	55.15	65.22	83.90	26.62	42.71	63.56	77.64
SSSS	38.01	59.10	59.10	85.32	23.70	51.04	51.04	80.02
CSSS	41.28	61.27	67.58	92.35	27.32	53.32	60.17	87.13
CCSS	44.57	69.21	69.78	98.39	30.64	61.88	62.36	93.66
CSCS	46.87	64.10	76.80	100.07	32.47	55.41	70.37	95.06
CCCS	50.51	72.22	78.62	106.22	35.51	64.76	72.13	101.40
CCCC	58.04	80.84	80.92	112.54	40.26	74.17	74.43	108.66

$$U_{x=a} = \frac{1}{2} \int_{y=0}^{y=b} \left\{ k_x u_0^2(a,y) + k_y v_0^2(a,y) + k_z w_0^2(a,y) + k_\psi \left(\frac{\partial w_0(a,y)}{\partial x} \right)^2 \right\} dy$$

(17)

This is to be added to the expression for PE_{max}. Similar treatment can be made for springs at y =b.

For solving the free vibration problem, the displacement functions are substituted into the energy functional equations in order to get an expression for the maximum strain energy (PE_{max}) and maximum kinetic energy (KE_{max}). The Ritz method requires

minimization of the functional $(T_{\max} - U_{\max})$ with respect to the coefficient α_{ij}, β_{kl} and

γ_{mn} which can be accomplished by setting:

$$\frac{\partial(KE_{\max} - PE_{\max})}{\partial \alpha_{ij}} = 0, \qquad i = i_0, i_0 + 1, ..., I; \qquad j = j_0, j_0 + 1, ..., J;$$

$$\frac{\partial(KE_{\max} - PE_{\max})}{\partial \beta_{k\ell}} = 0, \qquad k = k_0, k_0 + 1, ..., K; \qquad \ell = \ell_0, \ell_0 + 1, ..., L;$$

$$\frac{\partial(KE_{\max} - PE_{\max})}{\partial \gamma_{mn}} = 0, \qquad m = m_0, m_0 + 1, ..., M; \qquad n = n_0, n_0 + 1, ..., N \tag{18}$$

which yields a total of $(I + i_0 + 1) \times (J - j_0 + 1) + (K - k_0 + 1) \times (L - l_0 + 1) + (M - m_0 + 1) \times$

$(N - n_0 + 1)$ simultaneous, linear, homogenous equations in an equal number of

unknowns α_{ij}, β_{kl} and γ_{mn}. Those equations can be described by {K- Ω_2 M} a = 0;

where K and M are the stiffness and mass matrices, respectively; Ω is the frequency

parameter, and a is the vector of unknown coefficients α_{ij}, β_{kl} and γ_{mn}.

The determinant of the coefficient matrix is set equal to zero which will yield a set

of eigenvalues. Substituting each eigenvalue back into (18) yields the corresponding

eigenvector (amplitude ratio) in the usual manner. The mode shape corresponding to each

frequency can be determined by substituting the eigenvector back into the displacement

functions.

3.3. Vibrations of shallow shells

Symmetry of the problem results in 21 combination of classical boundary

conditions for plates [30]. Such symmetry exists here for spherical and hyperbolic

paraboloidal shells (assuming only one version for each of the four possible combinations depending on inplane displacement constraints). This symmetry is mostly lost for cylindrical shells yielding different boundary conditions if $R_y = \infty$ instead of R_x. The symmetry is retained, however, for FFFF, SSSS, CCCC, SSFF, CCSS, CCFF boundaries and whether $R_y = \infty$ or $R_x = \infty$, the same results are obtained.

A shell of square planform (a=b) is selected with a thickness being 20th of that of the side length. Poisson's ratio of 0.3 is selected. Three types of curvature are studied; spherical, cylindrical and hyperbolic paraboloidal. For each of these curvatures, two curvature values are studied; one with the radius five times the side length and the second with the side radius twice the length. Table 3.1 shows the results for the 21 boundary conditions of plates. They are reported here as a reference and to benchmark our results against those of Ref. [30] who obtained exact solutions for 6 of the 21 boundary conditions (two opposite edges being simply supported) and used the Ritz method with beam functions for the remaining 15 boundary conditions. The 49-term results reported here are showing better (smaller) results than those of the 36-term solutions presented in [30]. Ill conditioning is observed here if a higher number of terms is selected in the present analysis.

Table 3.2 shows the 147 term solution for a spherical shell with curvature ratios (a/R) of 0.2 and 0.5. Note here that both the 75-term solutions and 108-term solutions were obtained and convergence is observed to be within 1% for almost all the reported results. In many cases convergence is observed to the third significant figure. Only four

Table 3.3: Frequency parameters $\omega a^2 \sqrt{\rho h / D}$ of shallow cylindrical shells, $R_x = \infty$, a/ b = 1, a / h = 20, v = 0.3.

B.C.	a/Ry = 0.5				a/Ry = 0.2			
FFFF	13.44	21.28	28.12	34.69	13.46	20.12	24.77	34.79
SFFF	6.640	19.43	25.80	26.10	6.643	15.76	25.45	26.01
CFFF	5.164	8.594	24.65	28.10	3.806	8.526	21.98	27.29
SSFF	3.347	17.93	22.68	40.57	3.365	17.61	19.79	38.57
CSFF	6.779	19.53	28.28	45.24	5.621	19.16	25.35	43.42
CCFF	8.440	25.57	29.56	51.11	7.218	24.30	27.08	48.21
SFSF	13.10	16.41	37.22	43.26	10.29	16.18	36.80	39.67
CFSF	18.64	21.00	40.21	53.51	15.33	20.66	39.98	49.68
SSSF	14.78	29.57	44.94	61.91	12.30	28.03	41.88	59.53
CSSF	19.73	33.15	54.56	64.20	17.42	31.42	52.08	64.02
CCSF	20.08	39.72	54.05	74.34	18.13	36.59	52.47	71.62
CFCF	25.12	26.85	44.33	64.01	22.36	26.43	43.59	61.59
SCSF	15.79	36.41	45.24	64.32	13.34	33.60	42.36	63.59
CSCF	25.96	37.66	65.26	66.90	23.67	36.16	63.21	66.65
CCCF	26.75	43.68	66.05	77.50	24.34	40.53	62.56	76.47
SSSS	25.48	49.61	55.84	80.46	20.78	49.39	50.44	79.19
CSSS	29.05	52.11	64.19	87.56	24.60	51.75	59.57	86.50
CCSS	34.16	61.76	66.44	94.71	28.45	60.83	61.66	93.05
CSCS	33.69	55.30	73.85	95.62	29.63	54.99	69.69	94.48
CCCS	37.38	63.67	76.00	99.98	32.87	63.48	71.64	100.78
CCCC	46.08	74.02	78.10	109.68	37.56	72.59	72.66	108.41

significant results are reported here for all the results. The boundary conditions of SFFF, CFFF, SSFF, CSFF, CCFF were among the fastest converging with accuracy achieved up to the third significant results for the first four frequency parameters. Another observation is made here that boundaries where the support is restrained using springs (at x=a and y = b) tend to yield ill-conditioned matrices faster. It should be mentioned here that many of these boundary conditions yields zero frequencies corresponding to rigid body modes. These are not reported.

Compare the results obtained for a spherical shallow shell with a curvature ratio of 0.2 with those obtained for flat plates. It is clear that the spherical curvature, although extremely shallow, had a considerable effect on some frequencies for most boundary conditions. For example, the third mode of the extremely shallow shell having FFFF boundary is 6.4 % higher than plate. The other three modes seem to vary within 1%. For a curvature ratio of 0.5, still a shallow shell, the third mode of FFFF boundary condition shows 34 % higher frequency than that of a plate. Still, even at this curvature the other three frequencies varied very little (within 1%) from that of a plate.

Table 3.4: Frequency parameters $\omega a^2 \sqrt{\rho h / D}$ of shallow cylindrical shells, $R_y = \infty$, a/ b = 1, a / h = 20, v = 0.3.

B.C	a/Rx = 0.5				a/Rx = 0.2			
FFFF	13.44	21.29	28.12	34.69	13.46	20.12	24.77	34.79
SFFF	6.554	14.96	25.16	30.71	6.629	14.93	25.34	26.89
CFFF	3.437	8.274	21.14	28.67	3.468	8.473	21.31	27.98
SSFF	3.347	17.93	22.68	40.57	3.365	17.61	19.79	38.57
CSFF	5.286	22.22	24.74	46.70	5.343	19.82	24.61	43.67
CCFF	8.439	25.57	29.56	51.11	7.218	24.30	27.07	48.21
SFSF	9.554	15.70	38.83	44.55	9.621	16.06	38.09	38.93
CFSF	14.77	25.93	47.87	48.89	15.14	21.60	41.94	49.54
SSSF	11.51	34.82	41.06	59.64	11.66	29.01	41.35	59.29
CSSF	19.51	39.35	51.39	68.96	17.28	32.61	51.41	65.06
CCSF	21.30	43.49	51.98	72.42	18.21	37.38	51.83	71.32
CFCF	35.27	38.05	52.60	60.49	24.74	28.56	45.10	60.86
SCSF	14.72	39.37	41.65	63.66	13.05	34.16	41.69	63.11
CSCF	36.08	45.81	62.47	73.20	25.85	37.36	62.61	67.80
CCCF	36.43	49.52	62.90	81.78	26.51	41.40	62.94	75.78
SSSS	25.48	49.61	55.84	80.46	20.78	49.39	50.44	79.18
CSSS	31.31	58.56	59.67	88.62	25.08	52.83	58.80	86.47
CCSS	34.16	61.76	66.44	94.71	28.36	60.80	61.68	93.01
CSCS	40.65	62.24	69.80	96.37	31.07	55.92	69.17	94.62
CCCS	42.85	69.49	71.49	101.95	33.83	64.52	70.85	100.67
CCCC	46.08	73.88	78.10	109.68	37.56	72.59	72.66	108.41

A similar observation is made for most boundary conditions. For example, the first frequency of a CFFF increased by 7.5 % when a spherical curvature of 0.2 is introduced and increased by 36% when curvature is 0.5. For the boundary conditions of CCFF , CFCF, CCCF, SSSS, CSSS, CCSS, CSCS, CCCS, CCCC, the first frequency increased by more than 10 % when the curvature ratio is 0.2 and more than 50% when it is 0.5; with maximum increase for the simply supported case. Increase in the other frequencies is moderate. The second frequencies of CFSF, SSSF, CSSF, and CCSF seem to be impacted significantly by curvature. Another interesting observation is that some frequencies tend to have a small reduction with the increase in curvature. Such reduction is all within 1%.

Table 3.3 and 3.4 show the 147 term solutions for cylindrical shell with curvature ratios of 0.2 and 0.5. Note here that diagonal symmetry is lost and Table 3.3 shows results for (a/Rx = 0) and Table 3.4 shows the same results for (a/Ry = 0). Note that diagonal symmetry is regained for 6 boundary conditions (FFFF, SSFF, CCFF, SSSS, CCSS and CCCC) and they yield the same results in Table 3.3 and 3.4. Again both the 75-term solutions and 108-term solutions were obtained and convergence is observed to be within 1%. In many cases convergence is observed to the third significant figure. Only four significant results are reported here for all the results. The boundary conditions of SFFF, CFFF, SSFF, CSFF, and CCFF were among the fastest converging with accuracy achieved up to the third significant results for the first four frequency parameters. Boundaries where the support is restrained using springs (at x=a and y = b) tend to yield ill-conditioned matrices faster.

One basic observation is that having the restraint on the curved edge is yielding higher frequencies than having it on the straight edge. This is clear when one compares the CFFF boundary with a/Ry = 0.5 (Table 3.3) with the same boundary with a/Rx = 0.5 (Table 3.4). The first has the curved surface clamped and is 48% higher than plate for the fundamental frequency, while the other is actually slightly lower than plate. The second frequency for SFFF is 29 % higher than its plate equivalent in Table 3.3 (curved edge

Table 3.5:   Frequency parameters $\omega a^2 \sqrt{\rho h / D}$ of shallow hyperbolic paraboloidal shells $R_x / R_y = -1$, a/ b = 1, a / h = 20, v = 0.3.

B.C.	a/R = 0.5				a/R = 0.2			
FFFF	13.41	24.10	31.23	35.45	13.46	21.90	24.24	34.94
SFFF	6.549	19.02	25.57	31.45	6.628	16.06	25.42	26.76
CFFF	4.837	8.317	25.11	29.30	3.814	8.480	22.38	27.89
SSFF	3.309	19.42	24.89	37.88	3.358	18.78	19.32	38.16
CSFF	6.345	24.22	28.37	44.75	5.621	20.37	25.09	43.35
CCFF	7.558	28.62	32.68	51.19	7.071	25.58	27.03	48.22
SFSF	12.91	15.94	41.28	43.78	10.41	16.11	37.45	39.77
CFSF	18.41	25.99	45.72	53.08	15.86	21.64	40.72	50.06
SSSF	14.05	29.79	45.09	59.40	12.20	28.06	41.86	59.11
CSSF	21.71	36.52	54.76	68.60	17.76	32.05	39.42	39.42
CCSF	25.79	41.98	55.37	73.62	19.19	37.03	52.48	71.69
CFCF	36.86	38.15	51.50	63.14	25.07	28.62	44.92	61.47
SCSF	20.85	36.11	45.78	64.32	14.38	33.59	42.43	63.31
CSCF	37.40	45.11	65.41	72.28	26.16	37.49	63.13	67.60
CCCF	38.20	49.57	66.06	81.85	26.78	41.60	63.92	77.26
SSSS	19.25	52.79	52.79	78.46	19.66	49.92	49.92	78.85
CSSS	28.80	56.32	62.38	86.72	24.59	51.78	59.24	80.69
CCSS	34.99	65.23	65.47	93.89	28.52	61.38	61.57	92.91
CSCS	41.15	61.24	72.16	95.50	31.19	55.88	69.64	94.61
CCCS	44.49	69.45	74.64	102.65	34.15	64.16	71.44	100.95
CCCC	50.54	78.44	78.52	109.57	38.51	74.09	73.97	108.00

restraint). When the straight edge is restrained, the frequency for SFFF shallow shell (Table 3.4) is close to that of plate.

The boundary conditions SFSF, CFSF, SSSF, and CSSF in Table 3.3 where there is at least one straight edge free showed higher frequencies than those for plates for the fundamental mode (by more than 10%). The same boundary conditions in Table 3.4 offer a curved free boundary are showing reduction in the fundamental mode when compared with plates. It is interesting that boundaries CCCF, SSSS, CSSS, CCSS, CSCS, CCCS and CCCC are showing much higher frequencies in Table 3.4 than those of plates. The second frequencies of CFSF, SSSF, CFCF are showing much higher frequencies for shells in Table 3.4 as compared with their counter parts in plates.

Table 3.6: Frequency parameters $\omega a^2 \sqrt{\rho h / D}$ of cantilevered shallow cylindrical shells using a finite element analysis (FEA) and Ritz method. a/ b = 1, a / h = 20, v = 0.3.

Curvature	Ritz				FEA			
Plate	3.472	8.512	21.29	27.20	3.493	8.603	21.33	27.29
$a / R_x = 0.2$	3.468	8.473	21.31	27.98	3.481	8.441	21.05	27.70
$a / R_x = 0.5$	3.437	8.274	21.14	28.67	3.585	8.323	20.86	28.04
$a / R_y = 0.2$	3.806	8.526	21.98	27.29	3.797	8.491	21.73	26.99
$a / R_y = 0.5$	5.164	8.594	24.65	28.10	5.176	8.630	24.46	27.82

Table 3.5 shows the 147 term solutions for hyperbolic paraboloidal shell with curvature ratios of 0.2 and 0.5. Note here that diagonal symmetry is regained. Again both

88

the 75-term solutions and 108-term solutions were obtained and convergence is observed to be within 1%. In general, less ill conditioning in the matrices is observed with this shell than spherical and cylindrical ones. In many cases convergence is observed to the third significant figure. Only four significant results are reported here for all the results.
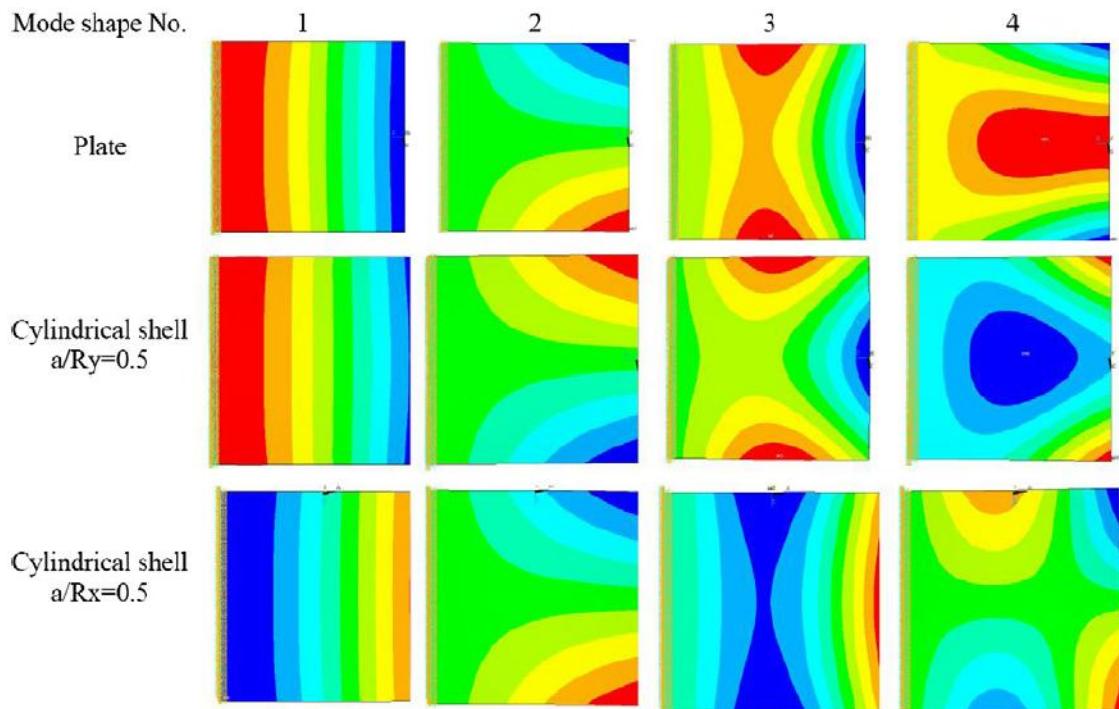
Figure 3.4: Countour plots for the first four mode shapes of a cantilever plate and cylindrical shells.

Similar to earlier findings for spherical and cylindrical shells, the boundary conditions of SFFF, CFFF, SSFF, CSFF, and CCFF were among the fastest converging with accuracy achieved up to the third significant results for the first four frequency parameters.

It is interesting to see that for these shells, the second and third frequencies of FFFF shallow shells are significantly higher than those for plates while the first and fourth are close to those of plates. The second and fourth frequencies of SFFF, the first and third for CFFF, the third for SSFF and CCFF, the first for most other boundaries (with the strange exception of SSSS) deliver much higher frequencies for hyperbolic paraboloidal shells than plates. The second modes have higher frequencies associated with them for CFCF and CCCF boundary conditions.

It should be mentioned here that many of the results presented here have been validated with a commercial finite element software package (ANSYS®). The results show agreement with a fine finite element mesh (100 by 100). Table 3.6 shows an example of such comparisons for a CFFF (cantilvered) boundary condition case. Figure 3.4, shows the mode shapes obtained using finite element for cantilevered plate and cylindrical shell with curvatures of a/Rx = 0.5. Also, in Fig. 3.4, results are given for a cylindrical shell with a/Ry = 0.5. Notice here that the mode shapes of the later are similar to those of the plate. This is confirming the finding that in order to maximize the natural frequencies, one needs to fix the curved edge of the shell.

3.4.   Conclusions

Reasonably accurate natural frequency parameters are delivered for a wide set of boundary conditions. Their accuracy is established through extensive convergence studies that yielded accuracy up to the third significant figure for many situations. These results can be used for benchmarking by researchers in future references. They can also be used

by practicing engineers to gain more insight on the behavior of these shells undergoing a vibrational motion.

In addition, this paper discussed interesting impact of shell curvature on shell frequencies. Only certain modes seem to be impacted significantly by curvature while others do not. Curvature and the boundary condition are interacting to deliver the frequency pattern for each of the 21 cases studie**d.**

3.5.   References

1.   Qatu MS. Vibration of Laminated Shells and Plates. Elsevier, 2004.

2.   Qatu MS. Theory and vibration analysis of laminated barrel thin shells. J Vib Cont 2004; 5: 851-889.

3.   Leissa AW, Qatu MS. Vibration of Continuous Systems. McGraw Hills, 2011.

4.   Qatu MS. Free vibration and static analysis of laminated composite shallow shells. PhD Dissertation, Ohio State University, 1989.

5.   Soedel W. Vibrations of Shells and Plates, 3rd Edition. New York, Marcel Dekker, 2004.

6.   Qatu MS. Review of shallow shell vibration research. Shock Vib Dig 1992; 24: 3-15.

7.   Liew KM, Lim CW, Kitipornchai S. Vibration of shallow shells: a review with bibliography. Appl Mech Rev 1997; 50: 431-444.

8.   Qatu MS. Recent Research Advances in the Dynamic Behavior of Shells. Part 2: Homogeneous Shells. Appl Mech Rev 2002; 55: 415-434.

9.   Qatu MS, Sullivan RW, Wang W. Recent research advances on the dynamic analysis of composite shells: 2000-2009. Comp Struct 2010; 93: 14-31.

10.   Leissa AW, Narita Y. Vibrations of completely free shallow shells of rectangular planform. J Sound Vib 1984; 96: 207-218.

11.   Narita Y, Leissa AW. Vibrations of corner point supported shallow shells of rectangular planform. Earth Engng Struct Dyn 1984; 12: 651-661.

12.   Liew KM, Lim CW. Vibratory characteristics of cantilevered rectangular shallow shells of variable thickness. AIAA J 1994; 32: 387-396.

13.   Liew KM, Lim CW. Vibration of perforated doubly-curved shallow shells with rounded corners. Int J Solids Struct 1994; 31: 1519-1536.

14.   Liew KM, Lim CW. Vibratory behavior of doubly curved shallow shells of curvilinear planform. J Engng Mech 1995; 121: 1277-1284.

15.   Leissa AW, Lee JK, Wang AJ. Vibrations of cantilevered shallow cylindrical shells of rectangular planform. J Sound Vib 1981; 78: 311-328, 1981.

16.   Liew KM, Lim CW, Ong LS. Flexural vibration of doubly-tapered cylindrical shallow shells. Int J Mech Sci 1994; 36: 547-565.

17. Leissa AW, Lee JK, Wang AJ. Vibrations of cantilevered doubly curved shallow shells. Int J Solids Struct 1983; 19: 411-424.

18. Leissa AW, Lee JK, Wang AJ. Rotating blade vibration analysis using shells. J Engng Power 1962; 104: 296-302.

19. Qatu MS. Mode shape analysis of laminated composite shallow shells. J Acoust Soc America 1992; 92: 1509-1520.

20. Qatu MS, Leissa AW. Vibrations of shallow shells with two adjacent edges clamped and the others free. J Mech Struct Mach 1993; 21: 285-301.

21. Qatu MS, Leissa AW. Effects of edge constraints upon shallow shell frequencies. Thin-Walled Struct 1992; 14: 347-379.

22. Qatu MS. Effect of inplane edge constraints on natural frequencies of simply supported doubly curved shallow shells. Thin-Walled Struct 2011; 49: 797-803.

23. Lim CW, Liew KM, Kitipornchai S. Free vibration of pretwisted, cantilevered composite shallow conical shells. American Inst Aeron Astron J 1997; 35: 327-333.

24. Liew KM, Lim MK, Lim CW, Li DB, Zhang YR. Effects of initial twist and thickness variation on the vibration behavior of shallow conical shells. J Sound Vib 1995; 180: 271-296.

25. Liew KM, Lim CW, Ong LS. Vibration of pretwisted cantilever shallow conical shells. Int J Solids Struct 1994; 31: 2463-2476.

26. Lim CW, Liew KM. A pb-2 Ritz formulation for flexural vibration of shallow cylindrical shells of rectangular planform. J Sound Vib 1994; 173: 343-375.

27. Lim CW, Liew KM. Vibratory behaviour of shallow conical shells by a global Ritz formulation. Engng Struct 1995; 17: 63-70.

28. Qatu MS. Vibration studies on completely free shallow shells having triangular and trapezoidal planforms. Appl Acoust 1995; 44: 215-231.

29. Qatu MS. Vibration analysis of cantilevered shallow shells with right triangular and trapezoidal planforms. J Sound Vib 1996; 191: 219-231.

30. Leissa AW. The free vibration of rectangular plates. J Sound Vib 1973; 31: 257-293.

CHAPTER 4

STATIC AND VIBRATION ANALYSES OF THICK DEEP LAMINATED

CYLINDERICAL SHELLS USING 3D AND VARIOUS

SHEAR DEFORMATION

THEORIES

Most of the engineering structures such as automotive, aerospace and submarine structures can be assumed as shells where one dimension of the structure, namely the thickness, is small in comparison to the other two dimensions. A shallow shell (or a plate) is a shell where the radii of its curvature are large (or infinity) compared with the span lengths or half sine waves in a vibration analysis.

Theories that treat shell structures are based upon the three dimensional (3D) theory of elasticity. Thus, 3D analyses of shells are considered the most accurate. However, they are the most complicated and time consuming analyses. Even for today's computers a 3D finite element analysis (FEA) for most practical problems is not feasible. Moreover, composite shells which are fairly common in today's engineering structures, where each layer in the composite shell needs to be one or more element, make 3D analyses even more complicated. Shell theories redeem the difficulty of shell analyses by employing certain assumptions on the behavior of displacements in the thickness direction; First-order expansion of in-plane displacements give rise to first order shear

deformation shell theories (FSDT) and higher-order expansion results in higher order

shear deformation theories (HSDT). Both set of theories reduce the problem from three

dimensions to two dimensions. Classical shell theories, on the other hand, ignore the

effects of shear deformation and rotary inertia. These theories are not accurate for treating

composite shells because such shells are, in general, thicker and more flexible in shear

than metallic ones. In addition, they are not accurate for higher frequencies in a vibration

analysis as the thickness to half sine wave lengths for these frequencies become higher.

On the other hand, HSDTs introduce difficulties when dealing with twisting curvature

and treating boundary terms, e.g. Yaghoubshahi et al. [1]. Thus, FSDT theories are

appropriate for use in moderately thick structures.

In the basic equations derived for shells, difficulties arise as a term $(1+z/R)$

appears in both the strain displacement and stress resultant equations. This term

introduced difficulty early in the development of shell theories. Some researchers

included the term even for thin isotropic shells like Flügge [2] and Vlasov [3] while other

ignored it like Love [4]. Significant analyses of isotropic thin shells showed that indeed

the term is negligible for such shells.

The term was neglected by first analysts of composite thin shells (e.g.

Ambartsumian [5]). While this is understandable for thin shells, the importance of the

inclusion of the term needs to be tested for thicker shells. In addition to the inclusion of

this term, both shear deformation and rotary inertia should be included for composite

thick shells. Early treatment of composite thick shells [6,7] included both shear

deformation and rotary inertia but failed to include the z/R terms. We will refer to these

95

as simply the first order shear deformation theory (FSDT). Interestingly, some researchers developed higher order theories while still neglecting the term, e.g. [8-10]. Qatu [11,12] presented equations where the term is carefully considered in the shell equations for composite deep thick shells. We will refer to his equations as the first order shear deformation shell theory by Qatu (FSDTQ). These equations will be described in detail here. Much of the literature on shell analysis is reviewed [13-16] recently showing a significant portion where inaccurate equations are still used.

The equations of motion with required boundary conditions for doubly curved composite deep and thick shells with twisting curvature are presented using FSDTQ. Clear relations are presented for FSDT showing that they are a simplification from FSDTQ where effects of the depth of shells, $(1+z/R)$ term, is neglected. Moreover, exact static and free vibration solutions for isotropic and symmetric and anti-symmetric orthotropic cross-ply cylindrical shells with shear diaphragm boundary conditions for different length-to-thickness and length-to-radius ratios varying from thin and shallow to moderately thick and very deep shells are obtained using both FSDT and FSDTQ and compared with those of a converged 3D finite element analysis obtained using a commercial software package (ANSYS®). Dimensionless transverse displacement, moment and force resultants in a static analysis and the first five natural frequency parameters in the dynamic analysis are studied for eighteen different cylindrical shells and compared with 3D results. Also, Errors of FSDTQ and FSDT results (when comparing them to those of the 3D results) are obtained and discussed.

96

4.1. Static and free vibration formulation of the shells

A doubly curved shell with in-plane axes α and β, and a normal to the middle-plane axis z, principal radii R_α and R_β in α and β directions, respectively, and a twisting radius $R_{\alpha\beta}$ is considered. The boundaries of the shell coincide with the principal axes. The Hamilton's principle [17] for the equations of motion of a body with surface S and volume V between two arbitrary time intervals t_0 and t_1 requires that

$$\int_{t_0}^{t_1} \{ \int_V [\sigma_\alpha \delta\varepsilon_\alpha + \sigma_\beta \delta\varepsilon_\beta + \sigma_z \delta\varepsilon_z + \sigma_{\alpha\beta} \delta\gamma_{\alpha\beta} + \sigma_{\alpha z} \delta\gamma_{\alpha z} + \sigma_{\beta z} \delta\gamma_{\beta z}$$

$$- \rho(\dot{u}\delta\dot{u} + \dot{v}\delta\dot{v} + \dot{w}\delta\dot{w})]dV - \int_S \delta W_{ext} dS dt = 0, \tag{1}$$

where $\sigma_{...}$ and $\varepsilon_{...}$ are stress and strain components, respectively, ρ is the mass density, W_{ext} is external work, and $\dot{u}, \dot{v},$ and $\dot{w}$ are velocity components in the $\alpha, \beta,$ and z-directions, respectively. Employing the first-order shear deformation model, the displacement components approximate as [e.g. 17]

$$u(\alpha, \beta, z, t) = u_0(\alpha, \beta, t) + z\psi_\alpha(\alpha, \beta, t),$$

$$v(\alpha, \beta, z, t) = v_0(\alpha, \beta, t) + z\psi_\beta(\alpha, \beta, t),$$

$$w(\alpha, \beta, z, t) = w_0(\alpha, \beta, t), \tag{2}$$

where $-h/2 \le z \le h/2$ and h is the shell thickness, u_0, v_0, and w_0 are midsurface displacements of the shell, and ψ_α and ψ_β are midsurface rotations. Eqs. (2) constitute

97

the only assumption needed to reduce a 3D elasticity equations in curvilinear coordinates to the shell theory by Qatu [11,12,17]. The strain-displacement relationships in the principal coordinates of a doubly-curved shell are [17]

$$\varepsilon_\alpha = \frac{1}{(1+z/R_\alpha)}(\frac{1}{A}\frac{\partial u}{\partial \alpha} + \frac{v}{AB}\frac{\partial A}{\partial \beta} + \frac{w}{R_\alpha}),$$

$$\varepsilon_\beta = \frac{1}{(1+z/R_\beta)}(\frac{1}{B}\frac{\partial v}{\partial \beta} + \frac{u}{AB}\frac{\partial B}{\partial \alpha} + \frac{w}{R_\beta}),$$

$$\varepsilon_z = \frac{\partial w}{\partial z},$$

$$\gamma_{\alpha\beta} = \frac{1}{(1+z/R_\alpha)}(\frac{1}{A}\frac{\partial v}{\partial \alpha} - \frac{u}{AB}\frac{\partial A}{\partial \beta} + \frac{w}{R_{\alpha\beta}}) + \frac{1}{(1+z/R_\beta)}(\frac{1}{B}\frac{\partial u}{\partial \beta} - \frac{v}{AB}\frac{\partial B}{\partial \alpha} + \frac{w}{R_{\alpha\beta}}),$$

$$\gamma_{\alpha z} = \frac{1}{A(1+z/R_\alpha)}\frac{\partial w}{\partial \alpha} + A(1+z/R_\alpha)\frac{\partial}{\partial z}(\frac{u}{A(1+z/R_\alpha)}) - \frac{v}{R_{\alpha\beta}(1+z/R_\alpha)},$$

$$\gamma_{\beta z} = \frac{1}{B(1+z/R_\beta)}\frac{\partial w}{\partial \beta} + B(1+z/R_\beta)\frac{\partial}{\partial z}(\frac{v}{B(1+z/R_\beta)}) - \frac{u}{R_{\alpha\beta}(1+z/R_\beta)}, \qquad (3)$$

In Eqs (5), $A^2 = (\partial \bar{r}/\partial \alpha).(\partial \bar{r}/\partial \alpha)$, $B^2 = (\partial \bar{r}/\partial \beta).(\partial \bar{r}/\partial \beta)$ where r is the position vector of a point on the middle surface of the shell. By substituting Eqs (2) into (3), strain-displacement equations become

$$\varepsilon_\alpha = \frac{1}{(1+z/R_\alpha)}(\varepsilon_{0\alpha} + z\kappa_\alpha), \qquad \varepsilon_\beta = \frac{1}{(1+z/R_\beta)}(\varepsilon_{0\beta} + z\kappa_\beta), \qquad \varepsilon_z = 0,$$

$$\varepsilon_{\alpha\beta} = \frac{1}{(1+z/R_\alpha)}(\varepsilon_{0\alpha\beta} + z\kappa_{\alpha\beta}), \qquad \varepsilon_{\beta\alpha} = \frac{1}{(1+z/R_\beta)}(\varepsilon_{0\beta\alpha} + z\kappa_{\beta\alpha}),$$

$$\gamma_{\alpha z}=\frac{1}{(1+z/R_{\alpha})}[\gamma_{0\alpha z}-z(\psi_{\beta}/R_{\alpha\beta})], \qquad \gamma_{\beta z}=\frac{1}{(1+z/R_{\beta})}[\gamma_{0\beta z}-z(\psi_{\alpha}/R_{\alpha\beta})], \tag{4}$$

The functions on the right-hand side of Eqs (4) are

$$\varepsilon_{0\alpha}=\frac{1}{A}\frac{\partial u_0}{\partial\alpha}+\frac{v_0}{AB}\frac{\partial A}{\partial\beta}+\frac{w_0}{R_{\alpha}}, \qquad \varepsilon_{0\beta}=\frac{1}{B}\frac{\partial v_0}{\partial\beta}+\frac{u_0}{AB}\frac{\partial B}{\partial\alpha}+\frac{w_0}{R_{\beta}},$$

$$\varepsilon_{0\alpha\beta}=\frac{1}{A}\frac{\partial v_0}{\partial\alpha}-\frac{u_0}{AB}\frac{\partial A}{\partial\beta}+\frac{w_0}{R_{\alpha\beta}}, \qquad \varepsilon_{0\beta\alpha}=\frac{1}{B}\frac{\partial u_0}{\partial\beta}-\frac{v_0}{AB}\frac{\partial B}{\partial\alpha}+\frac{w_0}{R_{\alpha\beta}},$$

$$\gamma_{0\alpha z}=\frac{1}{A}\frac{\partial w_0}{\partial\alpha}-\frac{u_0}{R_{\alpha}}-\frac{v_0}{R_{\alpha\beta}}+\psi_{\alpha}, \qquad \gamma_{0\beta z}=\frac{1}{B}\frac{\partial w_0}{\partial\beta}-\frac{v_0}{R_{\beta}}-\frac{u_0}{R_{\alpha\beta}}+\psi_{\beta},$$

$$\kappa_{\alpha}=\frac{1}{A}\frac{\partial\psi_{\alpha}}{\partial\alpha}+\frac{\psi_{\beta}}{AB}\frac{\partial A}{\partial\beta}, \qquad \kappa_{\beta}=\frac{1}{B}\frac{\partial\psi_{\beta}}{\partial\beta}+\frac{\psi_{\alpha}}{AB}\frac{\partial B}{\partial\alpha},$$

$$\kappa_{\alpha\beta}=\frac{1}{A}\frac{\partial\psi_{\beta}}{\partial\alpha}-\frac{\psi_{\alpha}}{AB}\frac{\partial A}{\partial\beta}, \qquad \kappa_{\beta\alpha}=\frac{1}{B}\frac{\partial\psi_{\alpha}}{\partial\beta}-\frac{\psi_{\beta}}{AB}\frac{\partial B}{\partial\alpha}. \tag{5}$$

The stress resultants are defined as

$$\begin{bmatrix} N_{\alpha} & N_{\alpha\beta} & Q_{\alpha} & M_{\alpha} & M_{\alpha\beta} & P_{\alpha} \end{bmatrix}^{T}=\int_{-h/2}^{h/2}\begin{bmatrix} \sigma_{\alpha} & \sigma_{\alpha\beta} & \sigma_{\alpha z} & z\sigma_{\alpha} & z\sigma_{\alpha\beta} & z\sigma_{\alpha z} \end{bmatrix}^{T}(1+\frac{z}{R_{\beta}})dz,$$

$$\begin{bmatrix} N_{\beta} & N_{\beta\alpha} & Q_{\beta} & M_{\beta} & M_{\beta\alpha} & P_{\beta} \end{bmatrix}^{T}=\int_{-h/2}^{h/2}\begin{bmatrix} \sigma_{\beta} & \sigma_{\beta\alpha} & \sigma_{\beta z} & z\sigma_{\beta} & z\sigma_{\beta\alpha} & z\sigma_{\beta z} \end{bmatrix}^{T}(1+\frac{z}{R_{\alpha}})dz, \tag{6}$$

where the superscript T stands for the transpose of a vector. The applied load per unit area on the middle surface of a shell is taken as $\bar{q}=q_{\alpha}\bar{e}_{\alpha}+q_{\beta}\bar{e}_{\beta}+q_{z}\bar{e}_{z}$, where the unit vectors $\bar{e}_{\alpha}$ and $\bar{e}_{\beta}$ are tangent to the principal axes and $\bar{e}_{z}$ is perpendicular to the shell

99

surface, respectively. Let $\sigma_{0\alpha}$, $\sigma_{0\alpha\beta}$ and $\sigma_{0\alpha z}$ be the components of applied traction on the edges α = constant and $\sigma_{0\beta}$, $\sigma_{0\beta\alpha}$ and $\sigma_{0\beta z}$ be the components of applied traction on the edges β = constant. The external work done by external loads on the shell yields

$$\delta w_{ext} = \int_{t_0}^{t_1} [\int_{\alpha}\int_{\beta} (q_\alpha \delta u + q_\beta \delta v + q_z \delta w) AB \, d\alpha \, d\beta + \oint_{\beta}\int_{-h/2}^{h/2} (\sigma_{0\alpha}\delta u + \sigma_{0\alpha\beta}\delta v$$
$$+ \sigma_{0\alpha z}\delta w) B(1+z/R_\beta) dz \, d\beta + \oint_{\alpha}\int_{-h/2}^{h/2} (\sigma_{0\beta}\delta v + \sigma_{0\beta\alpha}\delta u + \sigma_{0\beta z}\delta w) A(1+z/R_\alpha) dz \, d\alpha] dt. \quad (7)$$

In Eq. (7), the second and third integrals should be taken along the boundaries of the shell. Substituting Eqs. (6) into Eq. (7), the resultant equation with Eqs. (4) into Eq. (1), employing the definitions (6), setting $\sigma_z = 0$, and carrying out the required manipulations results in following equations of motion [13]

$$\frac{\partial(BN_\alpha)}{\partial\alpha} + \frac{\partial(AN_{\beta\alpha})}{\partial\beta} + N_{\alpha\beta}\frac{\partial A}{\partial\beta} - N_\beta\frac{\partial B}{\partial\alpha} + \frac{AB}{R_\alpha}Q_\alpha + \frac{AB}{R_{\alpha\beta}}Q_\beta + ABq_\alpha = AB\bar{I}_1\ddot{u}_0 + AB\bar{I}_2\ddot{\psi}_\alpha,$$

$$\frac{\partial(AN_\beta)}{\partial\beta} + \frac{\partial(BN_{\alpha\beta})}{\partial\alpha} + N_{\beta\alpha}\frac{\partial B}{\partial\alpha} - N_\alpha\frac{\partial A}{\partial\beta} + \frac{AB}{R_\beta}Q_\beta + \frac{AB}{R_{\alpha\beta}}Q_\alpha + ABq_\beta = AB\bar{I}_1\ddot{v}_0 + AB\bar{I}_2\ddot{\psi}_\beta,$$

$$\frac{\partial(BQ_\alpha)}{\partial\alpha} + \frac{\partial(AQ_\beta)}{\partial\beta} - AB(\frac{N_\alpha}{R_\alpha} + \frac{N_{\alpha\beta}+N_{\beta\alpha}}{R_{\alpha\beta}} + \frac{N_\beta}{R_\beta}) + ABq_z = AB\bar{I}_1\ddot{w}_0,$$

$$\frac{\partial(BM_\alpha)}{\partial\alpha} + \frac{\partial(AM_{\beta\alpha})}{\partial\beta} + M_{\alpha\beta}\frac{\partial A}{\partial\beta} - M_\beta\frac{\partial B}{\partial\alpha} - ABQ_\alpha + \frac{AB}{R_{\alpha\beta}}P_\beta = AB\bar{I}_2\ddot{u}_0 + AB\bar{I}_3\ddot{\psi}_\alpha,$$

$$\frac{\partial(AM_\beta)}{\partial\beta} + \frac{\partial(BM_{\alpha\beta})}{\partial\alpha} + M_{\beta\alpha}\frac{\partial B}{\partial\alpha} - M_\alpha\frac{\partial A}{\partial\beta} - ABQ_\beta + \frac{AB}{R_{\alpha\beta}}P_\alpha = AB\bar{I}_2\ddot{v}_0 + AB\bar{I}_3\ddot{\psi}_\beta, \quad (8)$$

where in Eq. (8)

$$\bar{I}_i = \left(I_i + I_{i+1} \left(\frac{1}{R_\alpha} + \frac{1}{R_\beta} \right) + \frac{I_{i+2}}{R_\alpha R_\beta} \right), \qquad i = 1, 2, 3,$$ (9)

where $[I_1, I_2, I_3, I_4, I_5] = \sum_{k=1}^{N} \int_{h_{k-1}}^{h_k} \rho^{(k)} [1, z, z^2, z^3, z^4] dz$. The stress resultant terms are shown

in Figs 2.3 and 2.4. Also, the remaining terms in the Hamilton's principle functional lead

to the natural and geometric boundary conditions for the shell. The boundary data on an

edge $\alpha = $ constant are

either $\quad N_{0\alpha} - N_\alpha = 0 \qquad$ or $\qquad u_0 = $ known

either $\quad N_{0\alpha\beta} - N_{\alpha\beta} = 0 \qquad$ or $\qquad v_0 = $ known

either $\quad Q_{0\alpha} - Q_\alpha = 0 \qquad$ or $\qquad w_0 = $ known

either $\quad M_{0\alpha} - M_\alpha = 0 \qquad$ or $\qquad \psi_\alpha = $ known

either $\quad M_{0\alpha\beta} - M_{\alpha\beta} = 0 \qquad$ or $\qquad \psi_\beta = $ known (10)

Depending upon the type of shell boundary, five boundary conditions should be chosen

from the above cases at each edge. The stress-strain relationships for a single orthotropic

lamina in a shell is

101

$$
\begin{Bmatrix} \sigma_{11} \\ \sigma_{22} \\ \tau_{2n} \\ \tau_{1n} \\ \tau_{12} \end{Bmatrix} = \begin{bmatrix} \bar{Q}_{11} & \bar{Q}_{12} & 0 & 0 & \bar{Q}_{16} \\ \bar{Q}_{12} & \bar{Q}_{22} & 0 & 0 & \bar{Q}_{26} \\ 0 & 0 & \bar{Q}_{44} & \bar{Q}_{45} & 0 \\ 0 & 0 & \bar{Q}_{45} & \bar{Q}_{55} & 0 \\ \bar{Q}_{16} & \bar{Q}_{26} & 0 & 0 & \bar{Q}_{66} \end{bmatrix} \begin{Bmatrix} \varepsilon_{11} \\ \varepsilon_{22} \\ \gamma_{2n} \\ \gamma_{1n} \\ \gamma_{12} \end{Bmatrix}
$$

(11)

The components of the matrix of material properties in Eqs (11) in terms of the stiffness coefficients in the direction of principal axes of material orthotropy may be written as

$$
\bar{Q}_{11} = Q_{11}m^4 + 2(Q_{12} + 2Q_{66})m^2 n^2 + Q_{22}n^4, \quad \bar{Q}_{12} = (Q_{11} + Q_{22} - 4Q_{66})m^2 n^2 + Q_{12}(m^4 + n^4),
$$

$$
\bar{Q}_{22} = Q_{11}n^4 + 2(Q_{12} + 2Q_{66})m^2 n^2 + Q_{22}m^4, \quad \bar{Q}_{45} = (Q_{55} - Q_{44})mn,
$$

$$
\bar{Q}_{16} = (Q_{11} - Q_{12} - 2Q_{66})m^3 n + (Q_{12} - Q_{22} + 2Q_{66})mn^3, \quad \bar{Q}_{44} = Q_{44}m^2 + Q_{55}n^2,
$$

$$
\bar{Q}_{26} = (Q_{11} - Q_{12} - 2Q_{66})mn^3 + (Q_{12} - Q_{22} + 2Q_{66})m^3 n, \quad \bar{Q}_{55} = Q_{44}n^2 + Q_{55}m^2,
$$

$$
\bar{Q}_{66} = (Q_{11} + Q_{22} - 2Q_{12})m^2 n^2 + Q_{66}(m^2 - n^2)^2
$$

(12)

In Eqs (12), $m = \cos\theta$, $n = \sin\theta$, where θ is the angle between a principal axis of material orthotropy and α-axis. The components of the material properties in Eqs (12) in terms of engineering constants are

$$
Q_{11} = E_1 / \Delta, \qquad Q_{12} = E_1 v_{21} / \Delta, \qquad Q_{22} = E_2 / \Delta,
$$

$$
Q_{44} = G_{23}, \qquad Q_{55} = G_{13}, \qquad Q_{66} = G_{12},
$$

(13)

where $\Delta = 1 - v_{12}v_{21}$. We substitute Eqs (4) into Eqs (11) the resultant equations into Eqs (6), carry out the integration in the thickness direction for a shell composed of M layers

102

while ignoring terms of $O(z/R)^2$ and arrive at the following relationships for the stress resultants [11,12,13,17]

$$
\begin{bmatrix} N_\alpha \\ N_\beta \\ N_{\alpha\beta} \\ N_{\beta\alpha} \\ M_\alpha \\ M_\beta \\ M_{\alpha\beta} \\ M_{\beta\alpha} \end{bmatrix} =
\begin{bmatrix}
\bar{A}_{11} & A_{12} & \bar{A}_{16} & A_{16} & \bar{B}_{11} & B_{12} & \bar{B}_{16} & B_{16} \\
A_{12} & \hat{A}_{22} & A_{26} & \hat{A}_{26} & B_{12} & \hat{B}_{22} & B_{26} & \hat{B}_{26} \\
\bar{A}_{16} & A_{26} & \bar{A}_{66} & A_{66} & \bar{B}_{16} & B_{26} & \bar{B}_{66} & B_{66} \\
A_{16} & \hat{A}_{26} & A_{66} & \hat{A}_{66} & B_{16} & \hat{B}_{26} & B_{66} & \hat{B}_{66} \\
\bar{B}_{11} & B_{12} & \bar{B}_{16} & B_{16} & \bar{D}_{11} & D_{12} & \bar{D}_{16} & D_{16} \\
B_{12} & \hat{B}_{22} & B_{26} & \hat{B}_{26} & D_{12} & \hat{D}_{22} & D_{26} & \hat{D}_{26} \\
\bar{B}_{16} & B_{26} & \bar{B}_{66} & B_{66} & \bar{D}_{16} & D_{26} & \bar{D}_{66} & D_{66} \\
B_{16} & \hat{B}_{26} & B_{66} & \hat{B}_{66} & D_{16} & \hat{D}_{26} & D_{66} & \hat{D}_{66}
\end{bmatrix}
\begin{bmatrix} \varepsilon_{0\alpha} \\ \varepsilon_{0\beta} \\ \varepsilon_{0\alpha\beta} \\ \varepsilon_{0\beta\alpha} \\ \kappa_\alpha \\ \kappa_\beta \\ \kappa_{\alpha\beta} \\ \kappa_{\beta\alpha} \end{bmatrix},
$$

$$
\begin{bmatrix} Q_\alpha \\ Q_\beta \\ P_\alpha \\ P_\beta \end{bmatrix} =
\begin{bmatrix}
\bar{A}_{55} & A_{45} & \bar{B}_{55} & B_{45} \\
A_{45} & \hat{A}_{44} & B_{45} & \hat{B}_{44} \\
\bar{B}_{55} & B_{45} & \bar{D}_{55} & D_{45} \\
B_{45} & \hat{B}_{44} & D_{45} & \hat{D}_{44}
\end{bmatrix}
\begin{bmatrix} \gamma_{0\alpha z} \\ \gamma_{0\beta z} \\ -\psi_\alpha / R_{\alpha\beta} \\ -\psi_\beta / R_{\alpha\beta} \end{bmatrix},
\tag{14}
$$

$$
\left.
\begin{aligned}
\bar{A}_{ij} &= A_{ij} - c_0 B_{ij}, & \hat{A}_{ij} &= A_{ij} + c_0 B_{ij}, \\
\bar{B}_{ij} &= B_{ij} - c_0 D_{ij}, & \hat{B}_{ij} &= B_{ij} + c_0 D_{ij}, \\
\bar{D}_{ij} &= D_{ij} - c_0 E_{ij}, & \hat{D}_{ij} &= D_{ij} + c_0 E_{ij},
\end{aligned}
\right\} \quad i,j = 1,2,4,5,6,
\tag{15}
$$

where $c_0 = \left(\dfrac{1}{R_\alpha} - \dfrac{1}{R_\beta} \right)$ and

$$
\left.
\begin{aligned}
A_{ij} &= \sum_{k=1}^{N} \bar{Q}_{ij}^{(k)} (h_k - h_{k-1}) \\
B_{ij} &= \frac{1}{2} \sum_{k=1}^{N} \bar{Q}_{ij}^{(k)} (h_k^2 - h_{k-1}^2) \\
D_{ij} &= \frac{1}{3} \sum_{k=1}^{N} \bar{Q}_{ij}^{(k)} (h_k^3 - h_{k-1}^3) \\
E_{ij} &= \frac{1}{4} \sum_{k=1}^{N} \bar{Q}_{ij}^{(k)} (h_k^4 - h_{k-1}^4)
\end{aligned}
\right\} \quad i,j = 1,2,6,
$$

$$
\left.
\begin{aligned}
A_{ij} &= \sum_{k=1}^{N} K_\alpha K_\beta \bar{Q}_{ij}^{(k)}(h_k - h_{k-1}) \\
B_{ij} &= \frac{1}{2} \sum_{k=1}^{N} K_\alpha K_\beta \bar{Q}_{ij}^{(k)}(h_k^2 - h_{k-1}^2) \\
D_{ij} &= \frac{1}{3} \sum_{k=1}^{N} K_\alpha K_\beta \bar{Q}_{ij}^{(k)}(h_k^3 - h_{k-1}^3)
\end{aligned}
\right\} \qquad i,j = 4,5,
\tag{16}
$$

$h_k - h_{k-1}$ is the thickness of k-th layer, and $K_\alpha,$ and K_β are the shear correction factors in α and β directions, respectively. Substitution of $\bar{\Lambda}_{ij}, \hat{\Lambda}_{ij}$ by $\Lambda_{ij}, i,j = 1,2,4,5,6,$ where $\Lambda = A, B, D$ leads to the formulation of FSDT which ignores effects of the shell depth [11, 12]. It is worth mentioning that for spherical shells $R_\alpha = R_\beta,$ $\bar{\Lambda}_{ij} = \hat{\Lambda}_{ij} = \Lambda_{ij}, i,j = 1,2,4,5,6, \quad \Lambda = A, B, D$, thus FSDTQ and FSDT are identical. Other publications which used a similar approach include those in references [18-20].

4.2.   Exact solution for cylindrical shells

A cylindrical laminated shell with length a and arc b under load per unit area, q in the thickness direction is considered here. Therefore, $A = B = 1,$ $1/R_\alpha = 1/R_{\alpha\beta} = 0$, and $R_\beta = R$ should be substituted in Eqs (6), (8-9), and (14) to arrive to the required formulations of cylindrical shells for both FSDT and FSDTQ. Consequently, Eqs (5) for cylindrical shells become

$$
\varepsilon_{0\alpha} = \frac{\partial u_0}{\partial \alpha}, \qquad \varepsilon_{0\beta} = \frac{\partial v_0}{\partial \beta} + \frac{w_0}{R}, \qquad \varepsilon_{0\alpha\beta} = \frac{\partial v_0}{\partial \alpha}, \qquad \varepsilon_{0\beta\alpha} = \frac{\partial u_0}{\partial \beta}, \qquad \gamma_{0\alpha z} = \frac{\partial w_0}{\partial \alpha} + \psi_\alpha,
$$

$$\gamma_{0\beta z}=\frac{\partial w_0}{\partial \beta}-\frac{v_0}{R}+\psi_\beta, \quad \kappa_\alpha=\frac{\partial \psi_\alpha}{\partial \alpha}, \quad \kappa_\beta=\frac{\partial \psi_\beta}{\partial \beta}, \quad \kappa_{\alpha\beta}=\frac{\partial \psi_\beta}{\partial \alpha}, \quad \kappa_{\beta\alpha}=\frac{\partial \psi_\alpha}{\partial \beta}. \tag{17}$$

In Eq. (15), $c_0=-1/R$, the first equation of (14) is still valid and the second equation of (14) becomes

$$\begin{bmatrix} Q_\alpha \\ Q_\beta \end{bmatrix}=\begin{bmatrix} \bar{A}_{55} & A_{45} \\ A_{45} & \hat{A}_{44} \end{bmatrix}\begin{bmatrix} \gamma_{0\alpha z} \\ \gamma_{0\beta z} \end{bmatrix}. \tag{18}$$

Equations of motion (8) for the cylindrical shell reduce to

$$\frac{\partial N_\alpha}{\partial \alpha}+\frac{\partial N_{\beta\alpha}}{\partial \beta}=\bar{I}_1\ddot{u}_0+\bar{I}_2\ddot{\psi}_\alpha, \qquad \frac{\partial N_\beta}{\partial \beta}+\frac{\partial N_{\alpha\beta}}{\partial \alpha}+\frac{Q_\beta}{R}=\bar{I}_1\ddot{v}_0+\bar{I}_2\ddot{\psi}_\beta,$$

$$\frac{\partial Q_\alpha}{\partial \alpha}+\frac{\partial Q_\beta}{\partial \beta}-\frac{N_\beta}{R}+q=\bar{I}_1\ddot{w}_0, \qquad \frac{\partial M_\alpha}{\partial \alpha}+\frac{\partial M_{\beta\alpha}}{\partial \beta}-Q_\alpha=\bar{I}_2\ddot{u}_0+\bar{I}_3\ddot{\psi}_\alpha,$$

$$\frac{\partial M_\beta}{\partial \beta}+\frac{\partial M_{\alpha\beta}}{\partial \alpha}-Q_\beta=\bar{I}_2\ddot{v}_0+\bar{I}_3\ddot{\psi}_\beta, \tag{19}$$

where $\bar{I}_i=\left(I_i+\frac{I_{i+1}}{R}\right)$, $i=1,2,3$. For a cross-ply cylindrical shell, $\Lambda_{16}=\Lambda_{26}=\Lambda_{45}=0$, $\Lambda=A,B,D,$ and E. For such shell with shear diaphragm boundary conditions, the following relations for middle surface displacements and rotations satisfy these conditions [17]

$$u_0=U_{mn}\cos(\alpha_m\alpha)\sin(\beta_n\beta)\sin(\omega_{mn}t), \quad v_0=V_{mn}\sin(\alpha_m\alpha)\cos(\beta_n\beta)\sin(\omega_{mn}t),$$

$$w_0=W_{mn}\sin(\alpha_m\alpha)\sin(\beta_n\beta)\sin(\omega_{mn}t), \quad \psi_\alpha=\psi_{\alpha mn}\cos(\alpha_m\alpha)\sin(\beta_n\beta)\sin(\omega_{mn}t),$$

$$\psi_\beta = \psi_{\beta mn} \sin(\alpha_m \alpha) \cos(\beta_n \beta) \sin(\omega_{mn} t). \tag{20}$$

where $\alpha_m = m\pi / a$ and $\beta_n = n\pi / b$. Substituting Eqs (20) into stress resultants relations and the results into Eq. (19) leads to the following five homogenous algebraic system of equations

$$\{[K] + \omega_{mn}^2 [M]\} \{\Delta\} = \{Q\}, \tag{21}$$

where

$$\{\Delta\} = \{U_{mn}, V_{mn}, W_{mn}, \psi_{\alpha mn}, \psi_{\beta mn}\}^T, \qquad \{Q\} = \{0, 0, q_{mn}, 0, 0\}^T,$$

$$K_{11} = -\bar{A}_{11}\alpha_m^2 - \hat{A}_{66}\beta_n^2, \qquad K_{12} = K_{21} = -(A_{12} + A_{66})\alpha_m\beta_n, \qquad K_{13} = K_{31} = \frac{A_{12}}{R}\alpha_m,$$

$$K_{14} = K_{41} = -\bar{B}_{11}\alpha_m^2 - \bar{B}_{66}\beta_n^2, \qquad K_{15} = K_{51} = -(B_{12} + B_{66})\alpha_m\beta_n,$$

$$K_{22} = -\bar{A}_{66}\alpha_m^2 - A_{22}\beta_n^2 - \frac{\hat{A}_{44}}{R^2}, \quad K_{23} = K_{32} = \frac{\hat{A}_{22} + \hat{A}_{44}}{R}\beta_n, \quad K_{24} = K_{42} = -(B_{12} + B_{16})\alpha_m\beta_n,$$

$$K_{25} = K_{52} = -\bar{B}_{66}\alpha_m^2 - \hat{B}_{22}\beta_n^2 + \frac{\hat{A}_{44}}{R}, \qquad K_{33} = -\bar{A}_{55}\alpha_m^2 - \bar{A}_{44}\beta_n^2 - \frac{\hat{A}_{22}}{R^2},$$

$$K_{34} = K_{43} = [-\bar{A}_{55} + \frac{B_{12}}{R}]\alpha_m, \quad K_{35} = K_{53} = [-\hat{A}_{44} + \frac{\hat{B}_{22}}{R}]\beta_n, \quad K_{44} = -\bar{A}_{55} - \hat{D}_{11}\alpha_m^2 - \hat{D}_{66}\beta_n^2,$$

$$K_{45} = K_{54} = -(D_{12} + D_{66})\alpha_m\beta_n, \qquad K_{55} = -\hat{A}_{44} - \bar{D}_{66}\alpha_m^2 - \hat{D}_{22}\beta_n^2, \tag{22}$$

q_{mn} are coefficients of double Fourier expansion of applied load q, and the non-zero components of M are

106

$$M_{ij} = M_{ji}, \qquad M_{11} = M_{22} = M_{33} = I_1 + \frac{I_2}{R},$$

$$M_{14} = M_{25} = I_2 + \frac{I_3}{R}, \qquad M_{44} = M_{55} = I_3 + \frac{I_4}{R}. \tag{23}$$

Eqs. (21) are actually valid for forced vibration analysis. For a free vibration problem, it suffices to put $\{Q\} = \{0\}$ in Eq. (21) and solve the resulting eigenvalue problems to find the natural frequencies, ω_{mn}, and corresponding mode shapes, $\{\Delta\}$. For static analyses, the natural frequency term $\omega_{mn} = 0$ should be substituted into Eq. (21). The resultant algebraic system of equations for middle surface displacements and rotations should then be solved. Stress resultants are first recovered from midsurface strain and curvature changes, then strains and stresses are recovered from the displacements in a normal manner.

4.3. Numerical results

In all of the following examples, cylindrical shells with length-to-arc ratio is one (i.e. $a/b = 1$), shear correction factors in both directions are $k^2 = 5/6$, and $v = 0.25$ for isotropic materials, and $E_1/E_2 = 25$, $G_{12}/E_2 = 0.5$, $G_{23}/E_2 = 0.2$, $G_{13} = G_{12}$, and $v_{12} = 0.25$ for orthotropic materials are considered. In static analyses, shells are under uniformly distributed load q. Thus, using a Fourier analysis, one finds the coefficients of a Fourier transform as $q_{mn} = 16q/mn\pi^2$ in Eq. (22). Numerical investigation showed that

the terms m and n did not need to exceed fifty for convergence of the results. Dimensionless transverse displacement, moment and force resultants

$$w^* = 10^3 E_2 h^3 w / q_n a^4, \quad M_i^* = 10^3 M_i / qa^2, \qquad N_i^* = 10^3 N_i / qa^3, \tag{24}$$

where $i = \alpha, \beta$, at the center of the shell are calculated based upon both FSDT and FSDTQ. In the dynamic analyses, the first five natural frequency parameters $\Omega_i = \omega_i a^2 \sqrt{\rho E_2 / h^2}, i = 1,...,5$ are obtained from those theories. In both analyses the results are calculated for isotropic, three-ply symmetric [0/90/0], and two-ply anti-symmetric [90/0] shells for different thickness ratios a / h and depth ratios a / R. Presented results from both FSDT and FSDTQ are compared against each others and against those obtained using 3D elasticity from finite element method (FEM). Figure 4.1 shows the mesh pattern of a typical cylindrical shell modeled using FEM wherein 3D elements are used. Moreover, W and V are set to zero at $\alpha -$ constant planes at boundary edges to make sure that $v_0 = w_0 = \psi_\beta = 0$ in presented theories and q is divided into two positive and negative pressures at the top and bottom planes of the shell; respectively, such that the whole force on the shell is equal to abq. Table 4.1 shows a convergence study for the first five natural frequency parameters obtained by three dimensional FEM analysis for an isotropic shell with a thickness ratio $a / h = 10$ (moderately thick shell) and a depth ratio $a / R = 2$ (deep shell). It is shown there that natural frequencies are converging to the fifth decimal place using a 30 by 30 by 4 quadratic solid elements. A smaller size mesh showed good convergence of the fundamental frequency.
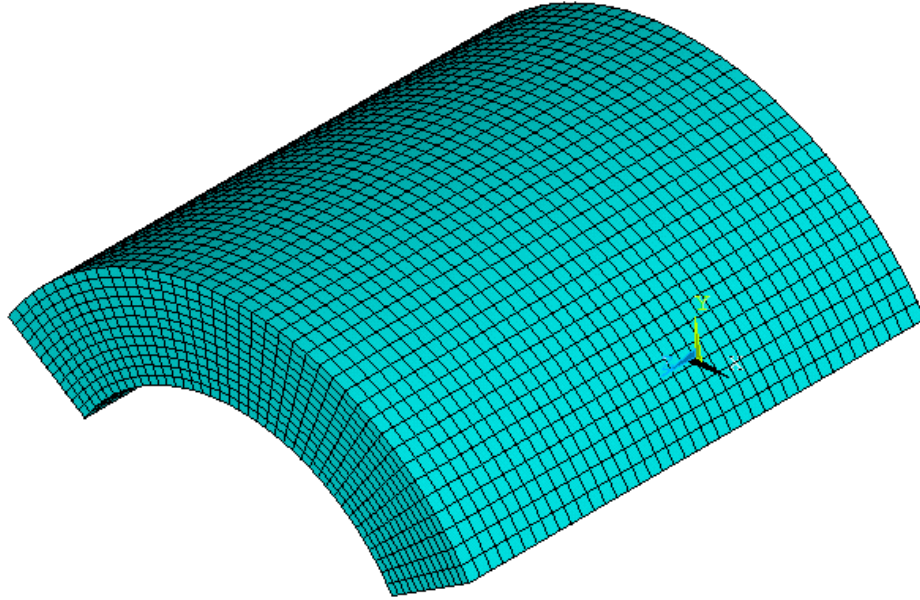
Figure 4.1:   Three dimensional mesh pattern of a moderately thick and deep cylindrical shell.

Table 4.1:   Convergence study of first five natural frequency parameters obtained by FEM three dimensional analysis for isotropic cylindrical shells.

Mesh	Ω_1	Ω_2	Ω_3	Ω_4	Ω_5
$10\times10\times2$	9.5801	8.437	19.666	21.429	24.211
$10\times10\times4$	9.5795	12.403	19.662	21.413	24.177
$10\times10\times8$	9.5795	12.402	19.662	21.413	24.175
$20\times20\times2$	9.5795	12.406	19.661	21.419	24.167
$20\times20\times4$	9.5791	12.398	19.657	21.403	24.135
$20\times20\times8$	9.5791	12.398	19.657	21.403	24.133
$30\times30\times2$	9.5795	12.406	19.661	21.419	24.165
$30\times30\times4$	9.5791	12.397	19.657	21.401	24.131
$30\times30\times8$	9.5791	12.397	19.657	21.401	24.131

4.3.1. Static analysis

Table 4.2 shows dimensionless displacement and force and moment resultants at the center of isotropic shells with different thickness ratios $a/h=$ 10, and 20 describing

Table 4.2:   Comparison of dimensionless displacement and moment and force resultants as in Eqs (24) of isotropic cylindrical shells.

a/h	a/R		w^*	M_α^*	M_β^*	N_α^*	N_β^*
		FSDTQ	26.679	25.215	24.340	1378.9	1281.9
	0	FSDT	26.596	25.032	24.376	1370.1	1281.6
		3D	26.698	25.304	24.377	1378.2	1281.0
		FSDTQ	11.388	9.4298	7.5046	1211.2	1090.3
	1	FSDT	11.337	9.1821	7.6363	1202.9	1087.8
20		3D	11.427	9.4918	7.4756	1212.4	1090.9
		FSDTQ	3.0070	1.5774	1.5604	713.13	633.06
	2	FSDT	2.9994	1.3327	1.3535	710.62	630.86
		3D	3.0350	1.6384	1.6121	715.48	633.99
		FSDTQ	40.956	38.905	37.929	535.51	470.14
	0	FSDT	40.699	38.584	37.928	526.14	472.81
		3D	40.875	39.151	38.108	530.95	465.63
		FSDTQ	28.333	26.042	23.237	746.57	651.79
	1	FSDT	28.009	25.301	23.395	730.05	650.49
10		3D	28.415	26.344	23.346	743.22	648.45
		FSDTQ	12.108	9.9288	4.5215	657.47	572.61
	2	FSDT	11.972	8.9645	5.1307	644.04	566.19
		3D	12.242	10.149	4.3759	658.16	573.24

moderately thick and thin shells, respectively. It also shows results for three different

depth ratios $a/R =$ 0.5, 1, and 2 representing shallow, deep, and very deep shells,

respectively. Although the error of dimensionless displacement calculated from both

FSDTQ and FSDT for thin shells for all depth ratios stays under 1%, FSDTQ's results are

Table 4.3:   Comparison of dimensionless displacements and moments and force
resultants as in Eqs. (24) of [90/0] orthotropic cylindrical shells.

a/h	a/R		w^*	M_α^*	M_β^*	N_α^*	N_β^*
		FSDTQ	11.632	52.953	28.801	1086.1	994.64
	0.5	FSDT	11.636	52.822	28.740	1083.4	996.77
		3D	11.612	53.689	29.643	1084.7	990.78
		FSDTQ	5.6782	31.255	5.5480	1070.5	959.45
	1	FSDT	5.6735	31.043	5.5104	1067.0	959.78
20		3D	5.6746	31.638	5.9669	1070.5	957.92
		FSDTQ	1.7117	13.077	6.4874	660.41	611.31
	2	FSDT	1.7089	12.899	6.4325	658.02	610.42
		3D	1.7106	13.250	6.2433	661.99	612.94
		FSDTQ	17.141	63.319	47.531	396.12	340.21
	0.5	FSDT	17.188	63.160	47.393	394.21	343.88
		3D	17.009	64.496	48.617	393.25	332.46
		FSDTQ	12.738	53.117	26.648	598.29	511.21
	1	FSDT	12.751	52.616	26.338	594.33	515.24
10		3D	12.679	54.318	27.476	595.02	503.90
		FSDTQ	5.9687	30.875	0.7428	574.42	511.74
	2	FSDT	5.9488	30.132	0.8399	568.08	511.26
		3D	5.9629	31.668	0.5844	574.34	510.95

closer to those of 3D. This error of FSDT's results for thicker shells increases to 2.2% as

the depth of the shells increases whereas it is still less than 1% for FSDTQ. For

dimensionless moment and force resultants, a similar observation is still valid here to that made earlier for dimensionless displacements. The error, however, for deeper and thicker shells reached higher than 10% for moment results using FSDT and remained at 3% where FSDTQ is used. This shows the significant improvement that has been made here by using FSDTQ as compared with FSDT. A similar observation is made recently by Khdeir [18].

Table 4.4:   Comparison of dimensionless displacements and moments and force resultants as in Eqs (24) of [0/90/0] orthotropic cylindrical shells.

a/h	a/R		w^*	M_α^*	M_β^*	N_α^*	N_β^*
		FSDTQ	6.1289	103.49	6.9507	573.31	559.77
	0.5	FSDT	6.1282	103.42	6.9604	571.68	559.67
		3D	6.3773	101.85	7.7181	596.06	576.85
		FSDTQ	3.8321	64.062	2.6818	720.17	709.00
	1	FSDT	3.8314	63.908	2.7087	718.62	708.66
20		3D	3.9303	62.260	2.9527	738.14	719.09
		FSDTQ	1.3646	22.235	1.8251	523.35	556.50
	2	FSDT	1.3654	22.040	1.7775	524.39	556.13
		3D	1.3753	21.468	1.9346	527.80	556.25
		FSDTQ	9.5159	115.57	11.341	224.27	201.89
	0.5	FSDT	9.5092	115.46	11.340	222.26	202.12
		3D	10.661	112.55	13.847	249.78	222.52
		FSDTQ	7.8589	95.411	7.9335	370.84	335.59
	1	FSDT	7.8418	95.117	7.9421	367.19	335.23
10		3D	8.6399	91.340	9.5561	405.29	362.88
		FSDTQ	4.4754	54.405	1.0161	424.23	398.24
	2	FSDT	4.4600	54.021	1.0879	420.58	396.17
		3D	4.7425	50.500	1.3337	446.10	415.31

In the next examples, the previous problem is investigated for two-layer [90/0] and three-layer [0/90/0] composite cylindrical shells and results are shown in Tables 4.3 and 4.4, respectively. Some stress resultant terms where in significant error using FSDT, while the error is much less when FSDTQ is employed. A similar observation on errors of FSDT for composite materials is made. It is concluded here that in almost all cases FSDTQ gives better results than FSDT comparing to the results of 3D finite element analysis.

Table 4.5:   Comparison of first five dimensionless natural frequency parameters of isotropic cylindrical shells.

a/h	a/R		Ω_1	Ω_2	Ω_3	Ω_4	Ω_5
		FSDTQ	7.5553	14.416	16.386	23.188	28.148
	0.5	FSDT	7.5651	14.422	16.401	23.200	28.149
		3D	7.5523	14.423	16.390	23.206	28.183
		FSDTQ	11.026	14.445	21.173	24.365	27.851
	1	FSDT	11.048	14.466	21.216	24.408	27.856
20		3D	11.017	14.444	21.166	24.368	27.884
		FSDTQ	14.585	17.957	26.700	28.360	33.469
	2	FSDT	14.656	17.977	26.723	28.482	33.550
		3D	14.562	17.945	26.727	28.324	33.455
		FSDTQ	6.0913	13.529	14.098	20.955	25.425
	0.5	FSDT	6.1020	13.531	14.113	20.963	25.412
		3D	6.0921	13.560	14.124	19.869	19.871
		FSDTQ	7.0900	13.281	15.439	21.039	25.131
	1	FSDT	7.1204	13.290	15.491	21.069	25.118
10		3D	7.0810	13.309	15.452	19.869	19.877
		FSDTQ	9.5961	12.381	19.660	21.378	23.986
	2	FSDT	9.6275	12.424	19.774	21.472	23.945
		3D	9.5791	12.397	19.657	21.401	24.131

4.3.2. Free vibration analysis

The same set of shells investigated in static analysis section are considered for free vibration analyses to find the first five natural frequency parameters with both FSDT and FSDTQ and compare them with the 3D elasticity results obtained by FEM. Those results for isotropic cylindrical shells are shown in Table 4.5. It can be seen that both shear

Table 4.6:   Comparison of first five dimensionless natural frequency parameters of [90/0] orthotropic cylindrical shells.

a/h	a/R		Ω_1	Ω_2	Ω_3	Ω_4	Ω_5
		FSDTQ	11.530	25.357	27.913	36.324	50.210
	0.5	FSDT	11.527	25.330	27.896	36.288	50.151
		3D	11.537	25.378	27.951	36.434	50.253
		FSDTQ	15.859	25.648	34.867	37.831	50.263
	1	FSDT	15.863	25.601	34.850	37.778	50.148
20		3D	15.861	25.658	34.890	37.942	50.297
		FSDTQ	24.809	26.193	42.664	49.382	51.170
	2	FSDT	24.809	26.132	42.627	49.166	51.144
		3D	24.805	26.162	42.743	49.359	51.167
		FSDTQ	9.4577	21.676	22.150	29.959	38.608
	0.5	FSDT	9.4450	21.624	22.112	29.890	38.512
		3D	9.4855	21.743	22.246	30.193	38.745
		FSDTQ	10.666	21.705	24.090	30.368	38.722
	1	FSDT	10.657	21.608	24.043	30.247	38.530
10		3D	10.686	21.767	24.191	30.614	38.896
		FSDTQ	13.771	21.037	29.574	31.200	38.073
	2	FSDT	13.768	20.873	29.535	31.033	37.696
		3D	13.772	21.040	29.639	31.411	38.266

deformation theories predict all five natural frequencies close to 3D results (less than 1% error for all cases). Table 4.6 and 4.7 compare frequency parameters for [90/0] and

114

[0/90/0] composite shells, respectively. It is worth mentioning that, while maximum error for anti-symmetric lay-up of FSDT results increases to 2%, it stills under 1% for FSDTQ results whereas the maximum error increases to 7.8% for symmetric lay-up in both shell theories. However, the general observation is that errors of both shear deformation theories in comparison to 3D results increase as the thickness and depth of the shell increase and for higher natural frequencies and in the same conditions the improvement of FSDTQ respect to FSDT toward 3D results increases too.

Table 4.7: Comparison of dimensionless first five dimensionless natural frequency parameters of [0/90/0] orthotropic cylindrical shells.

a/h	a/R		Ω_1	Ω_2	Ω_3	Ω_4	Ω_5
		FSDTQ	15.551	21.646	37.022	46.309	48.938
	0.5	FSDT	15.551	21.646	37.022	46.311	48.940
		3D	15.245	21.370	36.803	43.529	46.148
		FSDTQ	18.710	21.974	36.794	49.770	49.852
	1	FSDT	18.709	21.975	36.795	49.779	49.860
20		3D	18.471	21.703	36.567	47.074	47.416
		FSDTQ	23.178	25.978	35.923	52.746	57.077
	2	FSDT	23.177	25.959	35.925	52.769	58.869
		3D	22.924	25.840	35.668	50.360	56.448
		FSDTQ	12.443	18.677	30.839	31.323	34.456
	0.5	FSDT	12.445	18.678	30.839	31.331	34.462
		3D	11.769	18.159	28.600	30.471	31.928
		FSDTQ	13.187	18.524	30.564	32.232	34.523
	1	FSDT	13.192	18.528	30.562	32.258	34.546
10		3D	12.590	18.005	29.732	30.189	32.037
		FSDTQ	15.250	17.989	29.491	34.795	34.913
	2	FSDT	15.241	17.996	29.487	34.866	34.951
		3D	14.840	17.468	29.094	32.464	33.046

4.3.3. Modified FSDTQ

FSDTQ uses the radii of the midsurface of the shell in its equations for calculating moment of inertias and stress resultants (Eqs (9) and (15)). One may use the radii of each lamina instead of the mid-surface to modify those equations. Moment of inertia equation considering the radius of each lamina is

$$\bar{I}_i = \sum_{k=1}^{N} \left[I_i^k + I_{i+1}^k \left(\frac{1}{R_\alpha^k} + \frac{1}{R_\beta^k} \right) + \frac{I_{i+2}^k}{R_\alpha^k R_\alpha^k} \right], \quad i = 1, 2, 3, \tag{24}$$

Table 4.8: Comparison of dimensionless displacements and moments and force resultants of orthotropic cylindrical shells with shear diaphragm boundary condition ($a/h = 10$).

Lay-up	a/R		w^*	M_α^*	M_β^*	N_α^*	N_β^*
		present	12.739	53.104	26.670	598.35	511.09
		FSDTQ	12.735	53.137	26.605	598.11	511.48
	1	FSDT	12.751	52.616	26.338	594.33	515.24
[90/0]		3D	12.679	54.318	27.476	595.02	503.90
		present	5.9741	30.866	0.7133	574.96	511.63
		FSDTQ	5.9557	30.867	0.8112	573.06	512.16
	2	FSDT	5.9488	30.132	0.8399	568.08	511.26
		3D	5.9629	31.668	0.5844	574.34	510.95
		present	7.8601	95.406	7.9373	370.90	335.60
		FSDTQ	7.8514	95.432	7.9169	370.48	335.57
	1	FSDT	7.8418	95.117	7.9421	367.19	335.23
		3D	8.6399	91.340	9.5561	405.29	362.88
[0/90/0]		present	4.4781	54.393	1.0213	424.50	398.29
		FSDTQ	4.4578	54.441	0.9926	422.51	398.12
	2	FSDT	4.4600	54.021	1.0879	420.58	396.17
		3D	4.7425	50.500	1.3337	446.10	415.31

where $\left[I_1^k, I_2^k, I_3^k, I_4^k, I_5^k\right] = \int\limits_{h_{k-1}}^{h_k} \rho^k \left[1, z, z^2, z^3, z^4\right] dz$ and R_α^k and R_β^k are the radii of each

layer in the α and β directions, respectively. The stress resultant equations are

$$
\begin{bmatrix} N_\alpha \\ N_\beta \\ N_{\alpha\beta} \\ N_{\beta\alpha} \\ M_\alpha \\ M_\beta \\ M_{\alpha\beta} \\ M_{\beta\alpha} \end{bmatrix} = \begin{bmatrix} \overline{A}_{11} & A_{12} & \overline{A}_{16} & A_{16} & \overline{B}_{11} & B_{12} & \overline{B}_{16} & B_{16} \\ A_{12} & \hat{A}_{22} & A_{26} & \hat{A}_{26} & B_{12} & \hat{B}_{22} & B_{26} & \hat{B}_{26} \\ \overline{A}_{16} & A_{26} & \overline{A}_{66} & A_{66} & \overline{B}_{16} & B_{26} & \overline{B}_{66} & B_{66} \\ A_{16} & \hat{A}_{26} & A_{66} & \hat{A}_{66} & B_{16} & \hat{B}_{26} & B_{66} & \hat{B}_{66} \\ \overline{B}_{11} & B_{12} & \overline{B}_{16} & B_{16} & \overline{D}_{11} & D_{12} & \overline{D}_{16} & D_{16} \\ B_{12} & \hat{B}_{22} & B_{26} & \hat{B}_{26} & D_{12} & \hat{D}_{22} & D_{26} & \hat{D}_{26} \\ \overline{B}_{16} & B_{26} & \overline{B}_{66} & B_{66} & \overline{D}_{16} & D_{26} & \overline{D}_{66} & D_{66} \\ B_{16} & \hat{B}_{26} & B_{66} & \hat{B}_{66} & D_{16} & \hat{D}_{26} & D_{66} & \hat{D}_{66} \end{bmatrix} \begin{bmatrix} \varepsilon_{0\alpha} \\ \varepsilon_{0\beta} \\ \varepsilon_{0\alpha\beta} \\ \varepsilon_{0\beta\alpha} \\ \kappa_\alpha \\ \kappa_\beta \\ \kappa_{\alpha\beta} \\ \kappa_{\beta\alpha} \end{bmatrix},
$$

$$
\begin{bmatrix} Q_\alpha \\ Q_\beta \\ P_\alpha \\ P_\beta \end{bmatrix} = \begin{bmatrix} \overline{A}_{55} & A_{45} & \overline{B}_{55} & B_{45} \\ A_{45} & \hat{A}_{44} & B_{45} & \hat{B}_{44} \\ \overline{B}_{55} & B_{45} & \overline{D}_{55} & D_{45} \\ B_{45} & \hat{B}_{44} & D_{45} & \hat{D}_{44} \end{bmatrix} \begin{bmatrix} \gamma_{0\alpha z} \\ \gamma_{0\beta z} \\ -\psi_\alpha / R_{\alpha\beta} \\ -\psi_\beta / R_{\alpha\beta} \end{bmatrix},
\tag{25}
$$

$$
\left.\begin{aligned}
\overline{A}_{ij} &= \sum_{k=1}^N [A_{ij}^k - c_0^k B_{ij}^k], & \hat{A}_{ij} &= \sum_{k=1}^N [A_{ij}^k + c_0^k B_{ij}^k], \\
\overline{B}_{ij} &= \sum_{k=1}^N [B_{ij}^k - c_0^k D_{ij}^k], & \hat{B}_{ij} &= \sum_{k=1}^N [B_{ij}^k + c_0^k D_{ij}^k], \\
\overline{D}_{ij} &= \sum_{k=1}^N [D_{ij}^k - c_0^k E_{ij}^k], & \hat{D}_{ij} &= \sum_{k=1}^N [D_{ij}^k + c_0^k E_{ij}^k],
\end{aligned}\right\} \quad i,j = 1,2,4,5,6,
\tag{26}
$$

where $c_0^k = \left(\dfrac{1}{R_\alpha^k} - \dfrac{1}{R_\beta^k}\right)$ and

$$
\left.\begin{aligned}
A_{ij}^k &= \overline{Q}_{ij}^{(k)}(h_k - h_{k-1}) \\
B_{ij}^k &= \frac{1}{2}\overline{Q}_{ij}^{(k)}(h_k^2 - h_{k-1}^2) \\
D_{ij}^k &= \frac{1}{3}\overline{Q}_{ij}^{(k)}(h_k^3 - h_{k-1}^3) \\
E_{ij}^k &= \frac{1}{4}\overline{Q}_{ij}^{(k)}(h_k^4 - h_{k-1}^4)
\end{aligned}\right\} \quad i,j = 1,2,6, \qquad
\left.\begin{aligned}
A_{ij}^k &= K_\alpha K_\beta \overline{Q}_{ij}^{(k)}(h_k - h_{k-1}) \\
B_{ij}^k &= \frac{1}{2}K_\alpha K_\beta \overline{Q}_{ij}^{(k)}(h_k^2 - h_{k-1}^2) \\
D_{ij}^k &= \frac{1}{3}K_\alpha K_\beta \overline{Q}_{ij}^{(k)}(h_k^3 - h_{k-1}^3)
\end{aligned}\right\} \quad i,j = 4,5,
$$

$$
\tag{27}
$$

117

Table 4.8 shows the results of static analysis on a moderately thick composite ($a/h=10$) shell with different depth ratios for the present theory compared with FSDT, FSDTQ and 3D results. It can be seen that the present modification improves the results of FSDTQ significantly comparing with 3D results. Table 4.9 shows first five natural frequency parameters for the same problem as the last example. Present modification predicts natural frequency parameters better than other theories.

Table 4.9: Comparison of first five natural frequency parameters of orthotropic cylindrical shells with shear diaphragm boundary condition($a/h=10$).

Lay-up	a/R		Ω_1	Ω_2	Ω_3	Ω_4	Ω_5
		present	10.668	21.717	24.087	30.373	38.744
		FSDTQ	10.666	21.705	24.090	30.368	38.722
	1	FSDT	10.657	21.608	24.043	30.247	38.530
[90/0]		3D	10.686	21.767	24.191	30.614	38.896
		present	13.772	21.072	29.569	31.216	38.147
		FSDTQ	13.771	21.037	29.574	31.200	38.073
	2	FSDT	13.768	20.873	29.535	31.033	37.696
		3D	13.772	21.040	29.639	31.411	38.266
		present	13.186	18.531	30.581	32.229	34.524
		FSDTQ	13.187	18.524	30.564	32.232	34.523
	1	FSDT	13.192	18.528	30.562	32.258	34.546
		3D	12.590	18.005	29.732	30.189	32.037
[0/90/0]		present	15.245	18.001	29.548	34.800	34.904
		FSDTQ	15.250	17.989	29.491	34.795	34.913
	2	FSDT	15.241	17.996	29.487	34.866	34.951
		3D	14.840	17.468	29.094	32.464	33.046

4.4.   Conclusions

Both static and vibration analyses are performed on composite cylindrical shells using a first order shear deformation theory with plate-like stiffness coefficients (FSDT), a first order shear deformation theory by Qatu (FSDTQ) where these coefficients are integrated exactly or truncated to the first order and three dimensional elasticity (3D). FSDTQ offers a more accurate representation of the stiffness parameters and the stress resultant equations. Most analyses performed here show that there is an improvement (closer to 3D) obtained when FSDTQ is used. In addition, such improvement is observed to be higher for deeper and thicker shells than for thin shallow shells, especially in static analyses. Moreover, FSDTQ has been modified by using the radii of each laminate instead of the radii of mid-plane in the calculating of the moments of inertias and stress resultants. The results show that this modification improves FSDTQ's results significantly. This analysis can be a prelude to the derivation of a proper higher order shell theory (e.g. third order) where the term $(1+z/R)$ needs to be truncated at the third order.

4.5.   References

1.   Yaghoubshahi M, Asadi E, Fariborz SJ. A higher-order shell model applied to shells with mixed boundary conditions. J Mech Eng Sci IMechE 2011; 225: 292-303.

2.   Flügge W. Stresses in Shells. Berlin: Springer-Verlag; 1962.

3.   Vlasov VZ. General Theory of Shells and Its Application to Engineering. GITTL: Moskva-Leningrad; 1949, English Translation, NASA Technical Translation TTF-99; 1964.

4.   Love AEH. A Treatise on the Mathematical Theory of Elasticity, 1st Edition. Cambridge Univ. Press; 1892, 4th Edition, New York: Dover Publishing Inc.; 1944.

5.   Ambartsumian SA. Contribution to the theory of anisotropic laminated shells. Appl Mech Rev 1962; 15: 245-249.

6.   Rath BK, and Das YC. Vibration of layered shells. J Sound Vib 1973; 28: 737-757.

7.   Reddy JN. Exact solution of moderately thick laminated shells. J Eng Mech ASCE 1984; 110: 794-809.

8.   Librescu L, Khdeir AA, Frederick D. A shear-deformable theory for laminated composite shallow shell-type panels and their response analysis I: free vibration and buckling. Acta Mechanica 1989; 76: 1-33.

9.   Librescu L, Khdeir AA, Frederick D. A shear-deformable theory for laminated composite shallow shell-type panels and their response analysis II: static analysis. Acta Mechanica 1989; 77: 1-12.

10.   Reddy JN, Liu CF. A higher order shear deformation theory of laminated elastic shells. Int J Eng Sci 1985; 23(3): 440-447.

11.   Qatu MS. Accurate stress resultants equations for laminated composite deep thick shells. Compos Press Vessl Indust 1995; 302: 39-44.

12.   Qatu MS. Accurate equations for laminated composite deep thick shells. Int J Solids Struct 1999; 36: 2917-2941.

13.   Qatu MS, Sullivan RW, Wang W. Recent research advances in the dynamic behavior of composite shells: 2000-2009. Compos Struct 2010; 93: 14–31.

14.   Qatu MS, Asadi E, Wang W. Review of recent literature on static analysis of composite shells: 2000-2010. Accepted for publication, 2012.

15.   Carrera E. Historical review of zig-zag theories for multilayered plates and shells.

Appl Mech Rev 2003; 56: 287–309.

16. Carrera E. Theories and finite elements for multilayered, anisotropic, composite plates and shells. J Arch Comput Methods Eng 2002; 9: 87–140.

17. Qatu, MS. Vibration of Laminated Shells and Plates. Elsevier; 2004.

18. Carrera E., Campisi C., Cinefra M. and Soave M. Evaluation of various theories of the thickness and curvature approximations for free vibrational analysis of cylindrical and spherical shells. Int J Veh Noise Vib 2011; 7(1): 16 – 36.

19. Carrera E. The effects of shear deformation and curvature on buckling and vibrations of cross-ply laminated composite shells. J Sound Vib 1991; 150(3): 405-433

20. Khdeir AA. Comparative dynamic and static studies for cross ply shells based on a deep thick shell theory. Int J Veh Noise Vib 2011; 7(3): 195-210.

CHAPTER 5

STATIC ANALYSIS OF THICK LAMINATED SHELLS WITH

DIFFERENT BOUNDARY CONDITIONS

USING GDQ

Shells are commonly used in many engineering structures; such as automotive, aerospace and submarine structures. Composite shells are getting particularly more attention recently. Because of the simplicity of shell theories, it is favorable to analyze shell structures with shell theories instead of three dimensional (3D) theory of elasticity Shell theories redeem difficulty of shell analyses by employing certain assumptions on the behavior of displacements in the thickness direction; For instance, first-order expansion of in-plane displacements leads to first order shear deformation shell theories (FSDTs).

Difficulties rise as a term (1+z/R) appears in both the strain displacement and stress resultant equations in the derivation of the basic equation of shells. The term was neglected by first analysts of composite thin shells (e.g. Ambartsumian [1]) which is understandable for thin shells. Although the importance of the inclusion of the term has been tested for thicker shells with simply supported boundaries and proven to be essential [2], no attempt has been made to general boundary conditions. In addition to the inclusion of this term, both shear deformation and rotary inertia should be included for composite

thick shells. Earlier treatment of composite thick shells included both shear deformation and rotary inertia rotary but failed to include the z/R terms [3,4]. We will refer to these as simply the first order shear deformation theory (FSDT). Interestingly, some researchers developed higher order theories while still neglecting the (1+z/R) term, e.g. [5-7]. Qatu [8, 9] presented equations where the term is considered in the shell equations for composite deep thick shells. We will refer to his equations as the first order shear deformation shell theory by Qatu (FSDTQ). Asadi et al. [2] used FSDTQ to find exact static and free vibration solution of isotropic and composite deep shells with fully simply supported boundary conditions. They showed that using of FSDTQ instead of FSDT significantly improves the results when compared to 3D results. The effect of using FSDTQ on shells with different boundary conditions and general lay-ups of laminates needs to be examined. Much of the literature on shell analysis is reviewed recently showing that inaccurate equations are still used in a significant portion of shells works [10-13].

Equilibrium equations with required boundary conditions for doubly curved deep and thick composite shells are shown using FSDTQ. It is shown that FSDT is a simplification from FSDTQ where the effects of depth of shells are neglected. Equilibrium equations are put together with the equations of stress resultants to arrive to a system of seventeen first order differential equations. General Differential Quadrature (GDQ) method is employed to solve this system of first order differential equations. Isotropic, cross-ply, angle-ply and general lay-up cylindrical shells with six types of different boundary conditions which are combinations of simply supported, clamp, and free boundary conditions are examined using both FSDTQ and FSDT. The results

obtained here are compared with those obtained by different first order and higher order theories available in the literature for a fully S1-type isotropic cylindrical shell. Moreover, dimensionless transverse displacement, moment and force resultants of moderately thick and very deep shells are obtained using both FSDT and FSDTQ for three different lay-ups and six different boundary conditions and compared with those of a converged 3D finite element analysis obtained by ANSYS®. Also, Errors of FSDTQ and FSDT results (when comparing them to those of the 3D results) are obtained and discussed.

5.1. Formulation of shells with different BC for static analysis

The principle of virtual work for the equilibrium of a body with surface S and volume V requires that

$$\int_V [\sigma_\alpha \delta\varepsilon_\alpha + \sigma_\beta \delta\varepsilon_\beta + \sigma_z \delta\varepsilon_z + \sigma_{\alpha\beta}\delta\gamma_{\alpha\beta} + \sigma_{\alpha z}\delta\gamma_{\alpha z} + \sigma_{\beta z}\delta\gamma_{\beta z}]dV - \int_S \delta W_{ext} dS = 0, \qquad (1)$$

where $\sigma_{...}$ and $\varepsilon_{...}$; respectively, are stress and strain components and δW_{ext} is the virtual work done by external forces. A doubly curved shell wherein the boundaries of the shell coincides along the in-plane principal axes α, β with normal to the middle-plane axis z, principal radii R_α and R_β; respectively, in α and β directions, and twisting radius $R_{\alpha\beta}$ is considered in this study. First-order shear deformation model approximates the displacement components as

$$u(\alpha,\beta,z) = u_0(\alpha,\beta) + z\psi_\alpha(\alpha,\beta),$$

124

$$v(\alpha, \beta, z) = v_0(\alpha, \beta) + z\psi_\beta(\alpha, \beta),$$

$$w(\alpha, \beta, z) = w_0(\alpha, \beta), \tag{2}$$

where $-h/2 \leq z \leq h/2$ and h is the shell thickness, u_0, v_0, and w_0 are midsurface displacements of the shell, and ψ_α and ψ_β are midsurface rotations. By substituting Eqs (2) into the strain-displacement relationships in the principal coordinates of a doubly-curved shell [14], strain-displacement equations become

$$\varepsilon_\alpha = \frac{1}{(1+z/R_\alpha)}(\varepsilon_{0\alpha} + z\kappa_\alpha), \qquad \varepsilon_\beta = \frac{1}{(1+z/R_\beta)}(\varepsilon_{0\beta} + z\kappa_\beta), \qquad \varepsilon_z = 0,$$

$$\varepsilon_{\alpha\beta} = \frac{1}{(1+z/R_\alpha)}(\varepsilon_{0\alpha\beta} + z\kappa_{\alpha\beta}), \qquad \varepsilon_{\beta\alpha} = \frac{1}{(1+z/R_\beta)}(\varepsilon_{0\beta\alpha} + z\kappa_{\beta\alpha}),$$

$$\gamma_{\alpha z} = \frac{1}{(1+z/R_\alpha)}[\gamma_{0\alpha z} - z(\psi_\beta/R_{\alpha\beta})], \qquad \gamma_{\beta z} = \frac{1}{(1+z/R_\beta)}[\gamma_{0\beta z} - z(\psi_\alpha/R_{\alpha\beta})]. \tag{3}$$

The functions on the right-hand side of Eqs (3) are

$$\varepsilon_{0\alpha} = \frac{1}{A}\frac{\partial u_0}{\partial \alpha} + \frac{v_0}{AB}\frac{\partial A}{\partial \beta} + \frac{w_0}{R_\alpha}, \qquad \varepsilon_{0\beta} = \frac{1}{B}\frac{\partial v_0}{\partial \beta} + \frac{u_0}{AB}\frac{\partial B}{\partial \alpha} + \frac{w_0}{R_\beta},$$

$$\varepsilon_{0\alpha\beta} = \frac{1}{A}\frac{\partial v_0}{\partial \alpha} - \frac{u_0}{AB}\frac{\partial A}{\partial \beta} + \frac{w_0}{R_{\alpha\beta}}, \qquad \varepsilon_{0\beta\alpha} = \frac{1}{B}\frac{\partial u_0}{\partial \beta} - \frac{v_0}{AB}\frac{\partial B}{\partial \alpha} + \frac{w_0}{R_{\alpha\beta}},$$

$$\gamma_{0\alpha z} = \frac{1}{A}\frac{\partial w_0}{\partial \alpha} - \frac{u_0}{R_\alpha} - \frac{v_0}{R_{\alpha\beta}} + \psi_\alpha, \qquad \gamma_{0\beta z} = \frac{1}{B}\frac{\partial w_0}{\partial \beta} - \frac{v_0}{R_\beta} - \frac{u_0}{R_{\alpha\beta}} + \psi_\beta,$$

$$\kappa_\alpha = \frac{1}{A}\frac{\partial \psi_\alpha}{\partial \alpha} + \frac{\psi_\beta}{AB}\frac{\partial A}{\partial \beta}, \qquad \kappa_\beta = \frac{1}{B}\frac{\partial \psi_\beta}{\partial \beta} + \frac{\psi_\alpha}{AB}\frac{\partial B}{\partial \alpha},$$

$$\kappa_{\alpha\beta} = \frac{1}{A}\frac{\partial \psi_\beta}{\partial \alpha} - \frac{\psi_\alpha}{AB}\frac{\partial A}{\partial \beta}, \qquad \kappa_{\beta\alpha} = \frac{1}{B}\frac{\partial \psi_\alpha}{\partial \beta} - \frac{\psi_\beta}{AB}\frac{\partial B}{\partial \alpha}. \tag{4}$$

In Eqs (4), $A^2 = (\partial \bar{r}/\partial \alpha).(\partial \bar{r}/\partial \alpha)$, $B^2 = (\partial \bar{r}/\partial \beta).(\partial \bar{r}/\partial \beta)$ where $\bar{r}$ is the position vector of a point on the middle surface of the shell. The stress resultants are defined as

$$\begin{bmatrix} N_\alpha & N_{\alpha\beta} & Q_\alpha & M_\alpha & M_{\alpha\beta} & P_\alpha \end{bmatrix}^T = \int_{-h/2}^{h/2} \begin{bmatrix} \sigma_\alpha & \sigma_{\alpha\beta} & \sigma_{\alpha z} & z\sigma_\alpha & z\sigma_{\alpha\beta} & z\sigma_{\alpha z} \end{bmatrix}^T (1+\frac{z}{R_\beta})dz,$$

$$\begin{bmatrix} N_\beta & N_{\beta\alpha} & Q_\beta & M_\beta & M_{\beta\alpha} & P_\beta \end{bmatrix}^T = \int_{-h/2}^{h/2} \begin{bmatrix} \sigma_\beta & \sigma_{\beta\alpha} & \sigma_{\beta z} & z\sigma_\beta & z\sigma_{\beta\alpha} & z\sigma_{\beta z} \end{bmatrix}^T (1+\frac{z}{R_\alpha})dz, \tag{5}$$

where the superscript T stands for the transpose of a vector. The applied load per unit area on the middle surface of a shell is $\bar{q} = q_\alpha \bar{e}_\alpha + q_\beta \bar{e}_\beta + q_z \bar{e}_z$, where the unit vectors $\bar{e}_\alpha$ and $\bar{e}_\beta$ are tangent to the principal axes and $\bar{e}_z$ is perpendicular to the shell surface. The virtual work done by external loads on the shell yields

$$\delta w_{ext} = \int_\alpha \int_\beta (q_\alpha \delta u + q_\beta \delta v + q_z \delta w) AB\, d\alpha\, d\beta + \oint_\beta \int_{-h/2}^{h/2} (\sigma_{0\alpha}\delta u + \sigma_{0\alpha\beta}\delta v$$

$$+\sigma_{0\alpha z}\delta w)B(1+z/R_\beta)dz\,d\beta + \oint_\alpha \int_{-h/2}^{h/2} (\sigma_{0\beta}\delta v + \sigma_{0\beta\alpha}\delta u + \sigma_{0\beta z}\delta w)A(1+z/R_\alpha)dz\,d\alpha, \tag{6}$$

where $\sigma_{0\alpha}$, $\sigma_{0\alpha\beta}$ and $\sigma_{0\alpha z}$ are the components of applied traction on the edges $\alpha =$ constant and $\sigma_{0\beta}$, $\sigma_{0\beta\alpha}$ and $\sigma_{0\beta z}$ are the components of applied traction on the edges $\beta =$ constant. Also, the second and third integrals in Eq. (6) should be taken along the boundaries of the shell. Substituting Eqs (5) into Eq. (6), the resultant equation with Eqs (3) into Eq. (1), employing the definitions (5), setting $\sigma_z = 0$, and carrying out the

required manipulations results in

$$\int\limits_{\alpha_1}\int\limits_{\alpha_2} \{[\frac{\partial(BN_\alpha)}{\partial\alpha}+\frac{\partial(AN_{\beta\alpha})}{\partial\beta}+N_{\alpha\beta}\frac{\partial A}{\partial\beta}-N_\beta\frac{\partial B}{\partial\alpha}+\frac{AB}{R_\alpha}Q_\alpha+\frac{AB}{R_{\alpha\beta}}Q_\beta+ABq_\alpha]\delta u_0$$

$$+[\frac{\partial(AN_\beta)}{\partial\beta}+\frac{\partial(BN_{\alpha\beta})}{\partial\alpha}+N_{\beta\alpha}\frac{\partial B}{\partial\alpha}-N_\alpha\frac{\partial A}{\partial\beta}+\frac{AB}{R_\beta}Q_\beta+\frac{AB}{R_{\alpha\beta}}Q_\alpha+ABq_\beta]\delta v_0$$

$$+[\frac{\partial(BQ_\alpha)}{\partial\alpha}+\frac{\partial(AQ_\beta)}{\partial\beta}-AB(\frac{N_\alpha}{R_\alpha}+\frac{N_{\alpha\beta}+N_{\beta\alpha}}{R_{\alpha\beta}}+\frac{N_\beta}{R_\beta})+ABq_z]\delta w_0$$

$$+[\frac{\partial(BM_\alpha)}{\partial\alpha}+\frac{\partial(AM_{\beta\alpha})}{\partial\beta}+M_{\alpha\beta}\frac{\partial A}{\partial\beta}-M_\beta\frac{\partial B}{\partial\alpha}-ABQ_\alpha+\frac{AB}{R_{\alpha\beta}}P_\beta]\delta\psi_\alpha$$

$$+[\frac{\partial(AM_\beta)}{\partial\beta}+\frac{\partial(BM_{\alpha\beta})}{\partial\alpha}+M_{\beta\alpha}\frac{\partial B}{\partial\alpha}-M_\alpha\frac{\partial A}{\partial\beta}-ABQ_\beta+\frac{AB}{R_{\alpha\beta}}P_\alpha]\delta\psi_\beta\}d\alpha d\beta$$

$$+\oint\limits_\beta [(N_{0\alpha}-N_\alpha)\delta u_0+(N_{0\alpha\beta}-N_{\alpha\beta})\delta v_0+(Q_{0\alpha}-Q_\alpha)\delta w_0-M_\alpha\delta\psi_\alpha-M_{\alpha\beta}\delta\psi_\beta]Bd\beta$$

$$+\oint\limits_\alpha [(N_{0\beta\alpha}-N_{\beta\alpha})\delta u_0+(N_{0\beta}-N_\beta)\delta v_0+(Q_{0\beta}-Q_\beta)\delta w_0-M_{\beta\alpha}\delta\psi_\alpha-M_\beta\delta\psi_\beta]Ad\alpha=0.$$

(7)

By virtue of Eqs (7), the following five governing differential equations are derived, [14]

$$\frac{\partial(BN_\alpha)}{\partial\alpha}+\frac{\partial(AN_{\beta\alpha})}{\partial\beta}+N_{\alpha\beta}\frac{\partial A}{\partial\beta}-N_\beta\frac{\partial B}{\partial\alpha}+\frac{AB}{R_\alpha}Q_\alpha+\frac{AB}{R_{\alpha\beta}}Q_\beta+ABq_\alpha=0,$$

$$\frac{\partial(AN_\beta)}{\partial\beta}+\frac{\partial(BN_{\alpha\beta})}{\partial\alpha}+N_{\beta\alpha}\frac{\partial B}{\partial\alpha}-N_\alpha\frac{\partial A}{\partial\beta}+\frac{AB}{R_\beta}Q_\beta+\frac{AB}{R_{\alpha\beta}}Q_\alpha+ABq_\beta=0,$$

127

$$\frac{\partial(BQ_\alpha)}{\partial\alpha}+\frac{\partial(AQ_\beta)}{\partial\beta}-AB(\frac{N_\alpha}{R_\alpha}+\frac{N_{\alpha\beta}+N_{\beta\alpha}}{R_{\alpha\beta}}+\frac{N_\beta}{R_\beta})+ABq_z=0,$$

$$\frac{\partial(BM_\alpha)}{\partial\alpha}+\frac{\partial(AM_{\beta\alpha})}{\partial\beta}+M_{\alpha\beta}\frac{\partial A}{\partial\beta}-M_\beta\frac{\partial B}{\partial\alpha}-ABQ_\alpha+\frac{AB}{R_{\alpha\beta}}P_\beta=0,$$

$$\frac{\partial(AM_\beta)}{\partial\beta}+\frac{\partial(BM_{\alpha\beta})}{\partial\alpha}+M_{\beta\alpha}\frac{\partial B}{\partial\alpha}-M_\alpha\frac{\partial A}{\partial\beta}-ABQ_\beta+\frac{AB}{R_{\alpha\beta}}P_\alpha=0. \qquad (8)$$

The rests of the terms in Eq. (7) lead to the boundary conditions for the shell. The boundary data on an edge $\alpha=$ constant are

either $\quad N_{0\alpha}-N_\alpha=0 \qquad$ or $\qquad u_0=$ known,

either $\quad N_{0\alpha\beta}-N_{\alpha\beta}=0 \qquad$ or $\qquad v_0=$ known,

either $\quad Q_{0\alpha}-Q_\alpha=0 \qquad$ or $\qquad w_0=$ known,

either $\quad M_{0\alpha}-M_\alpha=0 \qquad$ or $\qquad \psi_\alpha=$ known,

either $\quad M_{0\alpha\beta}-M_{\alpha\beta}=0 \qquad$ or $\qquad \psi_\beta=$ known. $\qquad (9)$

The boundary conditions on an edge $\beta=$ constant can be found by replacing α and u_0 to β and v_0; respectively, and vise versa in Eqs (9). Depending upon the type of a shell boundary, five boundary conditions should be chosen from the above cases at each edge. Therefore, there are 32 possible types of boundary conditions at each edge. Amongst those possible boundary conditions, two simply supported, S1 and S2, a clamped edge, C, and a free edge, F, boundary conditions at the edge $\alpha=$ constant are selected in this work

as

$S1: \quad u_0 = N_{\alpha\beta} = w_0 = M_\alpha = \psi_\beta = 0, \qquad\qquad S2: \quad N_\alpha = v_0 = w_0 = M_\alpha = \psi_\beta = 0,$

$C: \quad u_0 = v_0 = w_0 = \psi_\beta = \psi_\alpha = 0, \qquad\qquad F: \quad N_\alpha = N_{\alpha\beta} = Q_\alpha = M_\alpha = M_{\alpha\beta} = 0. \qquad (10)$

The stress-strain relationships for a single orthotropic lamina is

$$
\begin{Bmatrix} \sigma_\alpha \\ \sigma_\beta \\ \sigma_{\beta z} \\ \sigma_{\alpha z} \\ \sigma_{\alpha\beta} \end{Bmatrix} = \begin{bmatrix} \bar{Q}_{11} & \bar{Q}_{12} & 0 & 0 & \bar{Q}_{16} \\ \bar{Q}_{12} & \bar{Q}_{22} & 0 & 0 & \bar{Q}_{26} \\ 0 & 0 & \bar{Q}_{44} & \bar{Q}_{45} & 0 \\ 0 & 0 & \bar{Q}_{45} & \bar{Q}_{55} & 0 \\ \bar{Q}_{16} & \bar{Q}_{26} & 0 & 0 & \bar{Q}_{66} \end{bmatrix} \begin{Bmatrix} \varepsilon_\alpha \\ \varepsilon_\beta \\ \gamma_{\beta z} \\ \gamma_{\alpha z} \\ \gamma_{\alpha\beta} \end{Bmatrix} \qquad (11)
$$

wherein Eq. (11) material properties are defined in terms of the stiffness coefficients as

$\bar{Q}_{11} = Q_{11}m^4 + 2(Q_{12} + 2Q_{66})m^2 n^2 + Q_{22}n^4$

$\bar{Q}_{12} = (Q_{11} + Q_{22} - 4Q_{66})m^2 n^2 + Q_{12}(m^4 + n^4)$

$\bar{Q}_{22} = Q_{11}n^4 + 2(Q_{12} + 2Q_{66})m^2 n^2 + Q_{22}m^4, \qquad \bar{Q}_{45} = (Q_{55} - Q_{44})mn,$

$\bar{Q}_{16} = (Q_{11} - Q_{12} - 2Q_{66})m^3 n + (Q_{12} - Q_{22} + 2Q_{66})mn^3, \qquad \bar{Q}_{44} = Q_{44}m^2 + Q_{55}n^2$

$\bar{Q}_{26} = (Q_{11} - Q_{12} - 2Q_{66})mn^3 + (Q_{12} - Q_{22} + 2Q_{66})m^3 n, \qquad \bar{Q}_{55} = Q_{44}n^2 + Q_{55}m^2,$

$\bar{Q}_{66} = (Q_{11} + Q_{22} - 2Q_{12})m^2 n^2 + Q_{66}(m^2 - n^2)^2, \qquad (12)$

In Eqs (12), $m = \cos\theta, n = \sin\theta$, where θ is the angle between the principal axis of

material orthotropy and α -axis. The components of the material properties in Eqs (12) in

129

terms of engineering constants are

$$Q_{11} = E_1 / (1 - v_{12}v_{21}), \qquad Q_{12} = E_1 v_{21} / (1 - v_{12}v_{21}), \qquad Q_{22} = E_2 / (1 - v_{12}v_{21}),$$

$$Q_{44} = G_{23}, \qquad\qquad Q_{55} = G_{13}, \qquad\qquad Q_{66} = G_{12} \qquad (13)$$

Substituting Eqs (3) into Eqs (11), the resultant equations into Eqs (5), and taking the integration in the thickness direction for a shell composed of M layers while ignoring terms of $O(z/R)^2$ lead to the following relationships for the stress resultants

$$
\begin{bmatrix} N_\alpha \\ N_\beta \\ N_{\alpha\beta} \\ N_{\beta\alpha} \\ M_\alpha \\ M_\beta \\ M_{\alpha\beta} \\ M_{\beta\alpha} \end{bmatrix}
=
\begin{bmatrix}
\bar{A}_{11} & A_{12} & \bar{A}_{16} & A_{16} & \bar{B}_{11} & B_{12} & \bar{B}_{16} & B_{16} \\
A_{12} & \hat{A}_{22} & A_{26} & \hat{A}_{26} & B_{12} & \hat{B}_{22} & B_{26} & \hat{B}_{26} \\
\bar{A}_{16} & A_{26} & \bar{A}_{66} & A_{66} & \bar{B}_{16} & B_{26} & \bar{B}_{66} & B_{66} \\
A_{16} & \hat{A}_{26} & A_{66} & \hat{A}_{66} & B_{16} & \hat{B}_{26} & B_{66} & \hat{B}_{66} \\
\bar{B}_{11} & B_{12} & \bar{B}_{16} & B_{16} & \bar{D}_{11} & D_{12} & \bar{D}_{16} & D_{16} \\
B_{12} & \hat{B}_{22} & B_{26} & \hat{B}_{26} & D_{12} & \hat{D}_{22} & D_{26} & \hat{D}_{26} \\
\bar{B}_{16} & B_{26} & \bar{B}_{66} & B_{66} & \bar{D}_{16} & D_{26} & \bar{D}_{66} & D_{66} \\
B_{16} & \hat{B}_{26} & B_{66} & \hat{B}_{66} & D_{16} & \hat{D}_{26} & D_{66} & \hat{D}_{66}
\end{bmatrix}
\begin{bmatrix} \varepsilon_{0\alpha} \\ \varepsilon_{0\beta} \\ \varepsilon_{0\alpha\beta} \\ \varepsilon_{0\beta\alpha} \\ \kappa_\alpha \\ \kappa_\beta \\ \kappa_{\alpha\beta} \\ \kappa_{\beta\alpha} \end{bmatrix},
$$

$$
\begin{bmatrix} Q_\alpha \\ Q_\beta \\ P_\alpha \\ P_\beta \end{bmatrix}
=
\begin{bmatrix}
\bar{A}_{55} & A_{45} & \bar{B}_{55} & B_{45} \\
A_{45} & \hat{A}_{44} & B_{45} & \hat{B}_{44} \\
\bar{B}_{55} & B_{45} & \bar{D}_{55} & D_{45} \\
B_{45} & \hat{B}_{44} & D_{45} & \hat{D}_{44}
\end{bmatrix}
\begin{bmatrix} \gamma_{0\alpha z} \\ \gamma_{0\beta z} \\ -\psi_\alpha / R_{\alpha\beta} \\ -\psi_\beta / R_{\alpha\beta} \end{bmatrix},
\qquad (14)
$$

$$
\left.
\begin{aligned}
\bar{A}_{ij} &= A_{ij} - c_0 B_{ij}, & \hat{A}_{ij} &= A_{ij} + c_0 B_{ij}, \\
\bar{B}_{ij} &= B_{ij} - c_0 D_{ij}, & \hat{B}_{ij} &= B_{ij} + c_0 D_{ij}, \\
\bar{D}_{ij} &= D_{ij} - c_0 E_{ij}, & \hat{D}_{ij} &= D_{ij} + c_0 E_{ij},
\end{aligned}
\right\} \quad i, j = 1,2,4,5,6, \qquad (15)
$$

where $c_0 = \left(\dfrac{1}{R_\alpha} - \dfrac{1}{R_\beta} \right)$ and

$$A_{ij} = \sum_{k=1}^{N} \bar{Q}_{ij}^{(k)} (h_k - h_{k-1})$$

$$B_{ij} = \frac{1}{2} \sum_{k=1}^{N} \bar{Q}_{ij}^{(k)} (h_k^2 - h_{k-1}^2)$$

$$D_{ij} = \frac{1}{3} \sum_{k=1}^{N} \bar{Q}_{ij}^{(k)} (h_k^3 - h_{k-1}^3)$$

$$E_{ij} = \frac{1}{4} \sum_{k=1}^{N} \bar{Q}_{ij}^{(k)} (h_k^4 - h_{k-1}^4)$$

$$i,j = 1,2,6,$$

$$A_{ij} = \sum_{k=1}^{N} K_\alpha K_\beta \bar{Q}_{ij}^{(k)} (h_k - h_{k-1})$$

$$B_{ij} = \frac{1}{2} \sum_{k=1}^{N} K_\alpha K_\beta \bar{Q}_{ij}^{(k)} (h_k^2 - h_{k-1}^2)$$

$$D_{ij} = \frac{1}{3} \sum_{k=1}^{N} K_\alpha K_\beta \bar{Q}_{ij}^{(k)} (h_k^3 - h_{k-1}^3)$$

$$i,j = 4,5, \tag{16}$$

$h_k - h_{k-1}$ is the thickness of the k-th layer, and K_α and K_β are correction factors in α and β directions, respectively. It is worth mentioning that the presence of the components of $\bar{A}\bar{B}\bar{D}$ and $\hat{A}\hat{B}\hat{D}$ with the components of ABD in Eq. (14) is the difference between the theories used here (FSDTQ) and FSDT. The relevant equations for FSDT may be found by letting $c_0 = 0$; thus, $\bar{\Lambda}_{ij} = \hat{\Lambda}_{ij} = \Lambda_{ij}$ where $i,j = 1,2,4,5,6$ and $\Lambda = A, B, D$.

In order to numerically investigate the bending of shells, Eqs (4) should be substitute into (14). We put the resultants with Eqs (8) and arrive to seventeen system of first-order equations (instead of substituting the resultant into Eqs (8) and arriving to second order derivatives). The system of equations is

$$[K]\bar{X} = \bar{q}, \tag{17}$$

where

$$\bar{X} = [u_0, v_0, w_0, \psi_\alpha, \psi_\beta, N_\alpha, N_\beta, N_{\alpha\beta}, N_{\beta\alpha}, M_\alpha, M_\beta, M_{\alpha\beta}, M_{\beta\alpha}, Q_\alpha, Q_\beta, P_\alpha, P_\beta]^T,$$

$$\bar{q} = [q_\alpha, q_\beta, q_z, 0, 0, 0, 0, 0, 0, 0, 0, 0, 0, 0, 0, 0]^T, \tag{18}$$

and the non-zero components of matrix K are

$$K(3k+1, 4k+6) = \frac{\partial B}{\partial \alpha} + B\frac{\partial}{\partial \alpha}, \qquad K(3k+1, 4k+7) = -\frac{\partial B}{\partial \alpha}, \qquad K(3k+1, 4k+8) = \frac{\partial A}{\partial \beta},$$

$$K(3k+1, 4k+9) = \frac{\partial A}{\partial \beta} + A\frac{\partial}{\partial \beta}, \qquad K(1, 14) = \frac{AB}{R_\alpha}, \qquad K(4, 14) = -AB,$$

$$K(3k+1, 2k+15) = \frac{AB}{R_{\alpha\beta}}, \qquad K(3k+2, 4k+6) = -\frac{\partial A}{\partial \beta}, \qquad K(3k+2, 4k+7) = \frac{\partial A}{\partial \beta} + A\frac{\partial}{\partial \beta},$$

$$K(3k+2, 4k+8) = \frac{\partial B}{\partial \alpha} + B\frac{\partial}{\partial \alpha}, \qquad K(3k+2, 4k+9) = \frac{\partial B}{\partial \alpha}, \qquad K(3k+2, 2k+14) = \frac{AB}{R_{\alpha\beta}},$$

$$K(2, 15) = \frac{AB}{R_\beta}, \qquad K(5, 15) = -AB, \qquad K(3, 6) = -\frac{AB}{R_\alpha},$$

$$K(3, 7) = -\frac{AB}{R_\beta}, \qquad K(3, 8) = -\frac{AB}{R_{\alpha\beta}}, \qquad K(3, 9) = -\frac{AB}{R_{\alpha\beta}},$$

$$K(3, 14) = B\frac{\partial}{\partial \alpha}, \qquad K(3, 15) = A\frac{\partial}{\partial \beta},$$

$$K(6+4k, 1) = \frac{\bar{A}_{11}}{A}\frac{\partial}{\partial \alpha} + \frac{A_{16}}{B}\frac{\partial}{\partial \beta} + \frac{A_{12}}{AB}\frac{\partial B}{\partial \alpha} - \frac{\bar{A}_{16}}{AB}\frac{\partial A}{\partial \beta}, \qquad K(6+4k, 2) = \frac{A_{12}}{B}\frac{\partial}{\partial \beta} + \frac{\bar{A}_{16}}{A}\frac{\partial}{\partial \alpha} + \frac{\bar{A}_{11}}{AB}\frac{\partial A}{\partial \beta} - \frac{A_{16}}{AB}\frac{\partial B}{\partial \alpha},$$

$$K(6+4k, 3) = \frac{\bar{A}_{11}}{R_\alpha} + \frac{A_{12}}{R_\beta} + \frac{A_{16} + \bar{A}_{16}}{R_{\alpha\beta}}, \qquad K(6+4k, 4) = \frac{\bar{B}_{11}}{A}\frac{\partial}{\partial \alpha} + \frac{B_{16}}{B}\frac{\partial}{\partial \beta} + \frac{B_{12}}{AB}\frac{\partial B}{\partial \alpha} - \frac{\bar{B}_{16}}{AB}\frac{\partial A}{\partial \beta},$$

$$K(6+4k, 5) = \frac{\bar{B}_{16}}{A}\frac{\partial}{\partial \alpha} + \frac{B_{12}}{B}\frac{\partial}{\partial \beta} - \frac{B_{16}}{AB}\frac{\partial B}{\partial \alpha} + \frac{\bar{B}_{11}}{AB}\frac{\partial A}{\partial \beta}, \qquad K(7+4k, 1) = \frac{A_{12}}{A}\frac{\partial}{\partial \alpha} + \frac{\hat{A}_{26}}{B}\frac{\partial}{\partial \beta} + \frac{\hat{A}_{22}}{AB}\frac{\partial B}{\partial \alpha} - \frac{A_{26}}{AB}\frac{\partial A}{\partial \beta},$$

$$K(7+4k,2) = \frac{\hat{A}_{22}}{B}\frac{\partial}{\partial\beta} + \frac{A_{26}}{A}\frac{\partial}{\partial\alpha} + \frac{A_{12}}{AB}\frac{\partial A}{\partial\beta} - \frac{\hat{A}_{26}}{AB}\frac{\partial B}{\partial\alpha}, \qquad K(7+4k,3) = \frac{A_{12}}{R_\alpha} + \frac{\hat{A}_{22}}{R_\beta} + \frac{\hat{A}_{26}+A_{26}}{R_{\alpha\beta}},$$

$$K(7+4k,4) = \frac{B_{12}}{A}\frac{\partial}{\partial\alpha} + \frac{\hat{B}_{26}}{B}\frac{\partial}{\partial\beta} + \frac{\hat{B}_{22}}{AB}\frac{\partial B}{\partial\alpha} - \frac{B_{26}}{AB}\frac{\partial A}{\partial\beta}, \qquad K(7+4k,5) = \frac{B_{26}}{A}\frac{\partial}{\partial\alpha} + \frac{\hat{B}_{22}}{B}\frac{\partial}{\partial\beta} - \frac{\hat{B}_{26}}{AB}\frac{\partial B}{\partial\alpha} + \frac{B_{12}}{AB}\frac{\partial A}{\partial\beta},$$

$$K(8+4k,1) = \frac{\overline{A}_{16}}{A}\frac{\partial}{\partial\alpha} + \frac{A_{66}}{B}\frac{\partial}{\partial\beta} + \frac{A_{26}}{AB}\frac{\partial B}{\partial\alpha} - \frac{\overline{A}_{66}}{AB}\frac{\partial A}{\partial\beta}, \qquad K(8+4k,2) = \frac{A_{26}}{B}\frac{\partial}{\partial\beta} + \frac{\overline{A}_{66}}{A}\frac{\partial}{\partial\alpha} + \frac{\overline{A}_{16}}{AB}\frac{\partial A}{\partial\beta} - \frac{A_{66}}{AB}\frac{\partial B}{\partial\alpha},$$

$$K(8+4k,3) = \frac{\overline{A}_{16}}{R_\alpha} + \frac{A_{26}}{R_\beta} + \frac{A_{66}+\overline{A}_{66}}{R_{\alpha\beta}}, \qquad\qquad K(8+4k,4) = \frac{\overline{B}_{16}}{A}\frac{\partial}{\partial\alpha} + \frac{B_{66}}{B}\frac{\partial}{\partial\beta} + \frac{B_{26}}{AB}\frac{\partial B}{\partial\alpha} - \frac{\overline{B}_{66}}{AB}\frac{\partial A}{\partial\beta},$$

$$K(8+4k,5) = \frac{\overline{B}_{66}}{A}\frac{\partial}{\partial\alpha} + \frac{B_{26}}{B}\frac{\partial}{\partial\beta} - \frac{B_{66}}{AB}\frac{\partial B}{\partial\alpha} + \frac{\overline{B}_{16}}{AB}\frac{\partial A}{\partial\beta}, \qquad K(9+4k,1) = \frac{A_{16}}{A}\frac{\partial}{\partial\alpha} + \frac{\hat{A}_{66}}{B}\frac{\partial}{\partial\beta} + \frac{\hat{A}_{26}}{AB}\frac{\partial B}{\partial\alpha} - \frac{A_{66}}{AB}\frac{\partial A}{\partial\beta},$$

$$K(9+4k,2) = \frac{\hat{A}_{26}}{B}\frac{\partial}{\partial\beta} + \frac{A_{66}}{A}\frac{\partial}{\partial\alpha} + \frac{A_{16}}{AB}\frac{\partial A}{\partial\beta} - \frac{\hat{A}_{66}}{AB}\frac{\partial B}{\partial\alpha}, \qquad K(9+4k,3) = \frac{A_{16}}{R_\alpha} + \frac{\hat{A}_{26}}{R_\beta} + \frac{\hat{A}_{66}+A_{66}}{R_{\alpha\beta}},$$

$$K(9+4k,4) = \frac{B_{16}}{A}\frac{\partial}{\partial\alpha} + \frac{\hat{B}_{66}}{B}\frac{\partial}{\partial\beta} + \frac{\hat{B}_{26}}{AB}\frac{\partial B}{\partial\alpha} - \frac{B_{66}}{AB}\frac{\partial A}{\partial\beta}, \qquad K(9+4k,5) = \frac{B_{66}}{A}\frac{\partial}{\partial\alpha} + \frac{\hat{B}_{26}}{B}\frac{\partial}{\partial\beta} - \frac{\hat{B}_{66}}{AB}\frac{\partial B}{\partial\alpha} + \frac{B_{16}}{AB}\frac{\partial A}{\partial\beta},$$

$$K(14+2k,1) = -\left(\frac{\overline{A}_{55}}{R_\alpha} + \frac{A_{45}}{R_{\alpha\beta}}\right), \qquad\qquad K(14+2k,2) = -\left(\frac{A_{45}}{R_\beta} + \frac{\overline{A}_{55}}{R_{\alpha\beta}}\right),$$

$$K(14+2k,3) = \frac{\overline{A}_{55}}{A}\frac{\partial}{\partial\alpha} + \frac{A_{45}}{B}\frac{\partial}{\partial\beta}, \qquad\qquad K(14+2k,4) = \overline{A}_{55} - \frac{\overline{B}_{55}}{R_{\alpha\beta}},$$

$$K(14+2k,5) = A_{45} - \frac{B_{45}}{R_{\alpha\beta}}, \qquad\qquad K(15+2k,1) = -\left(\frac{A_{45}}{R_\alpha} + \frac{\hat{A}_{44}}{R_{\alpha\beta}}\right),$$

$$K(15+2k,2) = -\left(\frac{\hat{A}_{44}}{R_\beta} + \frac{A_{45}}{R_{\alpha\beta}}\right), \qquad\qquad K(15+2k,3) = \frac{A_{45}}{A}\frac{\partial}{\partial\alpha} + \frac{\hat{A}_{44}}{B}\frac{\partial}{\partial\beta},$$

$$K(15+2k,4) = A_{45} - \frac{B_{45}}{R_{\alpha\beta}}, \qquad\qquad K(15+2k,5) = \hat{A}_{44} - \frac{\hat{B}_{44}}{R_{\alpha\beta}}, \quad k=0,1,$$

$$K(i,i) = -1, \quad i = 6,7,\ldots 17. \tag{19}$$

In the Eqs (19), in the terms containing k, for $k=1$ the components of matrixes $B, \overline{B}, \hat{B}$ should change to $D, \overline{D}, \hat{D}$, respectively; then $A, \overline{A}, \hat{A}$ should change to $B, \overline{B}, \hat{B}$,

respectively. The present formulation facilitates the direct application of all kinds of boundary conditions in the ensuing numerical treatment. The numerical solution of Eqs (17) is accomplished by means of the generalized differential quadrature (GDQ) method in this work. The method is utilized by several investigators [e.g. 15]. In the GDQ method the derivative of a function at any discrete point in a direction is approximated as a weighted linear sum of the function values at all the sampling points in that direction

$$\frac{dF(x_k)}{dx} = \sum_{l=1}^{N} C_{kl} F(x_l), \qquad k \in \{1, 2, ..., N\} \tag{20}$$

where N is the number of sampling points selected in the x-direction and Ckl are the weighting coefficients of the first derivative with respect to variable x. The coefficients in Eqs (20) are

$$C_{kl} = \frac{M(x_k)}{(x_k - x_l)M(x_l)}, \qquad k, l = 1, 2, ..., N, \qquad k \neq l$$

$$C_{kk} = -\sum_{\substack{l=1 \\ l \neq k}}^{N} C_{kl} \qquad k = 1, 2, ..., N \tag{21}$$

where $M(x_k) = \prod_{\substack{l=1 \\ l \neq k}}^{N} (x_k - x_l)$. In order to have a denser distribution of grid points near boundaries, the sampling points are chosen in the form of cosine distribution as

$$x_k = \frac{L_x}{2}[1 - cos(\frac{k-1}{N-1}\pi)], \qquad k = 1, 2, ..., N \tag{22}$$
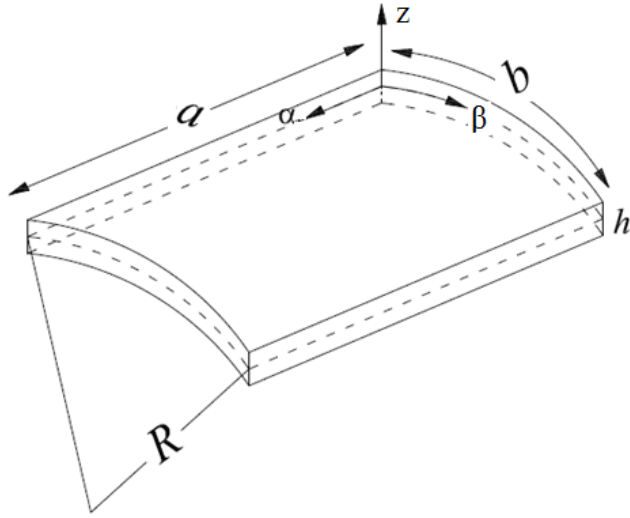
Figure 5.1:   Schematic view of a cylindrical shell.

where Lx is the length in x-direction. This described GDQ procedure should be applied to the system of first order differential equations (17) with conjunction of boundary conditions (10) to find unknown vector $\bar{X}$ in each grid points.

5.2.   Numerical results by GDQ

For the numerical analyses, laminated cylindrical panels with radius R are selected in this work (Fig. 5.1). Let the β-axis coincide with the curved edge of the cylindrical panel; thus, $R_\alpha = R_{\alpha\beta} = \infty$ and $A = B = 1$. The length-to-arc ratio, $a/b = 1$, thickness ratio, $a/h = 10$ (Moderately thick), depth ratio, $a/R = 2$ (very Deep) and equal shear correction factors in both directions, $k^2 = 5/6$ under uniformly distributed load q are considered unless otherwise mentioned. The material properties for orthotropic materials

135
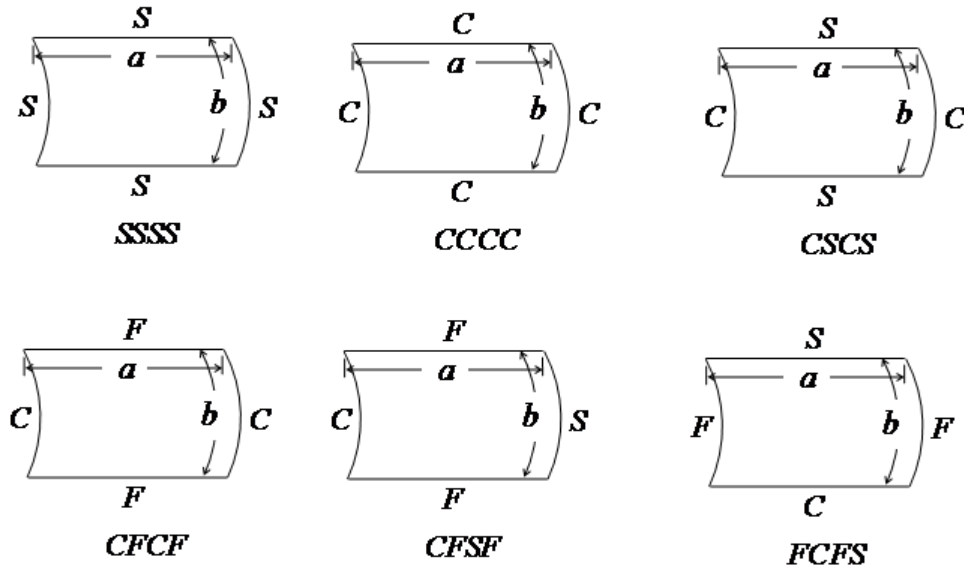
Figure 5.2:   Different type of boundary conditions.

are considered as $E_1/E_2 = 25$, $G_{12}/E_2 = 0.5$, $G_{23}/E_2 = 0.2$, $G_{13} = G_{12}$, and $v_{12} = 0.25$.

Dimensionless transverse displacement $w^* = 10^3 E_2 h^3 w / q_n a^4$, moment and force

resultants, respectively, $M_i^* = 10^3 M_i / qa^2$, and $N_i^* = 10^3 N_i / qa^3$, where $i = \alpha, \beta$ at the

center of the shell are calculated based on both FSDT and FSDTQ.

The convergence of the presented numerical method is studied with the increment

of GDQ grid points in Table 5.1. An isotropic shell with fully S-2 type boundary

condition (shear diaphragm) where the exact solution exists and reported by Asadi et al.

[2] is considered. The results show that the convergence of the center displacement

occurs with nine sampling points in each side which is faster than the convergence of the

moment and force resultants. However, all results converged to the exact solution by the

increment of sampling points to fifteen with the desired accuracy.

136

Table 5.1:   Convergence study of an isotropic cylindrical shell with $\nu = 0.25$.

GDQ	w^*	M_α^*	M_β^*	N_α^*	N_β^*
7×7	12.1113	9.9148	4.5266	657.10	573.42
9×9	12.1080	9.9278	4.5213	657.48	572.57
11×11	12.1080	9.9288	4.5215	657.46	572.60
13×13	12.1080	9.9288	4.5215	657.47	572.61
15×15	12.1080	9.9288	4.5215	657.47	572.61
Exact [9]	12.108	9.9288	4.5215	657.47	572.61

Dimensionless displacement and moment resultants of isotropic cylindrical panels with length-to-arc ratio, a/b = 3, and two different depth ratio, having fully S1-type simply-supported boundary condition, are presented in Table 5.2. In this example, results of presented theories (FSDT and FSDTQ) are compared against each others and those of other different FSDTs reported in Chaudhuri and Kabir [16] and a HSDT considering the effect of depth presented by Yaghoubshahi et al. [17]. Comparing the present theory with the cited theories reveals that the results of FSDTQ are in a better agreement with those of a HSDT including the effect of depth rather than other FSDTs.

For the rest of the numerical examples, orthotropic cylindrical shells with three different lay-ups, having six different types of boundary conditions are considered (Fig. 5.2). These are combinations of clamped, free and S2-type simply supported (called only simply supported after this) boundary conditions. Presented results from both FSDT and FSDTQ are compared against each others and against those obtained using 3D elasticity by finite element method (FEM). Figure 4.1 shows the mesh pattern of a typical

Table 5.2:   Comparison of different shell theories for isotropic cylindrical panels with $\nu = 0.3$

Shell Theory	w^*		M_α^*		M_β^*	
	R/b=10	R/b=1	R/b=10	R/b=1	R/b=10	R/b=1
Modified Sanders	123.37	12.97	37.10	3.23	109.68	11.16
Sanders	123.35	12.95	37.10	3.22	109.66	11.11
Reissner	123.37	12.97	37.10	3.23	109.68	11.16
Donnell	123.35	12.95	37.10	3.22	109.66	11.11
FSDT	126.39	13.19	37.03	3.24	109.23	11.05
FSDTQ	126.55	13.32	37.07	3.21	109.29	10.77
HSDT	126.60	13.32	37.07	3.21	109.27	10.93

cylindrical shell modeled using FEM wherein 3D elements are used. Moreover, uniformly distributed load, q, is divided into two positive and negative pressures at the top and bottom planes of the shell; respectively, such that the whole force on the shell is equal to abq. For simply supported boundary condition at $\alpha - $constant, W and V are set to zero at the relevant plane of the boundary condition to make sure that $v_0 = w_0 = \psi_\beta = 0$ in presented theories. Also, all three displacements of the plane at the boundary edge are set to zero and free in the 3D finite element analyses for clamped and free boundary conditions; respectively. Moreover, the number of quadratic solid elements used in FEM did not need to exceed $40 \times 40 \times 12$ for the convergence of the results. Dimensionless displacement, force and moment resultants of a cross-ply, $[0/90]_3$, cylindrical shell with six different boundary conditions are shown in Table 5.3. FSDTQ predicts the center displacement, moment resultants, and force resultants better than FSDT up to 2%, 17% and 4%, respectively (when compared with 3D results). Also,

Table 5.3:   Comparison of dimensionless displacements, moments and force resultants of $[0/90]_3$ cylindrical shells with different boundary conditions.

B.C.		w^*	M_α^*	M_β^*	N_α^*	N_β^*
SSSS	FSDT	5.2715	34.605	22.103	494.05	392.25
	FSDTQ	5.3092	34.841	21.767	500.66	396.76
	3D	5.4545	32.959	19.755	514.53	409.77
CCCC	FSDT	0.3056	0.9063	5.3758	11.194	482.39
	FSDTQ	0.3104	0.9120	4.6266	11.460	482.34
	3D	0.3124	1.0052	4.3571	9.3979	484.99
CSCS	FSDT	3.6668	20.459	14.838	131.97	324.27
	FSDTQ	3.7029	20.491	14.599	133.86	328.19
	3D	3.9818	18.849	14.150	139.45	351.29
CFCF	FSDT	3.5657	20.032	14.849	132.21	413.22
	FSDTQ	3.5876	19.982	14.721	132.70	418.01
	3D	3.8508	18.436	15.631	149.12	448.95
CFSF	FSDT	4.7281	28.411	18.685	419.50	473.51
	FSDTQ	4.7577	28.634	18.452	421.25	478.43
	3D	5.0026	27.018	19.257	447.13	503.75
FCFS	FSDT	14.851	0.7554	56.516	3.321	115.14
	FSDTQ	14.997	0.7886	56.539	3.507	115.26
	3D	17.609	0.8101	56.365	5.384	117.73

results for FCFS-type boundary condition are farthest results from the 3D results for the same lay-up. Similar results are presented in Table 5.4 for an angle-ply lay-up, namely $[-45/45]_3$. The error of dimensionless displacement in this lay-up for both FSDT

Table 5.4: Comparison of dimensionless displacements, moments and force resultants of $[-45/45]_3$ cylindrical shells with different boundary conditions.

B.C.		w^*	Error	M^*_α	Error	M^*_β	Error	N^*_α	Error	N^*_β	Error
SSSS	FSDT	0.7310	9.7%	0.1986	85.5%	0.3175	9.0%	729.40	2.1%	659.01	1.8%
	FSDTQ	0.7358	9.1%	1.2246	10.3%	0.3812	9.2%	736.34	1.2%	665.02	0.9%
	3D	0.8097		1.3651		0.3490		745.22		671.07	
CCCC	FSDT	0.5159	0.3%	1.9135	17.6%	1.9455	143%	402.13	2.4%	484.54	1.7%
	FSDTQ	0.5202	0.6%	1.9179	17.8%	1.1416	42.5%	406.33	1.4%	486.03	1.4%
	3D	0.5172		1.6277		0.8013		411.92		493.13	
CSCS	FSDT	0.6586	3.7%	0.1574	71.1%	0.2055	77.5%	615.38	4.3%	648.63	1.6%
	FSDTQ	0.6689	2.2%	0.6050	11.2%	0.7627	16.5%	620.18	3.5%	652.33	1.0%
	3D	0.6836		0.5439		0.9136		642.78		659.03	
CFCF	FSDT	1.1861	9.5%	3.2615	71.5%	7.0912	0.9%	1066.8	2.9%	1007.7	0.4%
	FSDTQ	1.1977	10.6%	0.9463	50.3%	5.9122	17.4%	1031.9	0.5%	995.34	0.8%
	3D	1.0829		1.9023		7.1575		1036.9		1003.3	
CFSF	FSDT	3.1296	3.2%	2.5474	21.8%	3.4083	19.7%	940.73	3.6%	1014.6	1.0%
	FSDTQ	3.1280	3.1%	4.5254	38.9%	2.4052	43.3%	909.63	0.1%	1012.2	1.3%
	3D	3.0328		3.2582		4.2455		908.46		1025.1	
FCFS	FSDT	24.247	9.7%	59.910	1.7%	70.491	0.2%	229.31	17.0%	276.34	11.7%
	FSDTQ	24.261	9.7%	59.483	0.8%	70.494	0.2%	196.62	0.3%	248.03	0.3%
	3D	26.863		58.989		70.608		196.01		247.72	

Table 5.5:   Comparison of dimensionless displacements, moments and force resultants of $[30/60/45]$ cylindrical shells with different boundary conditions.

B.C.		w^*	M_α^*	M_β^*	N_α^*	N_β^*
SSSS	FSDT	2.1496	10.089	9.5929	566.59	531.35
	FSDTQ	2.1552	11.176	9.5743	581.95	537.22
	3D	2.2130	11.626	9.7328	579.92	538.21
CCCC	FSDT	0.4794	2.7919	4.3264	300.33	476.94
	FSDTQ	0.4896	2.8885	3.8726	305.44	476.42
	3D	0.4938	2.9508	3.9819	307.92	477.42
CSCS	FSDT	1.3012	3.7353	5.0170	552.89	531.00
	FSDTQ	1.3189	4.6978	5.0165	567.31	539.31
	3D	1.3472	5.0247	5.1928	575.73	541.13
CFCF	FSDT	1.3267	1.8062	2.4559	636.00	677.02
	FSDTQ	1.3222	2.7661	2.1690	637.81	691.40
	3D	1.3651	3.4142	2.2485	647.31	697.87
CFSF	FSDT	2.9930	12.148	1.2989	462.19	691.47
	FSDTQ	3.0494	$\overline{1}3.953$	0.3287	457.20	700.49
	3D	3.2022	$\overline{1}5.023$	0.4257	459.31	708.15
FCFS	FSDT	35.975	60.918	71.845	101.28	321.54
	FSDTQ	36.462	64.326	72.414	132.12	326.32
	3D	36.940	63.947	73.632	133.11	329.68

and FSDTQ increases to ten percent. Although errors for all results increase in the angle-ply lay-up when compared to cross-ply lay-up. Moreover, the maximum errors in force resultants are 17% for FSDT whereas it is 3% for FSDTQ. The last example is the same as the two previous examples but for the lay-up of $[30/60/45]$ and its results are shown

in Table 5.5. Dimensionless displacement and moment resultants for all type of boundary conditions predicted by FSDTQ are in a better agreement with 3D results rather than those of FSDT for this general lay-up. Indeed, the FSDT predicts moment resultants out of order in some cases such as the case of CFSF wherein the error of 205% is observed whereas this error is nine percent for FSDTQ! Also, the maximum error of FSDTQ in force resultants is under two percent where it is around 24% for FSDT.

5.3.   Conclusions

Static analyses are performed on composite cylindrical shells with different boundary conditions and lay-ups using FSDT, FSDTQ and 3D using GQD. FSDTQ offers a more accurate representation of the stiffness parameters and the stress resultant equations by including the 1+z/R in the equations. Almost all analyses are showing that there is a significant improvement (closer to 3D and HSDTs that includes the effects of depth) obtained when FSDTQ is used. This improvement increases when angle-ply or generally laminated composites are used for shells. Also, it varies with the change of boundary conditions. This analysis is a prelude to the derivation of a proper higher order shell theory (e.g. third order) where the term (1+z/R) needs to be truncated at the third order.

5.4. References

1. Ambartsumian S.A. Contribution to the theory of anisotropic laminated shells. Appl Mech Rev 1962; 15: 245-249.

2. Asadi E., Wang W., Qatu M.S. Static and vibration analyses of thick deep laminated cylindrical shells using 3D and various shear deformation theories. Compos Struct 2011; DOI: 10.1016/j.compstruct.2011.08.011.

3. Rath B.K, Das Y.C. Vibration of layered shells. J Sound Vib 1973; 28: 737-757.

4. Reddy JN. Exact solution of moderately thick laminated shells. J Engng Mech ASCE 1984; 110: 794-809.

5. Librescu L., Khdeir A.A., Frederick D. A shear-deformable theory for laminated composite shallow shell-type panels and their response analysis I: free vibration and buckling. Acta Mechanica; 1989; 75: 1-33.

6. Librescu L., Khdeir A.A., Frederick D. A shear-deformable theory for laminated composite shallow shell-type panels and their response analysis II: static analysis. Acta Mechanica 1989; 77: 1-12.

7. Reddy JN, Liu C.F. A higher order shear deformation theory of laminated elastic shells. Int J Engng Sci 1985; 23: 440-447.

8. Qatu M.S. Accurate stress resultants equations for laminated composite deep thick shells. Compos Press Vessl Indust 1995; 302: 39-44.

9. Qatu M.S. Accurate equations for laminated composite deep thick shells. Int J Solids Struct 1999; 36: 2917-2941.

10. Qatu M.S., Sullivan R.W., Wang W. Recent research advances in the dynamic behavior of composite shells: 2000-2009. Compos Struct 2010; 93: 14–31.

11. Qatu M.S., Asadi E., Wang W. Review of recent literature on static analysis of composite shells: 2000-2010. Accepted for publication, Appl Mech Rev 2012.

12. Carrera E. Historical review of zig-zag theories for multilayered plates and shells. Appl Mech Rev 2003; 56: 287–309.

13. Carrera E. Theories and finite elements for multilayered, anisotropic, composite plates and shells. J Arch Comput Methods Engng 2002; 87: 87–140.

14. Qatu M.S. Vibration of Laminated Shells and Plates. Elsevier, 2004.

15. Asadi E., Fariborz S.J. Free vibration of composite plates with mixed boundary conditions based on higher-order shear deformation theory. Arch Appl Mech 2011;

DOI: 10.1007/s00419-011-0588-y.

16. Chaudhuri R.A., Kabir H.R.H. Boundary-discontinuous Fourier analysis of doubly-curved panels using classical shallow shell theories. Int J Engng Sci 1993; 31: 1551-1564.

17. Yaghoubshahi M., Asadi E., Fariborz S.J. A higher-order shell model applied to shells with mixed boundary conditions. J Mech Engng Sci IMechE 2011; 225: 292-303.

CHAPTER 6

FREE VIBRATION OF THICK LAMINATED CYLINDERICAL

SHELLS WITH DIFFERENT BOUNDARY

CONDITIONS USING GDQ

Light weight and high stiffness of structures made of laminated composite materials have provided excellent new opportunities in the design of engineering structures such as automotive, aerospace and submarine ones. The simplicity of shell and plate theories and the complexity of composite structures making them hard to analyze by three dimensional (3D) elasticity methods have led to the development of different shell and plate theories. In the development of plate theories, the thickness ratio is the main issue in categorizing different plate theories which are mainly classified into Classical Theories, First-order Shear Deformation Theories (FSDTs) and Higher-order Shear Deformation Theories (HSDTs). Besides the effect of the thickness of shells, the effect of depth ratio of shells should be included in the development of shell theories. Some researchers included the effect of the depth ratio in the development of shell theories, e.g. Qatu [1,2], Asadi et al. [3] and Yaghoubshahi et al. [4]. However, in spite of the effects of thickness ratio, the effects of the depth ratios need to be examined in the development of different shell theories.

Appearance of the term (1+z/R) in both the strain displacement and stress resultant equations in the derivation of the basic equation of shells makes it difficult to include the effects of depth ratio in shell theories. The term was neglected by first analysts of composite thin shells e.g. Ambartsumian [5] which is understandable for thin shells. In addition to the inclusion of this term, both shear deformation and rotary inertia should be included for composite thick shells. Early shear deformation shell theories included both shear deformation and rotary inertia rotary but failed to include the z/R terms [6,7]. We will refer to these as simply the first order shear deformation theory (FSDT). Interestingly, some researchers developed higher order theories while still neglecting the term, e.g. Librescu et al. [8,9] and Reddy and Liu [10]). Qatu [1,2] presented equations where the term is considered in the shell equations for composite deep thick shells. We will refer to his equations as the first order shear deformation shell theory by Qatu (FSDTQ). Asadi et al. [3] used FSDTQ to find exact static and free vibration solution of isotropic and composite deep and thick shells with fully simply supported boundary conditions. They showed that using of FSDTQ instead of FSDT significantly improves the results comparing to 3D results. However the effect of using FSDTQ on shells with different boundary conditions and general lay-ups of laminates needs to be examined. Much of the literature on shell analysis is reviewed recently showing that inaccurate equations are still used in a significant portion of shells works (Qatu et al. [11,12] and Carrera [13,14].

Equations of motion with required boundary conditions for a deep and thick cylindrical composite shell are obtained using FSDTQ. It is shown that FSDT is a simplification from FSDTQ where the effects of the depth in shell analyses are neglected.

Equations of motion are put together with the equations of stress resultants to arrive at a system of fifteen first-order differential equations. General Differential Quadrature (GDQ) method is employed to solve this system of first-order differential equations to find the shell natural frequencies and mode shapes. Isotropic, cross-ply, angle-ply and general lay-up cylindrical shells with six types of different boundary conditions which are combinations of simply supported, clamped, and free boundary conditions are examined using both FSDTQ and FSDT. Moreover, the first five natural frequency parameters and relevant mode shapes for those shells are obtained and compared with those of a converged 3D finite element analysis done by ANSYS®. Also, Errors of FSDTQ and FSDT results (when comparing them to those of the 3D results) are obtained and discussed.

6.1.   Formulation of free vibration for composite cylindrical shells

A cylindrical shell with in-plane axis x in the direction of the axis of shell, circumferential in-plane axis β, normal to the middle-plane axis z and radius R, Fig. 5.1, is considered. The Hamilton's principle for a body with surface S and volume V between two arbitrary time intervals t_0 and t_1 requires that

$$\int_{t_0}^{t_1} \left\{ \int_V [\sigma_x \delta\varepsilon_x + \sigma_\beta \delta\varepsilon_\beta + \sigma_z \delta\varepsilon_z + \sigma_{x\beta} \delta\gamma_{x\beta} + \sigma_{xz} \delta\gamma_{xz} + \sigma_{\beta z} \delta\gamma_{\beta z} \right.$$

$$\left. - \rho(\dot{u}\delta\dot{u} + \dot{v}\delta\dot{v} + \dot{w}\delta\dot{w})]dV - \int_S \delta W_{ext} dS \right\} dt = 0, \tag{1}$$

where $\sigma_{...}$ and $\varepsilon_{...}$, respectively, are stress and strain components, ρ is the mass density, and δW_{ext} is the virtual work done by external forces. Employing the first-order shear deformation model, the displacement components approximate as

$$u(x,\beta,z,t) = u_0(x,\beta,t) + z\psi_x(x,\beta,t),$$

$$v(x,\beta,z,t) = v_0(x,\beta,t) + z\psi_\beta(x,\beta,t),$$

$$w(x,\beta,z,t) = w_0(x,\beta,t), \qquad (2)$$

where $-h/2 \le z \le h/2$ and h is the shell thickness, u_0, v_0, and w_0 are midsurface displacements of the shell, and ψ_x and ψ_β are midsurface rotations. The strain-displacement relationships in the principal coordinates of a cylindrical shell can be simplified from relevant equations for the general shell [15] as

$$\varepsilon_x = \frac{\partial u}{\partial x}, \qquad \varepsilon_\beta = \frac{1}{1+z/R}\left(\frac{\partial v}{\partial \beta} + \frac{w}{R}\right), \qquad \varepsilon_z = \frac{\partial w}{\partial z}, \qquad \gamma_{x\beta} = \frac{1}{1+z/R}\frac{\partial u}{\partial \beta} + \frac{\partial v}{\partial x},$$

$$\gamma_{xz} = \frac{\partial w}{\partial x} + \frac{\partial u}{\partial z}, \qquad \gamma_{\beta z} = \frac{1}{1+z/R}\frac{\partial w}{\partial \beta} + (1+z/R)\frac{\partial}{\partial z}\left(\frac{v}{1+z/R}\right). \qquad (3)$$

By substituting Eqs (2) into (3), strain-displacement equations become

$$\varepsilon_x = \frac{\partial u_0}{\partial x} + z\frac{\partial \psi_x}{\partial x}, \qquad \varepsilon_\beta = \frac{1}{1+z/R}\left(\frac{\partial v_0}{\partial \beta} + \frac{w_0}{R} + z\frac{\partial \psi_\beta}{\partial \beta}\right), \qquad \varepsilon_z = 0,$$

$$\varepsilon_{x\beta} = \frac{\partial v_0}{\partial x} + z\frac{\partial \psi_\beta}{\partial x}, \qquad \varepsilon_{\beta x} = \frac{1}{(1+z/R)}\left(\frac{\partial u_0}{\partial \beta} + z\frac{\partial \psi_x}{\partial \beta}\right),$$

148

$$\gamma_{xz} = \frac{\partial w_0}{\partial x} + \psi_x, \qquad \gamma_{\beta z} = \frac{1}{1+z/R}(\frac{\partial w_0}{\partial \beta} + \psi_\beta - \frac{v_0}{R}). \tag{4}$$

The stress resultants are defined as

$$\left[N_x \quad N_{x\beta} \quad Q_x \quad M_x \quad M_{x\beta} \right]^T = \int_{-h/2}^{h/2} \left[\sigma_x \quad \sigma_{x\beta} \quad \sigma_{xz} \quad z\sigma_x \quad z\sigma_{x\beta} \right]^T (1+\frac{z}{R})dz,$$

$$\left[N_\beta \quad N_{\beta x} \quad Q_\beta \quad M_\beta \quad M_{\beta x} \right]^T = \int_{-h/2}^{h/2} \left[\sigma_\beta \quad \sigma_{\beta x} \quad \sigma_{\beta z} \quad z\sigma_\beta \quad z\sigma_{\beta x} \right]^T dz, \tag{5}$$

where the superscript T stands for the transpose of a vector. The applied load per unit area on the middle surface of the shell is $\bar{q} = q_x \bar{e}_x + q_\beta \bar{e}_\beta + q_z \bar{e}_z$, where the unit vectors $\bar{e}_x$ and $\bar{e}_\beta$ are tangent to the principal axes and $\bar{e}_z$ is perpendicular to the shell surface. Let σ_{0x}, $\sigma_{0x\beta}$ and σ_{0xz} be the components of applied traction on the edges $x =$ constant and $\sigma_{0\beta}$, $\sigma_{0\beta x}$ and $\sigma_{0\beta z}$ be the components of applied traction on the edges $\beta =$ constant. The external work done by the external loads on the shell yields

$$\delta w_{ext} = \int_x \int_\beta (q_x \delta u + q_\beta \delta v + q_z \delta w) AB \, dx \, d\beta + \oint_\beta \int_{-h/2}^{h/2} (\sigma_{0x} \delta u + \sigma_{0x\beta} \delta v$$

$$+ \sigma_{0xz} \delta w)(1+z/R) dz \, d\beta + \oint_x \int_{-h/2}^{h/2} (\sigma_{0\beta} \delta v + \sigma_{0\beta x} \delta u + \sigma_{0\beta z} \delta w) \, dz \, dx. \tag{6}$$

Substituting Eqs (5) into Eq. (6), the resultant equation with Eqs (4) into Eq. (1), employing the definitions (5), setting $\sigma_z = 0$, and carrying out the required manipulations results in the following five equations of motion

$$\frac{\partial N_x}{\partial x} + \frac{\partial N_{\beta x}}{\partial \beta} + q_x = \bar{I}_1 \ddot{u}_0 + \bar{I}_2 \ddot{\psi}_x, \quad \frac{\partial N_{\beta}}{\partial \beta} + \frac{\partial N_{x\beta}}{\partial x} + \frac{Q_{\beta}}{R} + q_{\beta} = \bar{I}_1 \ddot{v}_0 + \bar{I}_2 \ddot{\psi}_{\beta},$$

$$\frac{\partial Q_x}{\partial x} + \frac{\partial Q_{\beta}}{\partial \beta} - \frac{N_{\beta}}{R} + q_z = \bar{I}_1 \ddot{w}_0,$$

$$\frac{\partial M_x}{\partial x} + \frac{\partial M_{\beta x}}{\partial \beta} - Q_x = \bar{I}_2 \ddot{u}_0 + \bar{I}_3 \ddot{\psi}_x, \quad \frac{\partial M_{\beta}}{\partial \beta} + \frac{\partial M_{x\beta}}{\partial x} - Q_{\beta} = \bar{I}_2 \ddot{v}_0 + \bar{I}_3 \ddot{\psi}_{\beta}, \qquad (7)$$

where

$$\bar{I}_i = \left(I_i + \frac{I_{i+1}}{R} \right), \quad i = 1, 2, 3, \qquad \left[I_1, I_2, I_3, I_4 \right]^T = \sum_{k=1}^{N} \int_{h_{k-1}}^{h_k} \rho^{(k)} \left[1, z, z^2, z^3 \right]^T dz. \qquad (8)$$

The boundary data on an edge $x = $ constant are

either $\quad N_{0x} - N_x = 0 \qquad$ or $\qquad u_0 = $ known,

either $\quad N_{0x\beta} - N_{x\beta} = 0 \qquad$ or $\qquad v_0 = $ known,

either $\quad Q_{0x} - Q_x = 0 \qquad$ or $\qquad w_0 = $ known,

either $\quad M_{0x} - M_x = 0 \qquad$ or $\qquad \psi_x = $ known,

either $\quad M_{0x\beta} - M_{x\beta} = 0 \qquad$ or $\qquad \psi_{\beta} = $ known. $\qquad (9)$

The boundary conditions on an edge $\beta = $ constant can be found by replacing x and u_0 to β and v_0, respectively, and vise versa in Eqs (9). Depending upon the type of the shell boundary, five boundary conditions should be chosen from the above cases at each edge. Therefore, there are 32 possible types of boundary conditions at each edge. Amongst

those possible boundary conditions, a simply supported edge, S, clamped edge, C, and free edge, F, boundary conditions are selected in this work. Theses boundary conditions at the edge $x=$constant can be expressed as

$$S: \quad N_x = v_0 = w_0 = M_x = \psi_\beta = 0, \qquad\qquad C: \quad u_0 = v_0 = w_0 = \psi_\beta = \psi_\alpha = 0,$$

$$F: \quad N_x = N_{x\beta} = Q_x = M_x = M_{x\beta} = 0. \tag{10}$$

The stress-strain relationships for a single orthotropic lamina in a cylindrical shell is

$$\begin{Bmatrix} \sigma_x \\ \sigma_\beta \\ \sigma_{\beta z} \\ \sigma_{xz} \\ \sigma_{x\beta} \end{Bmatrix} = \begin{bmatrix} \bar{Q}_{11} & \bar{Q}_{12} & 0 & 0 & \bar{Q}_{16} \\ \bar{Q}_{12} & \bar{Q}_{22} & 0 & 0 & \bar{Q}_{26} \\ 0 & 0 & \bar{Q}_{44} & \bar{Q}_{45} & 0 \\ 0 & 0 & \bar{Q}_{45} & \bar{Q}_{55} & 0 \\ \bar{Q}_{16} & \bar{Q}_{26} & 0 & 0 & \bar{Q}_{66} \end{bmatrix} \begin{Bmatrix} \varepsilon_x \\ \varepsilon_\beta \\ \gamma_{\beta z} \\ \gamma_{xz} \\ \gamma_{x\beta} \end{Bmatrix} \tag{11}$$

wherein Eq. (11) material properties are defined in terms of the stiffness coefficients as

$$\bar{Q}_{11} = Q_{11}m^4 + 2(Q_{12} + 2Q_{66})m^2 n^2 + Q_{22}n^4, \quad \bar{Q}_{12} = (Q_{11} + Q_{22} - 4Q_{66})m^2 n^2 + Q_{12}(m^4 + n^4),$$

$$\bar{Q}_{22} = Q_{11}n^4 + 2(Q_{12} + 2Q_{66})m^2 n^2 + Q_{22}m^4, \quad \bar{Q}_{45} = (Q_{55} - Q_{44})mn,$$

$$\bar{Q}_{16} = (Q_{11} - Q_{12} - 2Q_{66})m^3 n + (Q_{12} - Q_{22} + 2Q_{66})mn^3, \quad \bar{Q}_{44} = Q_{44}m^2 + Q_{55}n^2,$$

$$\bar{Q}_{26} = (Q_{11} - Q_{12} - 2Q_{66})mn^3 + (Q_{12} - Q_{22} + 2Q_{66})m^3 n, \quad \bar{Q}_{55} = Q_{44}n^2 + Q_{55}m^2,$$

$$\bar{Q}_{66} = (Q_{11} + Q_{22} - 2Q_{12})m^2 n^2 + Q_{66}(m^2 - n^2)^2. \tag{12}$$

In Eqs (12), $m = \cos\theta, n = \sin\theta$, where θ is the angle between the principal axis of material orthotropy and x-axis. The components of the material properties in Eqs (12) in

151

terms of engineering constants are

$$Q_{11} = E_1 / \Delta, \quad Q_{12} = E_1 v_{21} / \Delta, \quad Q_{22} = E_2 / \Delta, \quad Q_{44} = G_{23}, \quad Q_{55} = G_{13}, \quad Q_{66} = G_{12}, \tag{13}$$

where $\Delta = 1 - v_{12} v_{21}$. We substitute Eqs (4) into Eqs (11) the resultant equations into Eqs (5), carry out the integration in the thickness direction for a cylindrical shell composed of M layers while ignoring terms of $O(z/R)^2$ and arrive at the following relationships for the stress resultants

$$
\begin{bmatrix} N_x \\ N_\beta \\ N_{x\beta} \\ N_{\beta x} \\ M_x \\ M_\beta \\ M_{x\beta} \\ M_{\beta x} \end{bmatrix} =
\begin{bmatrix}
\bar{A}_{11} & A_{12} & \bar{A}_{16} & A_{16} & \bar{B}_{11} & B_{12} & \bar{B}_{16} & B_{16} \\
A_{12} & \hat{A}_{22} & A_{26} & \hat{A}_{26} & B_{12} & \hat{B}_{22} & B_{26} & \hat{B}_{26} \\
\bar{A}_{16} & A_{26} & \bar{A}_{66} & A_{66} & \bar{B}_{16} & B_{26} & \bar{B}_{66} & B_{66} \\
A_{16} & \hat{A}_{26} & A_{66} & \hat{A}_{66} & B_{16} & \hat{B}_{26} & B_{66} & \hat{B}_{66} \\
\bar{B}_{11} & B_{12} & \bar{B}_{16} & B_{16} & \bar{D}_{11} & D_{12} & \bar{D}_{16} & D_{16} \\
B_{12} & \hat{B}_{22} & B_{26} & \hat{B}_{26} & D_{12} & \hat{D}_{22} & D_{26} & \hat{D}_{26} \\
\bar{B}_{16} & B_{26} & \bar{B}_{66} & B_{66} & \bar{D}_{16} & D_{26} & \bar{D}_{66} & D_{66} \\
B_{16} & \hat{B}_{26} & B_{66} & \hat{B}_{66} & D_{16} & \hat{D}_{26} & D_{66} & \hat{D}_{66}
\end{bmatrix}
\begin{bmatrix}
\partial u_0 / \partial x \\
\partial v_0 / \partial \beta + w_0 / R \\
\partial v_0 / \partial x \\
\partial u_0 / \partial \beta \\
\partial \psi_x / \partial x \\
\partial \psi_\beta / \partial \beta \\
\partial \psi_\beta / \partial x \\
\partial \psi_x / \partial \beta
\end{bmatrix},
$$

$$
\begin{bmatrix} Q_x \\ Q_\beta \end{bmatrix} =
\begin{bmatrix} \bar{A}_{55} & A_{45} \\ A_{45} & \hat{A}_{44} \end{bmatrix}
\begin{bmatrix} \partial w_0 / \partial x + \psi_x \\ \partial w_0 / \partial \beta + \psi_\beta - v_0 / R \end{bmatrix}
$$

$$
\left.
\begin{aligned}
\bar{A}_{ij} &= A_{ij} - c_0 B_{ij}, & \hat{A}_{ij} &= A_{ij} + c_0 B_{ij}, \\
\bar{B}_{ij} &= B_{ij} - c_0 D_{ij}, & \hat{B}_{ij} &= B_{ij} + c_0 D_{ij}, \\
\bar{D}_{ij} &= D_{ij} - c_0 E_{ij}, & \hat{D}_{ij} &= D_{ij} + c_0 E_{ij},
\end{aligned}
\right\} \quad i,j = 1,2,4,5,6, \tag{14}
$$

where $c_0 = -1/R$ and

$$A_{ij} = \sum_{k=1}^{N} \bar{Q}_{ij}^{(k)}(h_k - h_{k-1})$$

$$B_{ij} = \frac{1}{2} \sum_{k=1}^{N} \bar{Q}_{ij}^{(k)}(h_k^2 - h_{k-1}^2)$$

$$D_{ij} = \frac{1}{3} \sum_{k=1}^{N} \bar{Q}_{ij}^{(k)}(h_k^3 - h_{k-1}^3) \qquad i, j = 1, 2, 6,$$

$$E_{ij} = \frac{1}{4} \sum_{k=1}^{N} \bar{Q}_{ij}^{(k)}(h_k^4 - h_{k-1}^4)$$

$$A_{ij} = \sum_{k=1}^{N} K_x K_\beta \bar{Q}_{ij}^{(k)}(h_k - h_{k-1})$$

$$B_{ij} = \frac{1}{2} \sum_{k=1}^{N} K_x K_\beta \bar{Q}_{ij}^{(k)}(h_k^2 - h_{k-1}^2) \qquad i, j = 4, 5, \qquad (15)$$

$h_k - h_{k-1}$ is the thickness of the k-th layer, and K_x and K_β are correction factors in x and

β directions, respectively. It is worth mentioning that the presence of the components of

$\overline{A}\overline{B}\overline{D}$ and $\hat{A}\hat{B}\hat{D}$ with ABD matrixes in Eq. (14) is the difference of the present theory

(FSDTQ) by FSDT. The relevant equations for FSDT may be found by letting $c_0 = 0$;

thus, $\overline{\Lambda}_{ij} = \hat{\Lambda}_{ij} = \Lambda_{ij}$ where $i, j = 1, 2, 4, 5, 6$ and $\Lambda = A, B, D$.

In order to numerically investigate the bending of shells, Eqs (4) should be

substitute into (14). We put the resultants with Eqs (7) and arrive to system of fifteen

first-order differential equations instead of substituting the resultant into Eqs (7) and

arriving to a system of five second-order differential equations. The system of fifteen

first-order differential equation is

$$\{[K] + [M]\frac{\partial^2}{\partial t^2}\}\overline{X} = \overline{q}, \qquad (16)$$

where $\bar{X} = [u_0, v_0, w_0, \psi_x, \psi_\beta, N_x, N_\beta, N_{x\beta}, N_{\beta x}, M_x, M_\beta, M_{x\beta}, M_{\beta x}, Q_x, Q_\beta]^T$, and

$\bar{q}_1 = q_x, \bar{q}_2 = q_\beta, \bar{q}_3 = q_z$ are the non-zero components of $\bar{q}$. The non-zero components of

matrix K are

$$K(3k+1, 4k+6) = \frac{\partial}{\partial x}, \qquad K(3k+1, 4k+9) = \frac{\partial}{\partial \beta}, \qquad K(4,14) = -1,$$

$$K(3k+2, 4k+7) = \frac{\partial}{\partial \beta}, \qquad K(3k+2, 4k+8) = \frac{\partial}{\partial x}, \qquad K(2,15) = \frac{1}{R},$$

$$K(5,15) = -1, \qquad K(3,7) = -\frac{1}{R}, \qquad K(3,14) = \frac{\partial}{\partial x},$$

$$K(3,15) = \frac{\partial}{\partial \beta}, \qquad K(6+4k,1) = \bar{A}_{11}\frac{\partial}{\partial x} + A_{16}\frac{\partial}{\partial \beta}, \qquad K(6+4k,2) = A_{12}\frac{\partial}{\partial \beta} + \bar{A}_{16}\frac{\partial}{\partial x},$$

$$K(6+4k,3) = \frac{A_{12}}{R}, \qquad K(6+4k,4) = \bar{B}_{11}\frac{\partial}{\partial x} + B_{16}\frac{\partial}{\partial \beta}, \qquad K(6+4k,5) = \bar{B}_{16}\frac{\partial}{\partial x} + B_{12}\frac{\partial}{\partial \beta},$$

$$K(7+4k,1) = A_{12}\frac{\partial}{\partial x} + \hat{A}_{26}\frac{\partial}{\partial \beta}, \qquad K(7+4k,2) = \hat{A}_{22}\frac{\partial}{\partial \beta} + A_{26}\frac{\partial}{\partial x}, \qquad K(7+4k,3) = \frac{\hat{A}_{22}}{R},$$

$$K(7+4k,4) = B_{12}\frac{\partial}{\partial x} + \hat{B}_{26}\frac{\partial}{\partial \beta}, \qquad K(7+4k,5) = B_{26}\frac{\partial}{\partial x} + \hat{B}_{22}\frac{\partial}{\partial \beta}, \qquad K(8+4k,1) = \bar{A}_{16}\frac{\partial}{\partial x} + A_{66}\frac{\partial}{\partial \beta},$$

$$K(8+4k,2) = A_{26}\frac{\partial}{\partial \beta} + \bar{A}_{66}\frac{\partial}{\partial x}, \qquad K(8+4k,3) = \frac{A_{26}}{R}, \qquad K(8+4k,4) = \bar{B}_{16}\frac{\partial}{\partial x} + B_{66}\frac{\partial}{\partial \beta},$$

$$K(8+4k,5) = \bar{B}_{66}\frac{\partial}{\partial x} + B_{26}\frac{\partial}{\partial \beta}, \qquad K(9+4k,1) = A_{16}\frac{\partial}{\partial x} + \hat{A}_{66}\frac{\partial}{\partial \beta}, \qquad K(9+4k,2) = \hat{A}_{26}\frac{\partial}{\partial \beta} + A_{66}\frac{\partial}{\partial x},$$

$$K(9+4k,3) = \frac{\hat{A}_{26}}{R}, \qquad K(9+4k,4) = B_{16}\frac{\partial}{\partial x} + \hat{B}_{66}\frac{\partial}{\partial \beta}, \qquad K(9+4k,5) = B_{66}\frac{\partial}{\partial x} + \hat{B}_{26}\frac{\partial}{\partial \beta},$$

$$K(14,2) = -\frac{A_{45}}{R}, \qquad K(14,3) = \bar{A}_{55}\frac{\partial}{\partial x} + A_{45}\frac{\partial}{\partial \beta}, \qquad K(14,4) = \bar{A}_{55},$$

$$K(14,5) = A_{45}, \qquad K(15,2) = -\frac{\hat{A}_{44}}{R}, \qquad K(15,3) = A_{45}\frac{\partial}{\partial x} + \hat{A}_{44}\frac{\partial}{\partial \beta},$$

$$K(15,4) = A_{45}, \qquad K(15,5) = \hat{A}_{44}, \qquad K(i,i) = -1, \quad i = 6,7,\ldots17, \qquad (17)$$

where in the above equations in the terms containing k, it takes values of 0 and 1 and the

components of matrixes $B, \bar{B}, \hat{B}$ should change to $D, \bar{D}, \hat{D}$, respectively; then $A, \bar{A}, \hat{A}$

should change to $B, \bar{B}, \hat{B}$, respectively, for $k = 1$. Also, the non-zero components of the

symmetric matrix M are

$$M(1,1) = M(2,2) = M(3,3) = -\bar{I}_1, M(4,4) = M(5,5) = -\bar{I}_3, M(1,4) = M(2,5) = -\bar{I}_2. \qquad (18)$$

154

It should be emphasized that the presence of all the components of displacement and stress resultants in the system of Eqs (16), facilitates the direct application of all kinds of boundary conditions in the ensuing numerical treatment. The system of Eqs (16) is the equations of motion of the cylindrical shell. Letting $\bar{q} = 0$ and substituting $\bar{X}(t) = \bar{X}_1 e^{i\omega t}$ in the Eq. (16) lead to

$$[K - \omega^2 M]\bar{X}_1 = 0, \tag{19}$$

which is the relevant eigenvalue problem to find natural frequencies of the shell. The numerical solution of Eqs (19) may be accomplished by means of the generalized differential quadrature (GDQ) method. The method is utilized by several investigators; see for instance [16]. In the GDQ method the derivative of a function at any discrete point in a direction is approximated as a weighted linear sum of the function values at all the sampling points in that direction

$$\frac{dF(x_k)}{dx} = \sum_{l=1}^{N} C_{kl} F(x_l), \qquad k \in \{1,2,...,N\} \tag{20}$$

where N is the number of sampling points selected in the x-direction and C_{kl} are the weighting coefficients of the first derivative with respect to variable x and

$$C_{kl} = \frac{M(x_k)}{(x_k - x_l)M(x_l)}, \qquad k,l = 1,2,...,N, \qquad k \neq l$$

$$C_{kk} = -\sum_{\substack{l=1 \\ l \neq k}}^{N} C_{kl}, \qquad k = 1,2,...,N, \tag{21}$$

where $M(x_k) = \prod_{\substack{l=1 \\ l \neq k}}^{N} (x_k - x_l)$. The sampling points are chosen in the form of cosine

155

distribution as

$$x_k = \frac{L_x}{2}[1 - cos(\frac{k-1}{N-1}\pi)], \qquad k = 1,2,...,N \tag{22}$$

where L_x is the length in x-direction. Application of Eqs (20) with respect to variables x and β to system of Eqs (19) in conjunction with boundary conditions (10) leads to a system of algebraic equations for displacements and stress resultants at the sampling points.

6.2.   Numerical results using GDQ

For the numerical analyses, laminated cylindrical shells with the length-to-arc ratio, $a/b = 1$, thickness ratio, $a/h = 10$ (Moderately thick), depth ratio, $a/R = 2$ (very Deep) and equal shear correction factors in both directions, $k^2 = 5/6$ are considered. The material properties for orthotropic materials are considered as $E_1/E_2 = 25$, $G_{12}/E_2 = 0.5$, $G_{23}/E_2 = 0.2$, $G_{13} = G_{12}$, and $v_{12} = 0.25$. The first five natural frequency parameters $\Omega_i = \omega_i a^2 \sqrt{\rho/E_2 h^2}$, $i = 1,...,5$ with relevant mode shapes are calculated based on both FSDT and FSDTQ.

The convergence of the presented numerical method is studied with the increment of the GDQ grid points in Table 6.1. An isotropic shell with fully simply supported boundary condition (shear diaphragm) where the exact solution exists and reported by Asadi et al. [3] is considered. The first natural frequency parameter converges with seven

sampling points which is very fast; however, eleven sampling points are required for the convergence of the other four natural frequencies.

Table 6.1:   Convergence study of first five natural frequency parameters for an isotropic cylindrical shell.

GDQ points	Ω_1	Ω_2	Ω_3	Ω_4	Ω_5
5×5	9.5816	14.3482	19.821	21.5114	21.6487
7×7	9.5961	12.3892	19.668	21.3934	22.7221
9×9	9.5961	12.3817	19.660	21.3792	23.9669
11×11	9.5961	12.3813	19.660	21.3784	23.9857
Exact	9.5961	12.381	19.660	21.378	23.986

For the rest of the numerical examples, orthotropic cylindrical shells with three different lay-ups and six different types of boundary conditions are considered, Fig. 5.2, which are combinations of clamped, free and simply supported boundary conditions. Presented results from both FSDT and FSDTQ are compared against each others and against those obtained using 3D elasticity from finite element method (FEM). Fig. 4.1 shows the Mesh pattern of a typical cylindrical shell modeled using FEM wherein 3D elements are used. For simply supported boundary condition at $\alpha-$constant, W and V are set to zero at the relevant plane of boundary condition to make sure that $v_0 = w_0 = \psi_\beta = 0$ in presented theories. Also, all three displacements of the plane at boundary edge are set to zero and free in the 3D finite element analyses for clamped and free boundary conditions, respectively. Moreover, the number of quadratic solid elements used in FEM did not

Table 6.2:   Comparison of first five natural frequency parameters of $[0/90]_3$ cylindrical shells with different boundary conditions.

B.C.		Ω_1	Ω_2	Ω_3	Ω_4	Ω_5
SSSS	FSDT	14.322	24.337	32.188	35.746	42.181
	FSDTQ	14.286	24.242	32.069	35.575	42.031
	3D	14.018	22.265	30.663	32.825	37.790
CCCC	FSDT	28.417	40.157	40.346	48.160	56.039
	FSDTQ	28.319	40.005	40.196	47.953	55.815
	3D	26.249	37.072	37.624	44.511	52.327
CSCS	FSDT	17.105	26.331	33.875	37.524	43.348
	FSDTQ	17.039	26.220	33.748	37.342	43.191
	3D	16.338	24.020	32.222	34.513	38.824
CFCF	FSDT	14.231	15.715	21.910	29.537	31.557
	FSDTQ	14.170	15.680	21.787	29.425	31.522
	3D	13.185	14.946	20.394	27.278	29.563
CFSF	FSDT	11.977	13.670	20.644	28.395	30.519
	FSDTQ	11.923	13.639	20.526	28.278	30.478
	3D	11.251	13.155	19.310	26.175	28.562
FCFS	FSDT	6.3624	11.783	21.895	23.421	24.217
	FSDTQ	6.3302	11.691	21.817	23.266	24.229
	3D	5.8467	11.398	19.907	21.586	24.115

exceed $40 \times 40 \times 12$ for the convergence of the results. Table 6.2 and Fig. 6.1 show first five natural frequency parameters and mode shapes, respectively, for a $[0/90]_3$ cylindrical shell for the six types of boundary conditions. In all types of boundary conditions, natural frequency parameters predicted by 3D are the lowest and FSDTQ gives lower natural frequency parameters than those of FSDT and closer to 3D results. However, all three theories predict the same mode shapes.
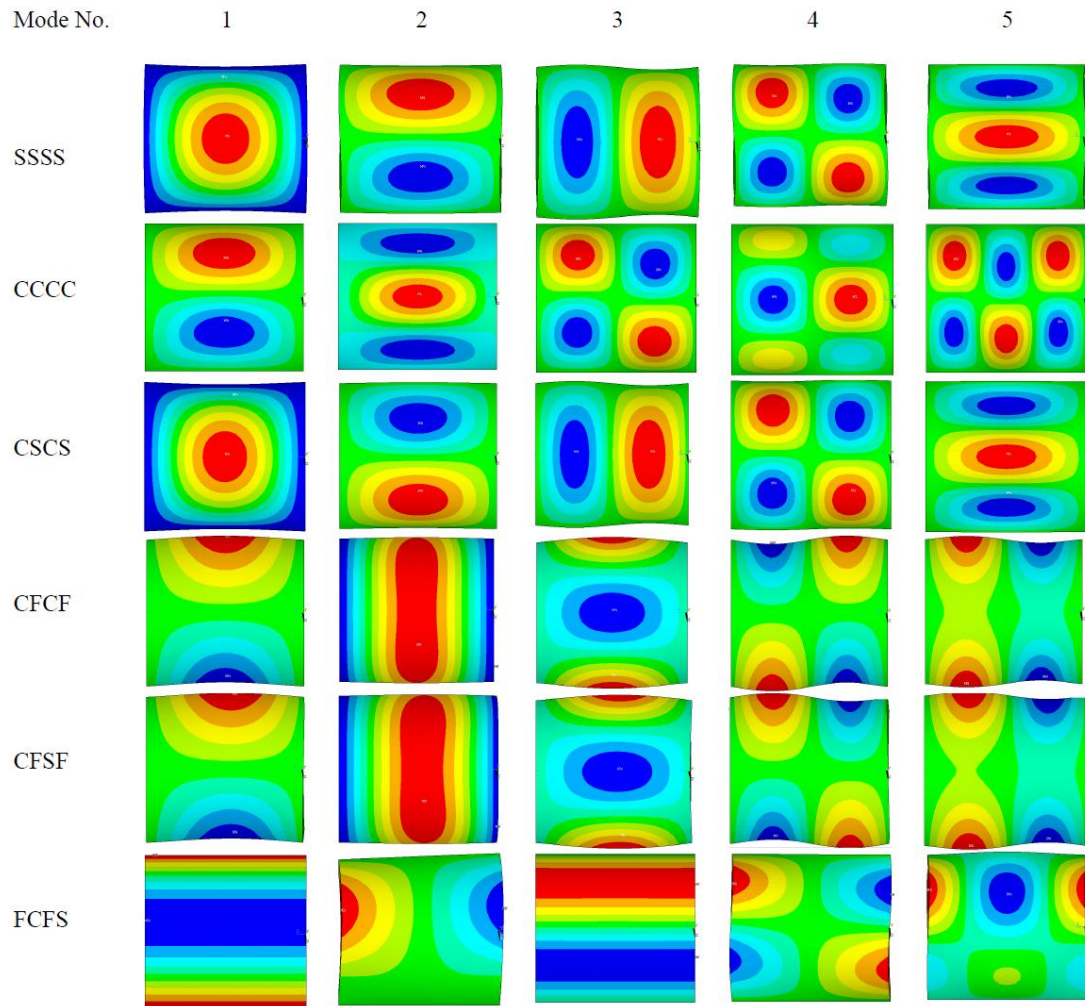
158

Figure 6.1:   First five mode shapes of a $[0/90]_3$ cylindrical shell with different boundary conditions.

Table 6.3: Comparison of first five natural frequency parameters of $[-45/45]_3$ cylindrical shells with different boundary conditions.

| B.C.		Ω_1	Error	Ω_2	Error	Ω_3	Error	Ω_4	Error	Ω_5	Error
SSSS	FSDT	24.859	8.8%	26.994	2.1%	41.519	10.0%	41.181	5.7%	43.027	4.7%
	FSDTQ	24.711	8.2%	27.023	2.2%	40.721	7.9%	41.241	5.8%	42.692	3.9%
	3D	22.842		26.432		37.744		38.975		41.111	
CCCC	FSDT	39.578	5.4%	41.011	5.9%	47.437	4.6%	50.070	5.8%	56.788	6.1%
	FSDTQ	39.462	5.1%	40.872	5.6%	46.916	3.4%	49.538	4.7%	56.500	5.5%
	3D	37.562		38.711		45.369		47.324		53.543	
CSCS	FSDT	29.705	7.3%	36.949	5.0%	41.861	8.9%	47.042	6.3%	52.652	7.7%
	FSDTQ	29.541	6.7%	36.743	4.4%	41.874	8.9%	46.489	5.0%	51.782	5.9%
	3D	27.675		35.182		38.499		44.261		48.880	
CFCF	FSDT	15.980	4.2%	18.462	3.7%	28.015	3.6%	30.252	6.1%	32.923	5.6%
	FSDTQ	16.158	5.3%	18.741	5.3%	27.508	2.3%	30.034	5.3%	33.255	6.7%
	3D	15.344		17.798		26.640		28.518		31.178	
CFSF	FSDT	13.916	6.0%	14.368	1.6%	22.996	6.7%	24.014	3.3%	29.325	6.2%
	FSDTQ	14.048	7.0%	14.661	3.6%	22.691	5.3%	23.639	1.7%	29.046	5.2%
	3D	13.127		14.149		21.550		23.253		27.606	
FCFS	FSDT	4.9792	5.2%	17.060	11.3%	18.186	6.9%	29.258	7.2%	29.487	2.8%
	FSDTQ	4.9697	5.0%	16.198	5.7%	18.107	6.4%	28.769	5.5%	29.241	2.0%
	3D	4.7332		15.322		17.011		27.282		28.683	
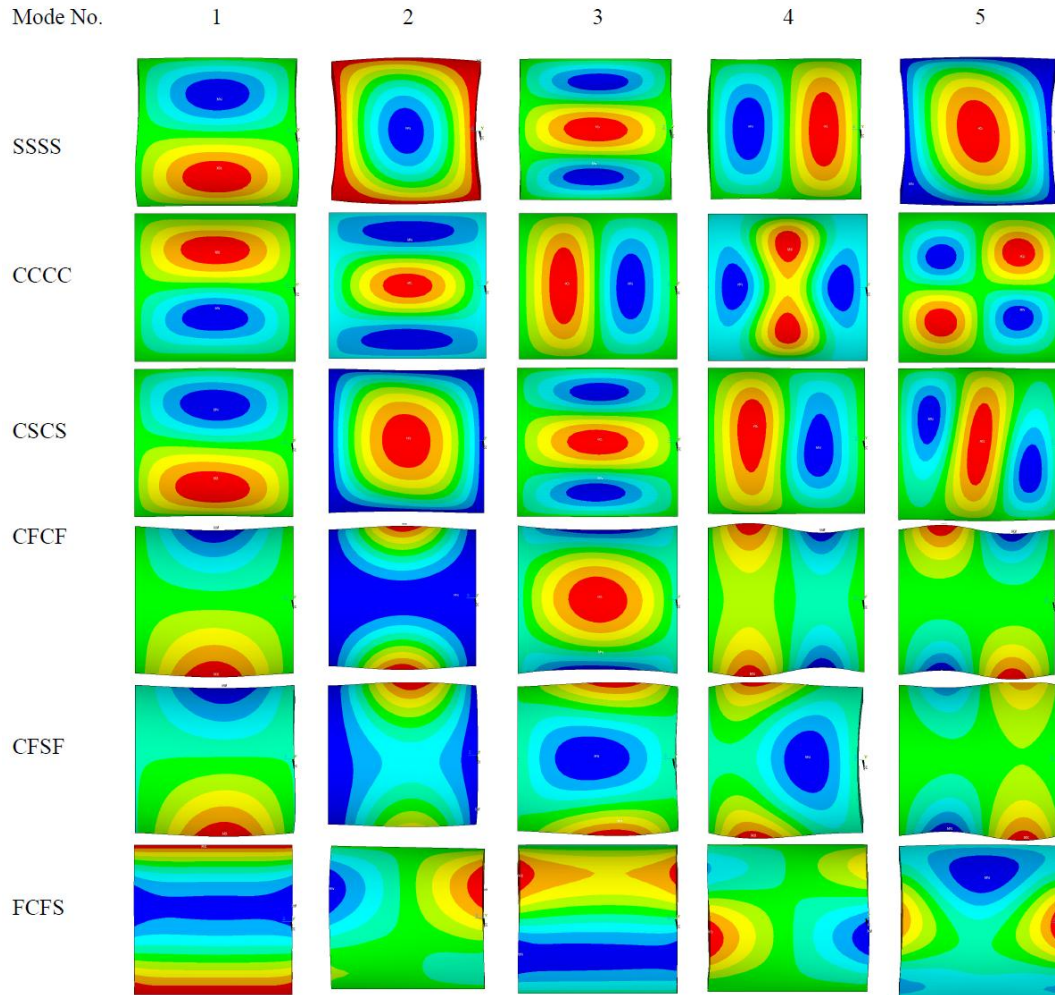
Figure 6.2: First five mode shapes of a $[-45/45]_3$ cylindrical shell with different boundary conditions.

Tables 6.3 and 6.4 show the same results as in the previous table but for angle-ply $[-45/45]_3$ and general $[30/60/45]$ lay-ups, respectively. Also, the mode shapes for angle-ply and general lay-ups cylindrical shells are depicted in Figures 6.2 and 6.3, respectively.

Table 6.4: Comparison of first five natural frequency parameters of [30/60/45] cylindrical shells with different boundary conditions.

B.C.		Ω_1	Ω_2	Ω_3	Ω_4	Ω_5
SSSS	FSDT	20.357	20.805	28.668	31.759	41.135
	FSDTQ	20.258	20.809	28.449	32.358	40.992
	3D	19.931	20.479	28.226	32.844	39.510
CCCC	FSDT	29.908	36.690	45.599	46.551	51.587
	FSDTQ	29.832	36.505	45.445	46.441	51.166
	3D	29.778	36.579	45.383	46.621	50.667
CSCS	FSDT	25.514	25.657	32.249	36.334	44.039
	FSDTQ	25.265	25.435	32.348	36.302	45.225
	3D	25.116	25.242	32.130	36.199	43.495
CFCF	FSDT	13.779	14.794	23.740	25.518	27.560
	FSDTQ	13.831	14.917	23.400	25.622	27.752
	3D	13.671	14.735	23.138	25.413	26.795
CFSF	FSDT	10.169	12.568	19.604	21.705	22.680
	FSDTQ	10.102	12.747	19.188	21.475	22.680
	3D	9.9874	12.561	18.859	21.079	22.410
FCFS	FSDT	4.0734	11.641	15.515	21.235	25.949
	FSDTQ	4.0603	11.164	15.241	20.856	25.568
	3D	4.0348	11.246	15.220	20.777	25.448

The same order in the calculated natural frequency parameters found in Table 1 is closely observed for the results in Tables 6.3 and 6.4. Also, both shear deformation theories give the same mode shapes as 3D results. It is worth mentioning that the difference between FSDT and FSDTQ and
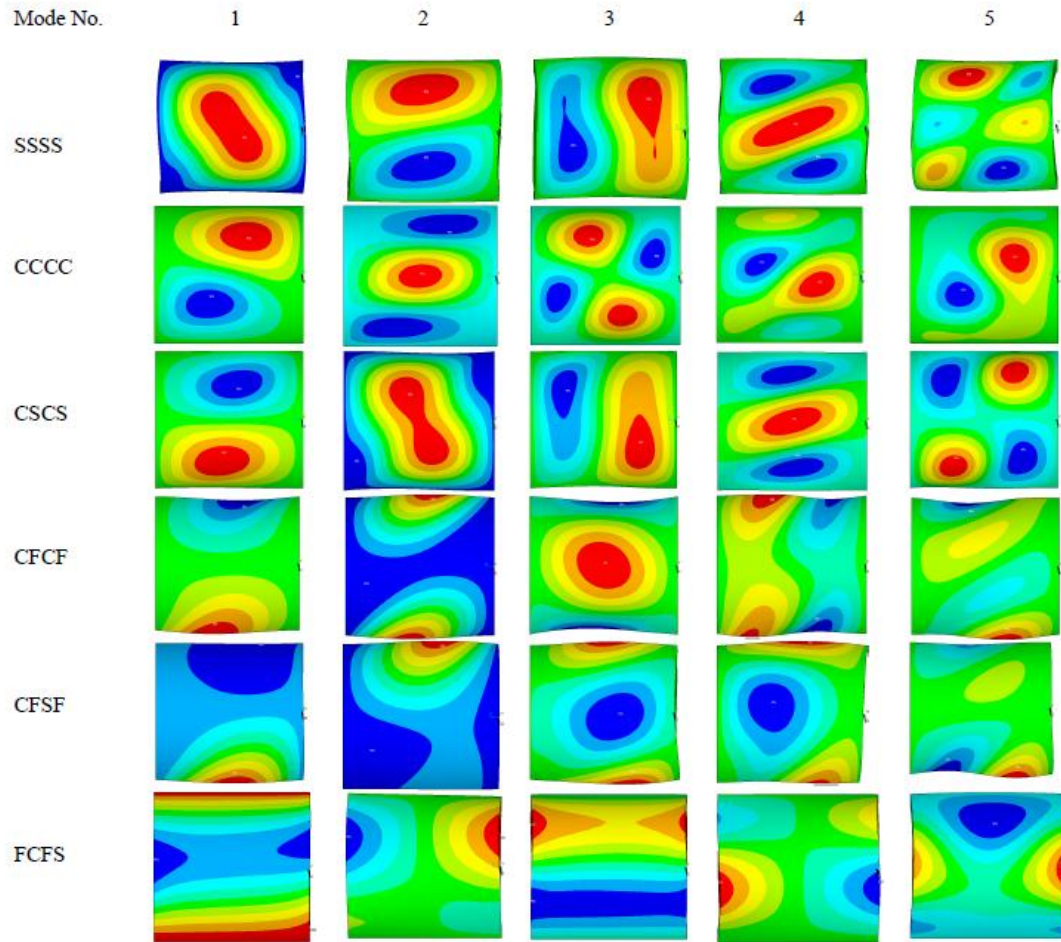
Figure 6.3:   First five mode shapes of a $[30/60/45]$ cylindrical shell with different boundary conditions.

the difference between both of them and 3D results increase as the number of natural frequency increases in all three sets of results. Moreover the biggest difference in the results of shear deformation theories occurs in the second natural frequency parameter for FCFS boundary condition and the angle-ply lay-up wherein FSDTQ predicts a natural frequency 5.6% better than FSDT when comparing both to 3D results.

6.3.   Conclusions

The equations of motion with required boundary conditions are obtained for composite cylindrical shells based on FSDTQ and FSDT. These equations of motion with stress resultants equations are put together to arrive to fifteen first-order differential equations for free the vibration problem. These equations are solved numerically for different types of boundary conditions and lay-ups by means of GDQ method. FSDTQ offers a more accurate representation of the stiffness parameters and the stress resultant equations by including the $1+z/R$ in the equations. Almost all analyses are showing that there is a significant improvement (closer to 3D) obtained when FSDTQ is used. This improvement increases when angle-ply or generally laminated composites are used for shells. Also, it varies with the change of boundary conditions. This analysis is a prelude to the derivation of a proper higher order shell theory (e.g. third order) where the term $(1+z/R)$ needs to be truncated at the third order.

6.4.   References

1.   Qatu M.S. Accurate stress resultants equations for laminated composite deep thick shells. Compos Press Vess Ind 1995; 302: 39-44.

2.   Qatu M.S. Accurate equations for laminated composite deep thick shells. Int Solids Struct 1999; 36: 2917-2941.

3.   Asadi E., Wang W. Qatu M.S. Static and vibration analyses of thick deep laminated cylindrical shells using 3D and various shear deformation theories. Compos Struct 2011; DOI: 10.1016/j.compstruct.2011.08.011.

4.   Yaghoubshahi M., Asadi E., Fariborz S.J. A higher-order shell model applied to shells with mixed boundary conditions. J Mech Engng Sci IMechE Part C 2011; 225: 292-303.

5.   Ambartsumian S.A. Contribution to the theory of anisotropic laminated shells. Appl Mech Rev 1962;15: 245-249.

6.   Rath B.K., Das Y.C. Vibration of layered shells. J Sound Vib 1973; 28: 737-757.

7.   Reddy J.N. Exact solution of moderately thick laminated shells. J Engng Mech ASCE 1984; 110: 794-809.

8.   Librescu L., Khdeir A.A. Frederick D. A shear-deformable theory for laminated composite shallow shell-type shells and their response analysis I: free vibration and buckling. Acta Mechanica 1989; 75: 1-33.

9.   Librescu L., Khdeir A.A., Frederick D. A shear-deformable theory for laminated composite shallow shell-type shells and their response analysis II: static analysis. Acta Mechanica 1989; 77: 1-12.

10.   Reddy J.N., Liu C.F. A higher order shear deformation theory of laminated elastic shells. Int J Engng Sci 1985; 23: 440-447.

11.   Qatu M.S., Sullivan R.W., Wang W. Recent research advances in the dynamic behavior of composite shells: 2000-2009. Compos Struct 2010; 93: 14–31.

12.   Qatu M.S., Asadi E., Wang W. Review of recent literature on static analysis of composite shells: 2000-2010. Accepted for publication, Appl Mech Rev 2012.

13.   Carrera E. Theories and finite elements for multilayered, anisotropic, composite plates and shells. Arch Comput Methods Engng 2002; 87: 87–140.

14.   Carrera E. Historical review of zig-zag theories for multilayered plates and shells. Appl Mech Rev 2003; 56: 287–309.

15. Qatu M.S. Vibration of Laminated Shells and Plates. Elsevier 2004.

16. Asadi E., Fariborz S.J. Free vibration of composite plates with mixed boundary conditions based on higher-order shear deformation theory. Arch Appl Mech 2011; DOI: 10.1007/s00419-011-0588-y.

CHAPTER 7

CONCLUSIONS AND RECOMMENDATIONS FOR FUTURE WORK

At first, reasonably accurate natural frequency parameters are delivered for a wide set of boundary conditions using the classical shell theory. The numerical Ritz method has been used for this purpose. Their accuracy is established through extensive convergence studies that yielded accuracy up to the third significant figure for many situations. These results can be used for benchmarking by researchers in future references. They can also be used by practicing engineers to gain more insight on the behavior of these shells undergoing a vibrational motion. In addition, the impact of shell curvature on shell frequencies is discussed. Only certain modes seem to be impacted significantly by curvature while others do not. Curvature and boundary condition are interacting to deliver the frequency pattern for each of the 21 cases studied.

Then, both static and vibration analyses are performed on composite cylindrical shells using a widely used first order shear deformation theory with plate-like stiffness coefficients (FSDT) and a first order shear deformation theory by Qatu (FSDTQ) where these coefficients are integrated exactly or truncated to the first order. For benchmarking we used finite element analyses based upon the three dimensional elasticity (3D). FSDTQ offers a more accurate representation of the stiffness parameters and the stress resultant equations. Most analyses performed here show that there is an improvement (closer to 3D) obtained when FSDTQ is used. In addition, such improvement is observed to be

higher for deeper and thicker shells than for thin shallow shells, especially in static analyses. It is worth mentioning that this study is the first study on the static analysis of composite shells by FSDTQ. Moreover, FSDTQ has been modified by the present author by using the radii of each laminate instead of the radii of the mid-plane in the calculating the moments of inertias and stress resultants. The results show that this modification improves FSDTQ's results in general and significantly in some cases.

In chapters five and six, FSDTQ's equations are derived for general shells and composite cylindrical shells in order to be solved numerically for shells with different boundary conditions. For the first time, these equations are presented in a system of seventeen first-order differential equations for general composite shells and a system of fifteen first-order differential equations for cylindrical shells. These equations were solved numerically by means of GDQ method. It is worth mentioning that this formulation facilitates the direct application of different boundary conditions and avoids ill-conditioned matrices. Almost all analyses are showing that there is a significant improvement (closer to 3D and HSDTs that includes the effects of depth) obtained when FSDTQ is used. This improvement increases when angle-ply or generally laminated composites are used for shells. Also, it varies with the change of boundary conditions and the difference between FSDT and FSDTQ is more significant in static analysis rather than in free vibration analysis.

It can be concluded from this dissertation that the limit of using FSDT is for the thickness ratio of ten and the depth ratio of 0.5 whereas the limit of the depth ratio was relaxed to the ratio of two by using FSDTQ. Also, FSDTQ gives better results even for thickness ratios bigger than ten and depth ratios smaller than two. Moreover, the run time

of codes written for FSDTQ is thirty times smaller than the run time of the same problem using 3D elasticity formulation. For example, for a typical shells solved in this dissertation the run time is around five minutes whereas it takes two and half hours to solve the same problem using 3D elements in FEM software. This emphasizes the value of using proposed shell theory instead of 3D elasticity in reducing of CPU time needed to solve complicated structures.

This analysis is a prelude to the derivation of a proper higher order shell theory (e.g. third order) where the term (1+z/R) needs to be truncated at the third order. In this HSDT, not only the effect of thickness (available HSDTS) but also the effect of the curvature of the shells should be included in the theory. Currently, it has been proven that FSDTQ presents more accurate results than other available FSDTs in literature. Also, commercial finite element software packages use some sort of FSDTs in their shell elements which are accurate when the curvature of the shell is relatively small (i.e. shallow shells). We argue that based upon the work done here that it can be improved by the FSDTQ and modified FSDTQ presented in this dissertation. Consequently, building an element based on the presented theory and the implementation of it in commercial software like ANSYS® would be another suggestion for future works.